April 2011

PWM Techniques: A Pure Sine Wave Inverter

Ho Fong Leung
Worcester Polytechnic Institute

Ian Francis Crowley
Worcester Polytechnic Institute

2010-2011 Worcester Polytechnic Institute Major Qualifying Project

PWM Techniques: A Pure Sine Wave Inverter

Advisor: Professor Stephen J. Bitar, ECE

Student Authors:

Ian F. Crowley

Ho Fong Leung

4/27/2011

Contents

Figures 3

Abstract 6

Introduction 7

Problem Statement 8

Background Research 10

- Prior Art 10
  - Comparison of Commercially Available Inverters 11
  - Examination of an Existing Design 15
- DC to AC Inversion 16
  - Square Wave Inverters 16
  - Modified Sine Wave Inverters 18
  - Pure Sine Wave Inverters 19
  - PWM 20
  - 2-Level PWM 20
  - 3-Level PWM 22
  - Examining 3-Level PWM in Practice 25
  - 5-Level PWM 27
  - IGBTs vs. Power MOSFETs 31
- Amplitude Modulation 32

H-Bridge Components and Power Losses 36

- IRFP460A MOSFET 36
- IR2304 MOSFET Driver IC 36
- Power Loss and Heat 38
  - Typical PWM 38
  - Our Design 39
- Filter Components 41

Control Signal Generation for 2-Level PWM 42

- A Stable Operation Voltage 42
- Triangle Wave Generator 45
- Sine Wave Generator 46

PWM Signal from Comparators 51
Signal Generation for 3-Level PWM 54
Features of the TL494 54
Programmable Switching Frequency 54
Two Error Amplifiers 54
Minimum Dead Time (Maximum Duty Cycle) 54
Using the TL494 55
Results 63
Low-Voltage Test 64
High Voltage Testing 66
200W Resistive Load 66
Inductive Load Test 70
Printed Circuit Board 71
Power Efficiency 75
Conclusion and Recommendations 77
References 79
Appendix A: Circuit Schematic 80
Appendix B: Parts List 91

Figures

Figure 1:Square, Modified Sine, and Sine Waves Comparison 11
Figure 2: A Modified Sine Wave Inverter 16
Figure 3: Square Wave 17
Figure 4: Square Wave Harmonic Analysis 17
Figure 5: Modified Sine Wave 18
Figure 6: Modified Sine Wave Harmonic Analysis 19
Figure 7: 2-Level PWM Comparison Signals 20
Figure 8: 2-Level PWM Output (Unfiltered) 21
Figure 9: 2-Level PWM Harmonic Analysis 21
Figure 10: 2-Level PWM Output (Filtered) 22
Figure 11: 3-Level PWM Comparison Control Signals 23
Figure 12: 3-Level PWM Simulation Circuit 23
Figure 13: Simulated 3-Level PWM Output (Unfiltered) 24

Figure 14: Simulated 3-Level PWM Output (Filtered) 24
Figure 15: 3-Level PWM Harmonics Analysis of Unfiltered Output 25
Figure 16: Block Diagram from "DC/AC Pure Sine Wave Inverter" MQP 26
Figure 17:5-Level PWM Simulation Circuit 28
Figure 18: 5-Level PWM Comparison Signals 29
Figure 19: PWM Bridge Control Signals (superimposed) 29
Figure 20: 5-Level PWM Output (unfiltered) 30
Figure 21: 5-Level PWM Output (filtered) 30
Figure 22: 5-Level PWM Harmonics Analysis of Unfiltered Output 31
Figure 23: Filtered Outputs ma 0.1 to 0.95 34
Figure 24: Bipolar PWM Test Circuit 35
Figure 25: IR2304 37
Figure 26: Voltage vs. State of Charge of a Sealed Lead Acid Battery 43
Figure 27: Dropout Voltage of the LM317 44
Figure 28: Voltage Regulation Circuit 44
Figure 29: Triangle Wave Generator Circuit 45
Figure 30: Output of the Triangle Wave Generator 46
Figure 31: Schmitt Trigger Oscillator 47
Figure 32: Butterworth Low-Pass Filter 48
Figure 33: Square and Sine Waves from the Above Circuits 49
Figure 34: Revised Sine Wave Generator 50
Figure 35: Sine Wave from the Revised Circuit 50
Figure 36: Comparison of Positive and Negative Swings of the 60 Hz Sine Wave 51
Figure 37: MC3302 Equivalent Circuit 52
Figure 38: Comparator Circuit 52
Figure 39 PWM Signals for Both Halves of the H-Bridge 53
Figure 40: TL494 Dead Time Control 55
Figure 41: TL494 Inputs 55
Figure 42: Precision Rectifiers for Half-Wave Generation 57
Figure 43: Half-Wave Rectifier Outputs 58
Figure 44: Inverting Gain Stage for the Half Waves 58
Figure 45: Outputs of the Inverting Amplfiers 59
Figure 46: TL494 Configuration 60
Figure 47: Sampling the Input with a Saw-Tooth Wave 60
Figure 48: Grounding the Bootstrap Capacitor 61
Figure 49: PWM Signal from the TL494 (Top) and its Inversion (Bottom) 62
Figure 50: Alternating PWM Signals for Both High Side Gate Half-Cycles 62
Figure 51: Final Inverter Design 63
Figure 52: Low-Voltage Test Half-Bridge Vgs Waveforms 64
Figure 53:Filtered Low-Voltage Output across 12VDC Headlight 65
Figure 54: Low-Voltage Output Cross-Over Distortion 66
Figure 55: High Voltage Half-Bridge Vgs Waveforms 67

Figure 56: High-Voltage Filtered Output Waveform (showing Breakdown Distortion) 68
Figure 57: Unfiltered High-Voltage Output with a 200W Load..... 68
Figure 58: Unfiltered Output FFT w/200W Resistive Load 69
Figure 59: Output FFT showing 60Hz peak 70
Figure 60: Unfiltered Output with Inductive Load..... 71
Figure 61: Sine Wave Inverter PCB 73
Figure 62: Populated PCB..... 73
Figure 63: PCB gate voltage waveforms (one half-bridge) 74
Figure 64: PCB filtered output waveform 74

Abstract

The ever-increasing reliance on electronic devices which utilize AC power highlights the problems associated with the unexpected loss of power from the electrical grid. In places where the electrical infrastructure is not well-developed, brown-outs can prove fatal when electronic medical instruments become unusable. Therefore, there is a need for inexpensive and reliable pure-sine wave inverters for use with medical devices in the underdeveloped world. This report documents the development of one component of an uninterruptible power supply, the DC-to-AC inverter. Through the use of analog signal processing techniques, a prototype which efficiently and accurately emulates the pure-sine wave power present on the power grid was created. The three-level PWM system within this report is created with the possibility of a feedback-regulated system to be implemented in the future.

Introduction

Conventionally, there are two ways in which electrical power is transmitted. Direct current (DC) comes from a source of constant voltage and is suited to short-range or device level transmission. Alternating current (AC) power consists of a sinusoidal voltage source in which a continuously changing voltage (and current) can be used to employ magnetic components. Long distance electrical transmission favors AC power, since the voltage can be boosted easily with the use of transformers. By boosting the voltage, less current is needed to deliver a given amount of power to a load, reducing the resistive loss through conductors.

The adoption of AC power has created a trend where most devices adapt AC power from an outlet into DC power for use by the device. However, AC power is not always available and the need for mobility and simplicity has given batteries an advantage in portable power. Thus, for portable AC power, inverters are needed. Inverters take a DC voltage from a battery or a solar panel as input, and convert it into an AC voltage output.

There are three types of DC/AC inverters available on the market, which are classified by their output type: square wave, modified-sine wave and pure sine wave. Off-the-shelf inverters are generally either square wave or modified-sine wave. These types of inverters are less expensive to make and the output, though delivering the same average voltage to a load, is not appropriate to delicate electronic devices which rely on precise timing. Pure sine wave inverters offer more accuracy and less unused harmonic energy delivered to a load, but they are more complex in design and more expensive. Pure sine wave inverters will power devices with more accuracy, less power loss, and less heat generation.

Pure sine wave inversion is accomplished by taking a DC voltage source and switching it across a load using an H-bridge. If this voltage needs to be boosted from the DC source, it can be accomplished either before the AC stage by using a DC-DC boost converter, or after the AC stage by using a boost transformer. The inverted signal itself is composed of a pulse-width-modulated (PWM) signal which encodes a sine wave. The duty cycle of the output is changed such that the power transmitted is exactly that of a sine-wave. This output can be used as-is or, alternatively, can be filtered easily into a pure sine wave. This report documents the design of a true sine wave inverter, focusing on the inversion of a DC high-voltage source. It therefore assumes the creation of a DC-DC boost phase.

Problem Statement

In developing countries, healthcare is often of limited access to the local inhabitants. The government is often unable, or unwilling, to direct its attention to the issue of public healthcare because the country is not yet economically or technologically mature enough to support a quality healthcare system. The lack of money available for building a reliable electrical infrastructure stunts the growth of electronics use, which includes the employment of instruments used in modern healthcare. In African villages, villagers may install a solar panel on their homes for the sole reason of charging a cell phone because there are no centralized production facilities or transmission lines for electrical energy.

The lack of reliable power severely limits the quality of healthcare available in developing countries. While it is true that these countries receive donations of medical instruments, the means to operate them reliably often does not exist. An ongoing issue with poorly developed electrical grids is that the production of electricity is not enough to meet demand. Brown-outs are commonplace, and the transients that result damage the donated equipment used in medical procedures. Imagine, during an operation, that a patient's heart stopped and no defibrillator was available because the grid suffered a brownout. Sadly, this is an all-too-common occurrence in much of the underdeveloped world.

Due to these problems, there is a market for uninterruptible power supplies which can provide a temporary remedy to the lack of electrical infrastructure in developing countries. Enter Waste to Watts, a company devoted to the recycling of electronic waste into useful products in developing countries. Their proposed flagship product, the ENZI interface[1], is a multipurpose power conditioner that will be compatible with grid power, battery, and solar power inputs to provide uninterrupted power. The mandatory characteristics of the ENZI interface are that it will be affordable, have high manufacturability, make use of waste electronic components local to the places they will be used, be capable of reliably powering medical equipment, and tolerate a wide range of power sources.

The design requirements of the ENZI dictate the specifications of a DC/AC power inverter that this project will endeavor to produce. First, the inverter will need to emulate grid power from a DC source such as a recycled battery or solar panel. The output must be a pure sine wave, to allow proper functioning of sensitive medical electronics. An output goal of 250 watts was set to allow the use of medical instruments. The form factor must be small enough to fit inside an enclosure or atop a battery.

[1] (Waste to Watts, 2010)

Transient response is also important in a device that is meant to curtail the effects of suddenly losing grid power. For the purpose of a project prototype, the use of waste electronics parts is a distant goal.

Background Research

Prior Art

Electrical power transmission is classified into two methods: alternating current and direct current. Alternating current can be found in AC motor drives and long distance power transmission. The cyclic nature of alternating current enables the use of transformers, which use magnetic principles to alter voltage levels. By stepping up an AC voltage, a large amount of power can be transferred over a long distance with less energy lost in heating up a conductor due to a lower current requirement, since $P=I^2R$. As such, AC power is more conventional than high voltage DC systems due to the ease of stepping up voltage for transmission and stepping voltage down to household outlet levels.

DC voltage also has a place in powering devices. Wherever there is a changing electrical current, a changing magnetic field accompanies it. In a device-level electrical circuit, the magnetic variations introduced by AC current manifest themselves as electrical noise. The effects of this can range from audible line hum in an audio system to inaccurate measurements in an electronic instrument. Thus, it is commonplace for a device such as an MP3 player to employ DC voltages that have been rectified and filtered from an AC wall outlet. An MP3 player also proves one other benefit of DC power transmission: it can be done with a compact form factor. Without a need for transformers or switching circuitry, battery-powered MP3 players, or any other portable device, can be made small enough to fit into a pocket.

However, there may come a time when household AC power is cut off due to a power outage. The multitude of devices that are designed around AC/DC power conversion (computers, for example) would then no longer be able to operate. One solution to this problem is an auxiliary AC power generator, like those powered by gasoline engines, or DC/AC power inverters which use energy stored in batteries (a DC source) and emulate a wall outlet AC output through voltage boosting and switching to create a changing voltage with the proper amplitude across a load. In practice, DC/AC conversion is done with topologies of varying precision. It can be as simple as applying voltages of equal amplitude in opposite directions across a load to generate a square wave. This method achieves the AC voltage requisite of a changing voltage across a load, but this rough approximation has consequences discussed later in this paper.

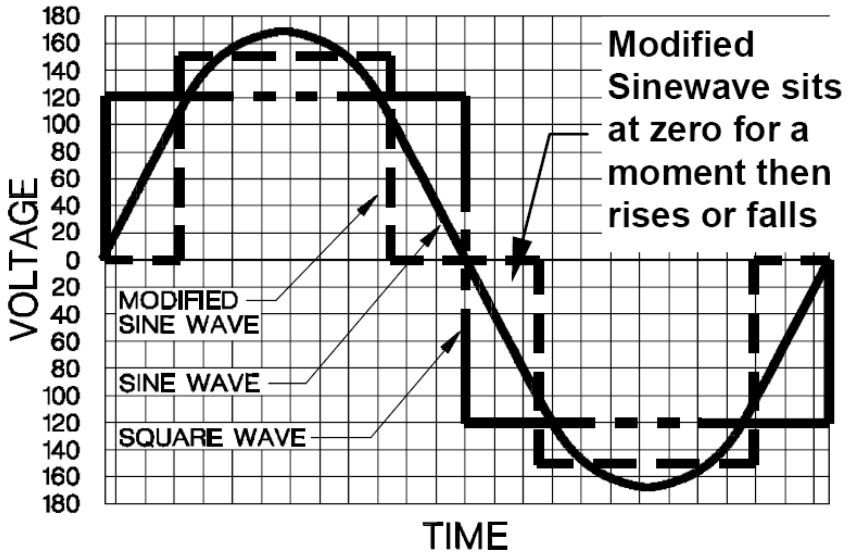

Figure 1:Square, Modified Sine, and Sine Waves Comparison[2]

A more precise method of DC/AC conversion is the modified sine wave, which introduces a dead time in a normal square wave output so that higher peak voltages can be used to produce the same average voltage as a sinusoidal wall-outlet output. This method produces fewer harmonics than square wave generation, but it still is not quite the same as the AC power that comes from an AC outlet. The harmonics that are still present in a modified sine wave make modified sine-wave inverters unsuitable for use while electrical noise is a concern, such as in medical devices which monitor the vital signs of a human.

Pure sine wave DC/AC conversion will introduce the least amount of harmonics into an electrical device, but are also the most expensive method. Since the AC sine wave must come from a DC source, switching must still take place. However, switching takes place with logic so that the energy delivered to a load approaches that of a pure sine wave. This means that extra components and design considerations are involved in the control circuitry of a pure sine wave inverter, driving up cost.

Comparison of Commercially Available Inverters

Market research revealed some generalizations that can be made about modified-sine and pure-sine wave inverters. A comparison was performed between Duracell (by Xantrex) modified sine wave inverters and the Samlex PST series of pure sine wave inverter. For a more relevant comparison, each series of inverters had variants available in 300-watt and 1000-watt ratings. In general, the Samlex

[2] (Doucet, 2007)

inverters have larger dimensions, compared to their modified-sine counterparts, and much higher cost. This is due to the added circuitry necessary to produce a pure sine wave. Note that all inverters operate from 12VDC input power. The commonalities that the inverters share hint at necessary features that any inverter should have. The inclusion of forced-air cooling, input protection, and overload protection are needed for the safe operation of inverters.

It should be noted that modified-sine wave inverters are not rated for Total Harmonic Distortion (THD). Rating a modified-sine wave inverter for harmonic distortion would be useless, for their intended use is not to reduce the harmonics introduced to devices. Their purpose is to provide affordable and portable AC power. A question of efficiency is brought up in the discussion of harmonics. The pure sine wave inverters are 5% less efficient, but this rating is from the conversion of battery energy to modified-sine-wave output. This does not take into consideration the effect of harmonics on battery-to-device output efficiency. As stated by Samlex America, "The high frequency harmonic content in a modified sine wave produces enhanced radio interference, higher heating effect in motors / microwaves and produces overloading due to lowering of the impedance of low frequency filter capacitors / power factor improvement capacitors."[3] A pure-sine-wave inverter may be less efficient in terms of battery energy conversion, but more of the output energy is used by the load.

[3] (Samlex Power, 2010)

Table 1: Comparison of Inverters, Pure Sine vs. Modified Sine of the Same Capacity [4]

	Model	Duracell Inverter 300	Duracell Inverter 1000	Samlex PST-30S-12A	Samlex PST-100S-12A
Specification					
Output Type		Modified Sine - 60 Hz	Modified Sine - 60 Hz	Pure Sine - 60 Hz	Pure Sine - 60 Hz
Rated Output		300W	1000W	300W	1000W
Overload Protection		Yes			
Maximum Output Surge (<1 sec)		500W	2000W	500W	2000W
Low Battery Shutdown		Yes			
Cooling		Thermostat-Controlled Forced Air			
Outlets		2	2	1	2
Dimensions		152 x 106 x 50 mm	305 x 152 x 76 mm	214 x 146 x 65 mm	395 x 236 x 83 mm
Thermal Shutdown		Yes			
Peak Efficiency		90%	90%	85%	85%
THD		Not Rated	Not Rated	<3%	<3%
Cost		$44	$129	$159	$479

[4] (Inverters R Us, 2010)

Table 2: Modified sine wave inverters

Model	Rated Output	Max Output	Outlets	Dimensions L x W x H	Efficiency	Cost
Cobra	150W	300W	1	3.25”x3.25”x.75”	85%	$25
Voltec	200W	400W	2	6.5”x4.125”x2”	87%	$29
Samlex	250W	500W	1	5.9”x4.5”x1.8”	90%	$25
Black&Decker	400W	800W	2	6”x5.25”x2”	90%	$37
AIMS	800W	1600W	2	10.25”x5.75”x2”	95%	$69
Xantrex	1000W	2000W	2	12”x6”x3”	90%	$129
Wagan	2000W	4000W	2	12.3”x6.4”x3”	90%	$219

Table 3: Pure sine inverters

Model	Rated Output	Max Output	Outlets	Dimensions L x W x H	Efficiency	Cost
Samlex	120W	240W	1	7.4”x4.3”x1.18”	88%	$99
Go Power	150W	260W	2	8”x5.3”x2.9”	90%	$150
Samlex	300W	500W	2	8.5”x5.8”x2.6”	90%	$149
AIMS	600W	1200W	2	9”x”x3”	86%	$189
Xantrex	900W	2000W	2	13.4”x8.7”x3.5”	90%	$299
Wagan	2000W	4000W	4	19”x7.5”x3.5”	90%	$499

Examination of an Existing Design

With the dissection of a commercially available DC/AC modified sine wave inverter, some lessons were learned about the design of power inverters. An exterior examination prompted thoughts about cooling, as this particular inverter had a plastic body, but with forced air cooling via an internal fan. There was also a 5V out USB port, but that is not important to this project which aims only to design a device capable of DC/AC inversion. The alligator clip battery leads were used since operation from a 12V car battery was intended. This inverter had two NEMA 5–15 (North American 15 A/125 V grounded) output plugs.

Opening the enclosure revealed some technical aspects of the inverter. The most prominent part was the large transformer used for high-voltage DC/DC conversion, as well as a 50-amp fuse and switching MOSFETs with heatsinks to deal with the high current. We also noted that the H-bridge MOSFETs did not have heat-sinks and the output was devoid of inductors. Operation of the inverter consisted of simply plugging in a device which, in our case, was a simple resistive load in the form of a soldering iron. A status indicator LED turned on with the connection of a load, and we noted the output waveform across the output terminals. The output waveform was a 60-hz modified sine wave with sharp voltage transitions and approximately 145V peak amplitude. This inverter was later used to provide our design with a 145V DC rail. To do so, we simply disassembled the inverter and tapped into the DC rail directly.

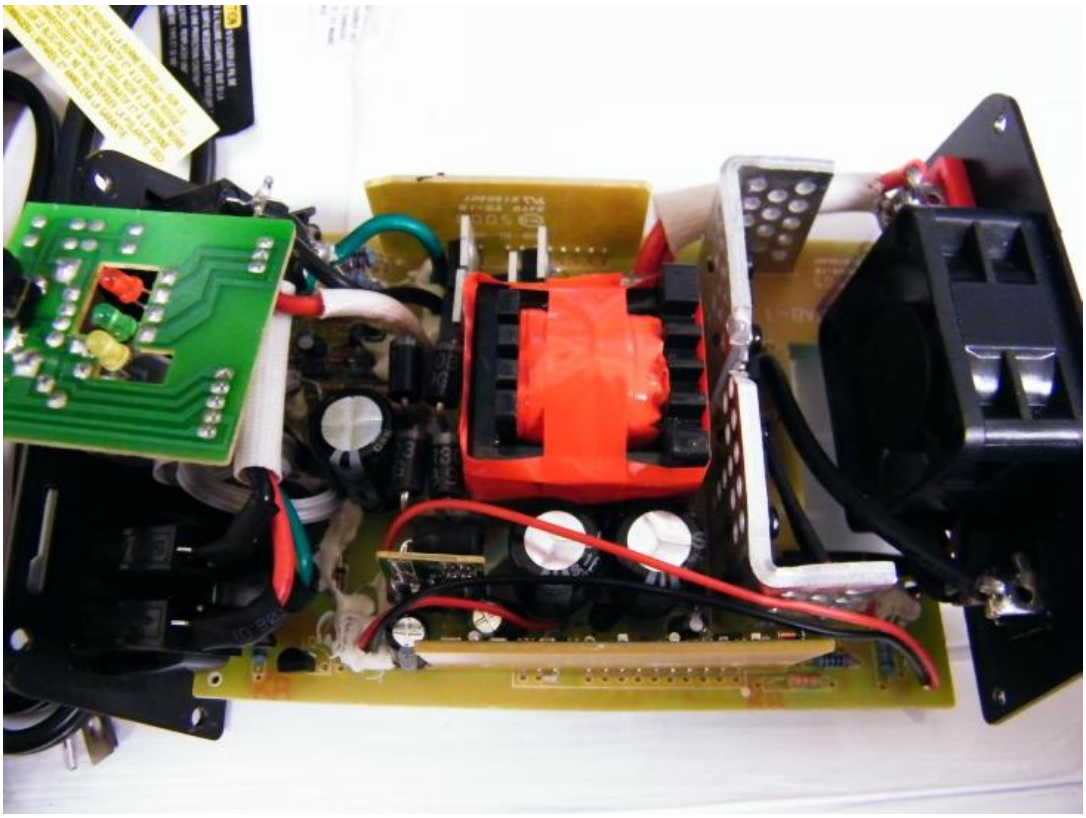

Figure 2: A Modified Sine Wave Inverter

DC to AC Inversion

Square Wave Inverters

DC to AC conversion is most commonly done through use of MOSFET inverter circuits, which can switch the voltage across the load, providing a digital approximation of the desired AC signal. The simplest variant of this inversion is the production of a square wave approximation of a sine wave (Figure 3). For a square wave, the load voltage must be switched merely from high to low, without the need for an intermediate step (i.e. 0V). In order to deliver the same power as the sine wave to be approximated, the amplitude of the square wave must be the sine wave's RMS value. This way, the average voltages, and therefore the power delivered, will be the same for the two waveforms. Square wave inverters are very rarely used in practice, as many devices which utilize timing circuits that rely on something close to the sine wave from the power company cannot operate with such a rough

approximation. In addition, a square wave has relatively large 3rd and 5th harmonic components (figure 4), which burn power and severely cut down on the efficiency of devices using such inverters as a power source.

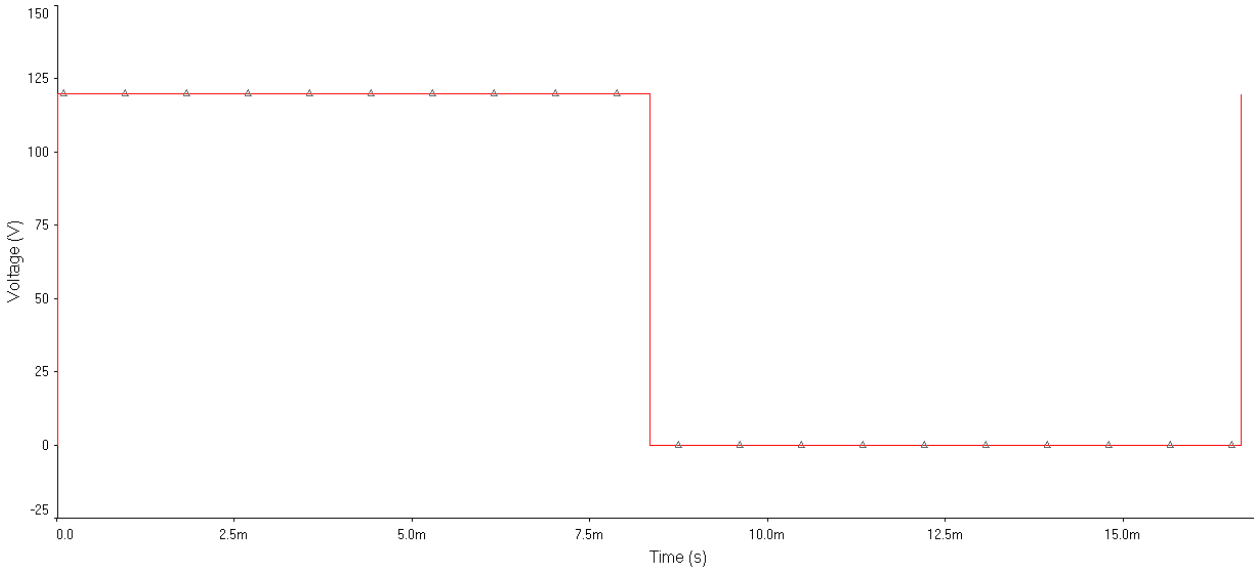

Figure 3: Square Wave

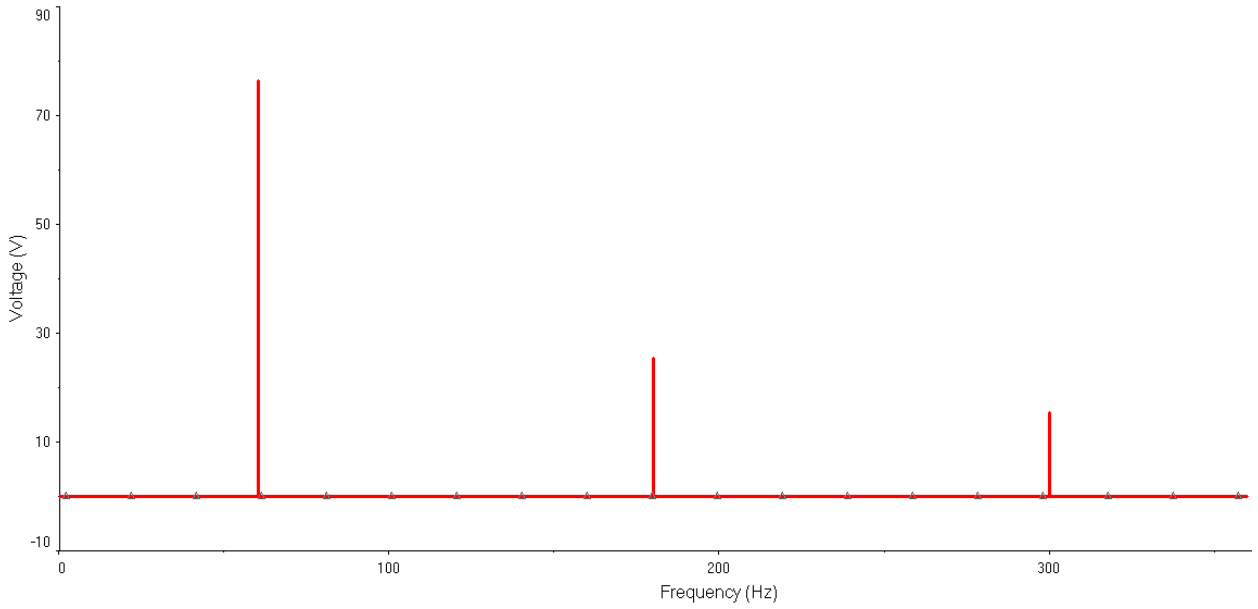

Figure 4: Square Wave Harmonic Analysis

Modified Sine Wave Inverters

A very common upgrade to the square wave inverter is the modified sine wave inverter. In the modified sine wave inverter, there are three voltage levels in the output waveform, high, low, and zero (figure 5), with a dead zone between the high and low pulses. The modified sine wave is a closer approximation of a true sine wave than is a square wave, and can be used by most household electrical devices. As such, it is extremely common to see this type of inversion in commercial quality inverters. Despite being much more viable than a simple square wave, the modified sine wave has some serious drawbacks. Like the square wave, modified sine waves have a large amount of power efficiency loss due to significant harmonic frequencies (figure 6), and devices that rely on the input power waveform for a clock timer will often not work properly. Despite the inherent drawbacks, many devices can work while powered by a modified sine source. This makes it an affordable design option for such implementations as household uninterruptible power supplies.

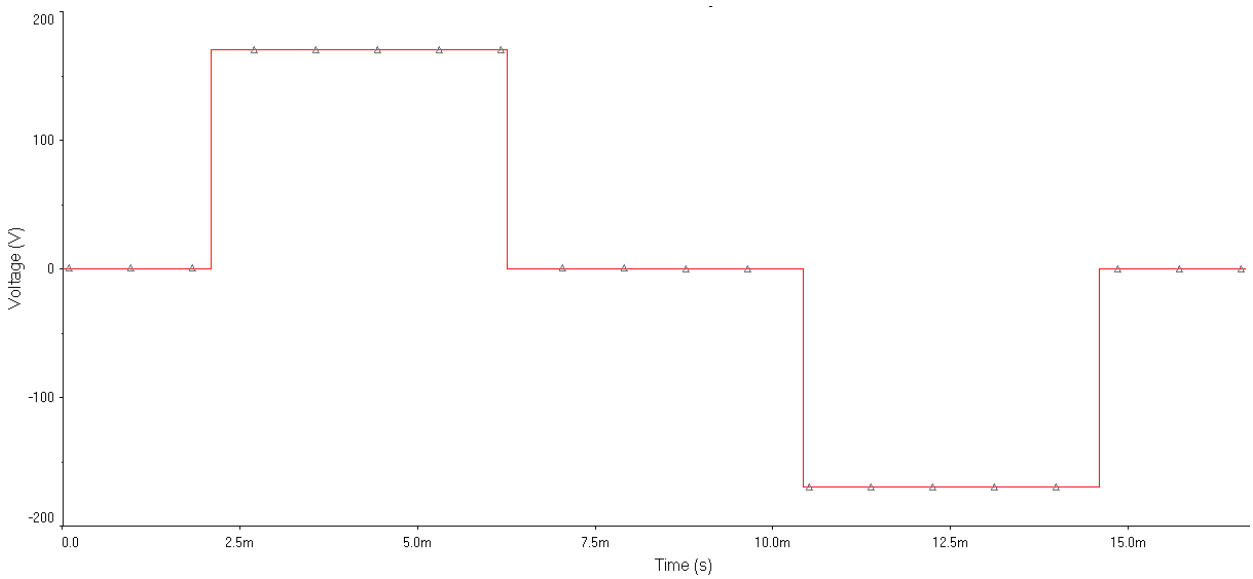

Figure 5: Modified Sine Wave

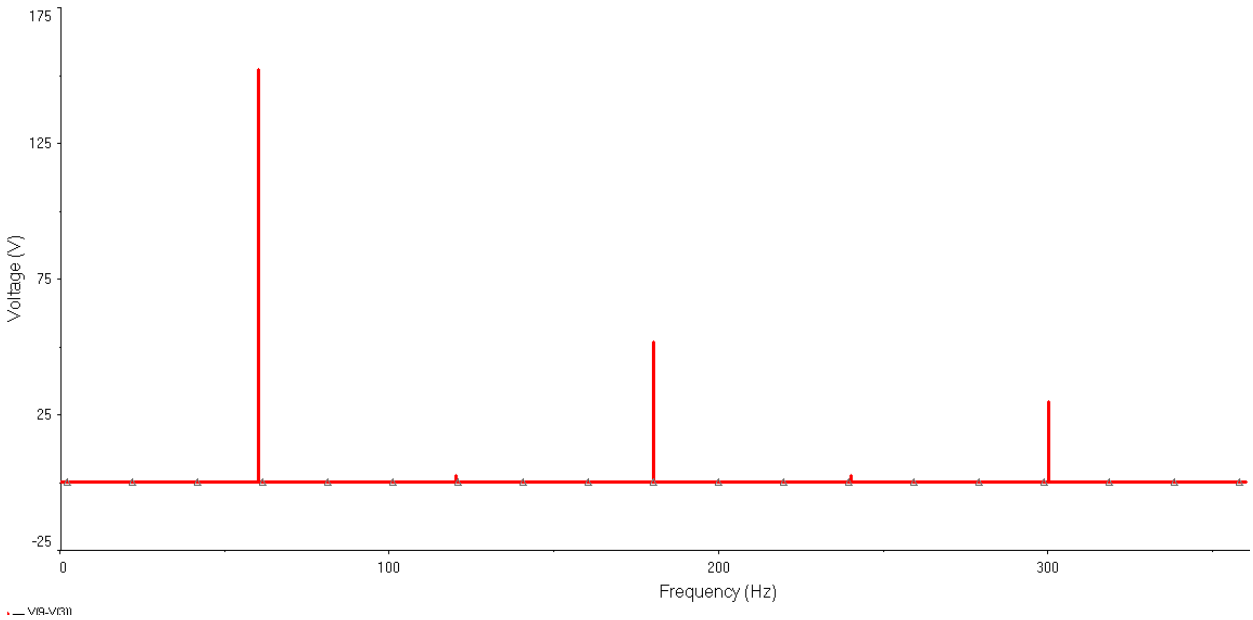

Figure 6: Modified Sine Wave Harmonic Analysis

Pure Sine Wave Inverters

The best power source for most applications is a pure 60Hz sine wave, identical to the 120Vrms source available from any US power company. All low power household plug-in devices are designed to work with this source (high power devices such as cooking ovens use a 240V source) and, as such, will be most likely to work properly and most efficiently on such a source. A true sine wave source is produced most easily for high power applications through rotating electrical machinery such as naval gas-turbine generators, house-hold diesel or gasoline backup generators, or the various generators employed by power companies that employ a shaft torque to create an AC current. These sources provide a relatively clean, pure sine wave (lacking significant harmonics and high frequency noise) thanks to their analog rotational make-up. Such rotating machinery can be inappropriate for low-power backup supply usage due to their high cost, large size and required maintenance. As such, a smaller, digital pure sine wave inverter can be extremely useful.

PWM

2-Level PWM

The most common and popular technique of digital pure-sine wave generation is pulse-width-modulation (PWM). The PWM technique involves generation of a digital waveform, for which the duty-cycle is modulated such that the average voltage of the waveform corresponds to a pure sine wave. The simplest way of producing the PWM signal is through comparison of a low-power reference sine wave with a triangle wave (figure 7). Using these two signals as input to a comparator, the output will be a 2-level PWM signal (figure 8). This PWM signal can then be used to control switches connected to a high-voltage bus, which will replicate this signal at the appropriate voltage. Put through an LC filter, this PWM signal will clean up into a close approximation of a sine wave (figure 10). Though this technique produces a much cleaner source of AC power than either the square or modified sine waves, the frequency analysis shows that the primary harmonic is still truncated, and there is a relatively high amount of higher level harmonics in the signal (figure 9).

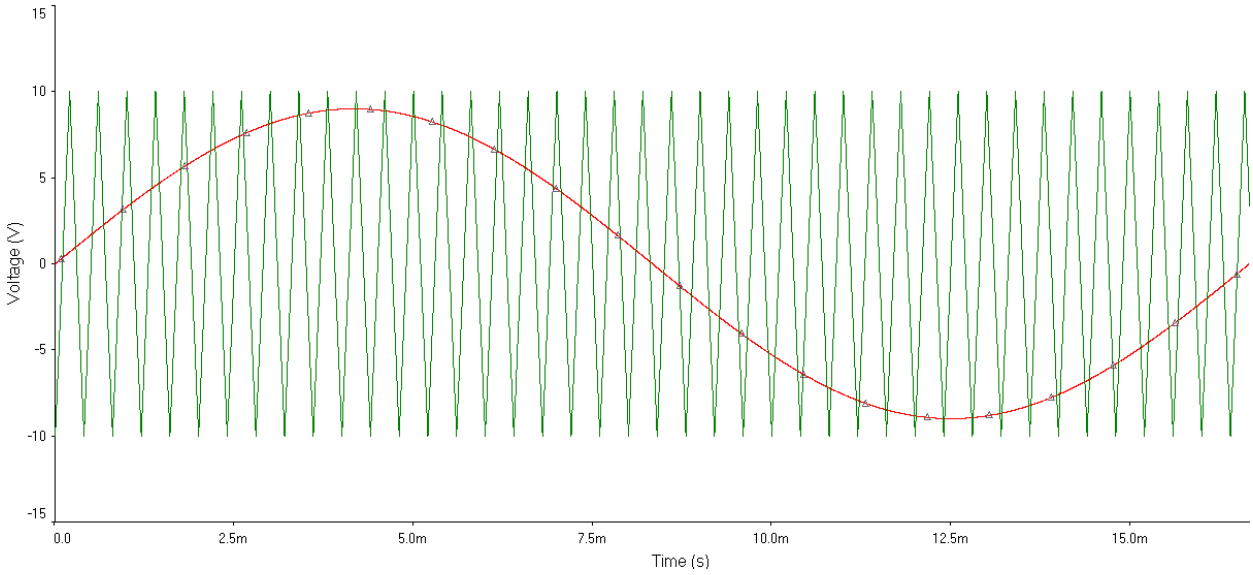

Figure 7: 2-Level PWM Comparison Signals

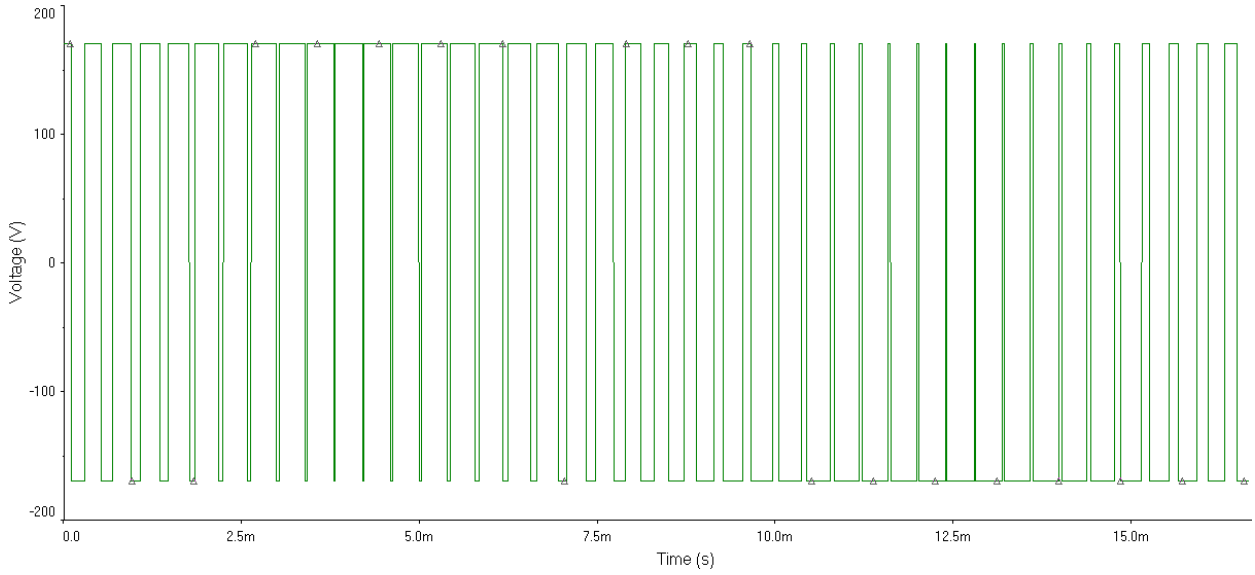

Figure 8: 2-Level PWM Output (Unfiltered)

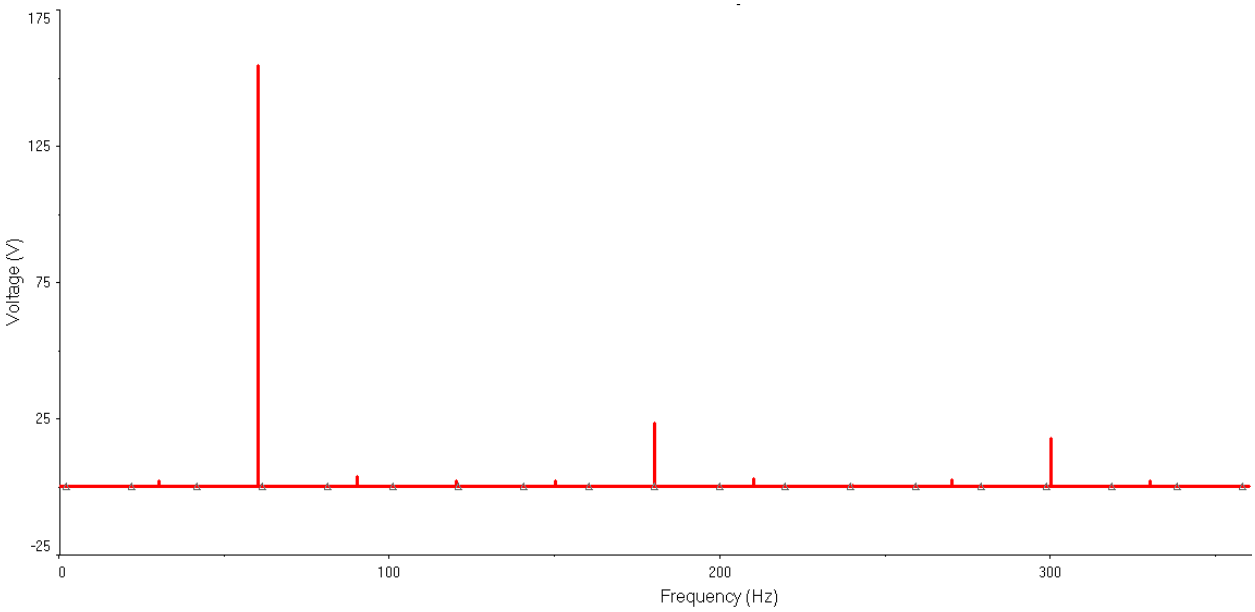

Figure 9: 2-Level PWM Harmonic Analysis

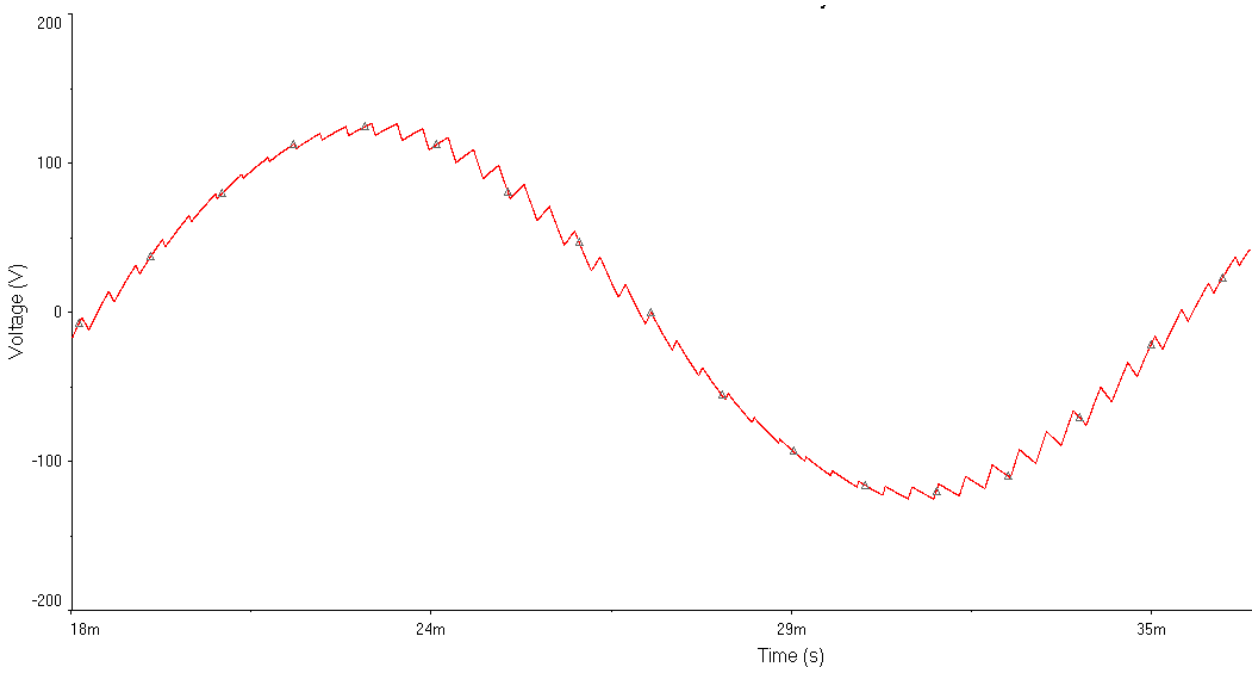

Figure 10: 2-Level PWM Output (Filtered)

3-Level PWM

In order to create a signal which is closer to a true sine wave, a 3 level PWM signal can be generated with high, low, and zero voltage levels. For the resulting 3-level PWM signal to correspond to a sine wave, the signal comparison stage must also be 3-level (figure 11). A triangle wave is used as it is in the 2-level PWM comparison, but it half the amplitude and summed with a square wave to compare one half of the sine reference signal at a time. The resulting PWM signal is used to control one half of an H-bridge (figure 12), which controls how long the bus voltage is allowed through to the load. The other half of the H-bridge controls the polarity of the voltage across the load, and is controlled by a simple square wave of the same frequency and in phase with the sine signal. Generally, this square wave can simply be created in a stage of the sine wave generation circuit. A virtual example of such a 3-level circuit we simulated is shown in figure 12. The resulting 3-level high-voltage PWM signal (figure 13) can be filtered into a very close approximation of the desired sine wave (figure 14). It should be noted that the simulations we did for this technique utilized a very low switching frequency for the triangle wave, so the PWM switching frequency is also low. This was done so that the waveforms would be easy to view and understand. In reality, a switching frequency above 20 kHz would be used to keep inductance ringing outside the range of human hearing.

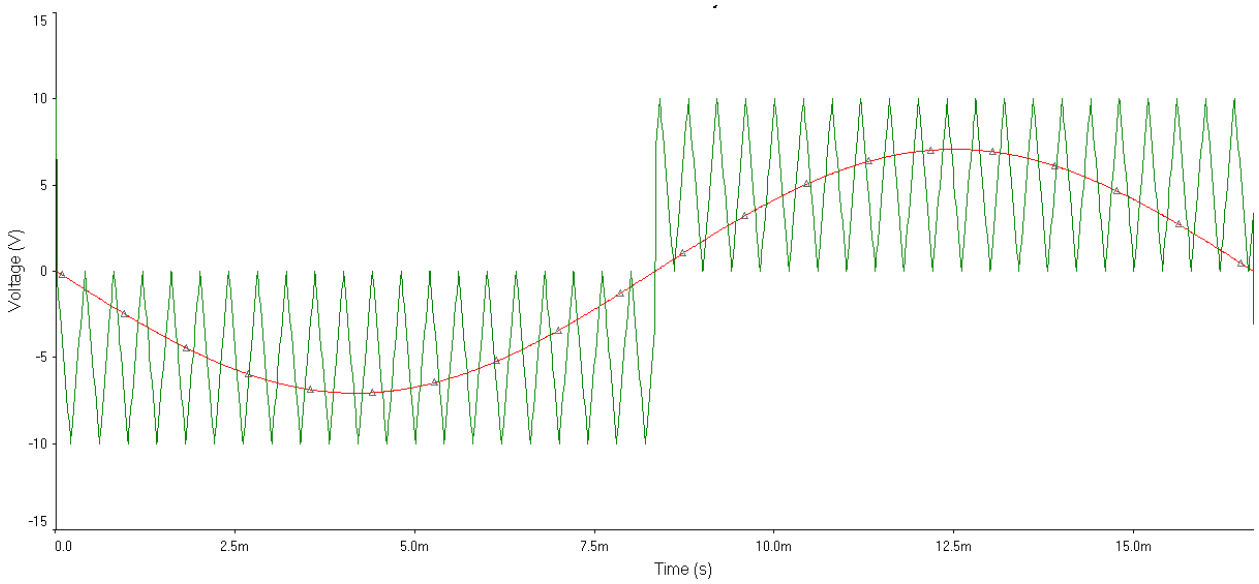

Figure 11: 3-Level PWM Comparison Control Signals

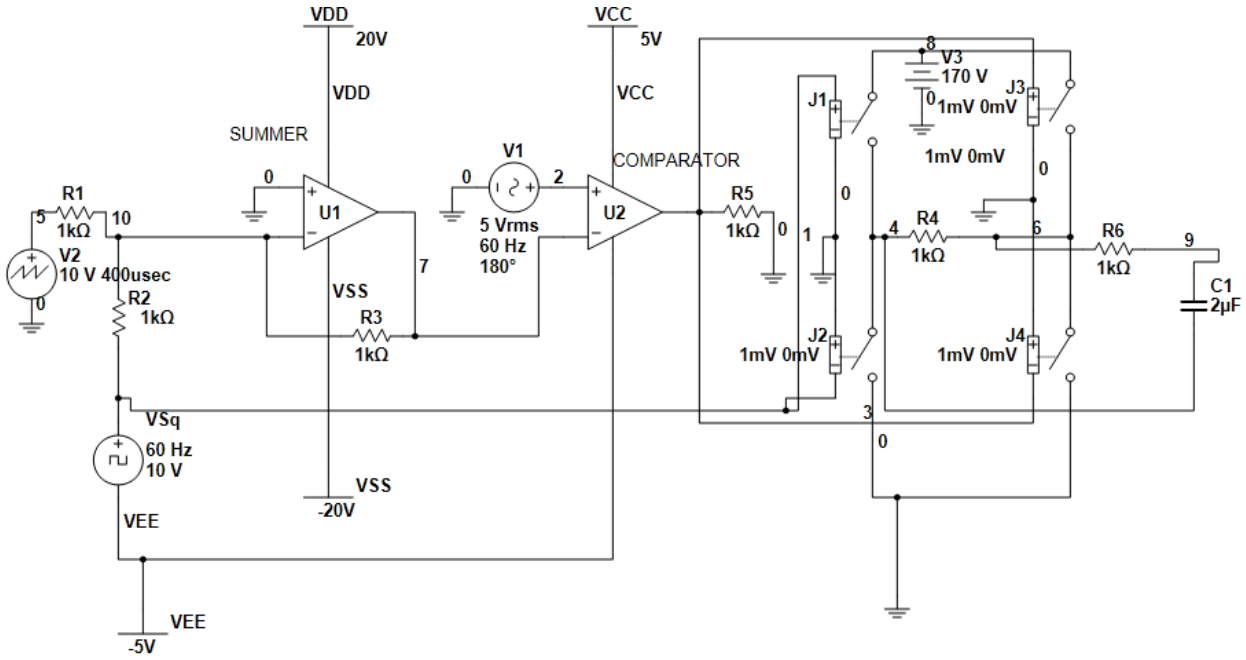

Figure 12: 3-Level PWM Simulation Circuit

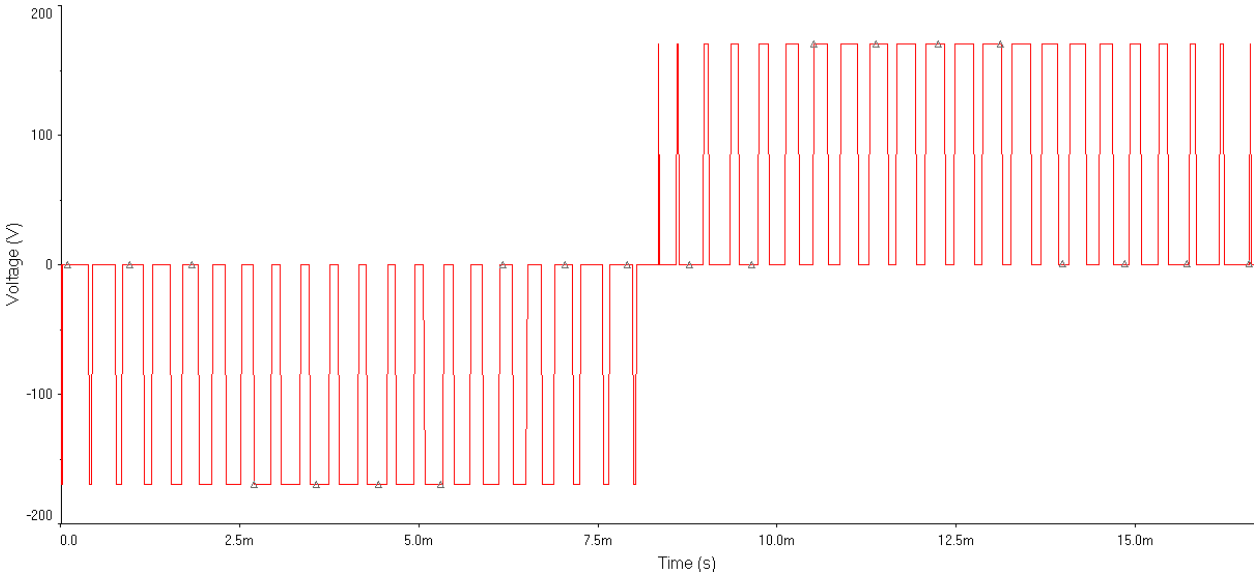

Figure 13: Simulated 3-Level PWM Output (Unfiltered)

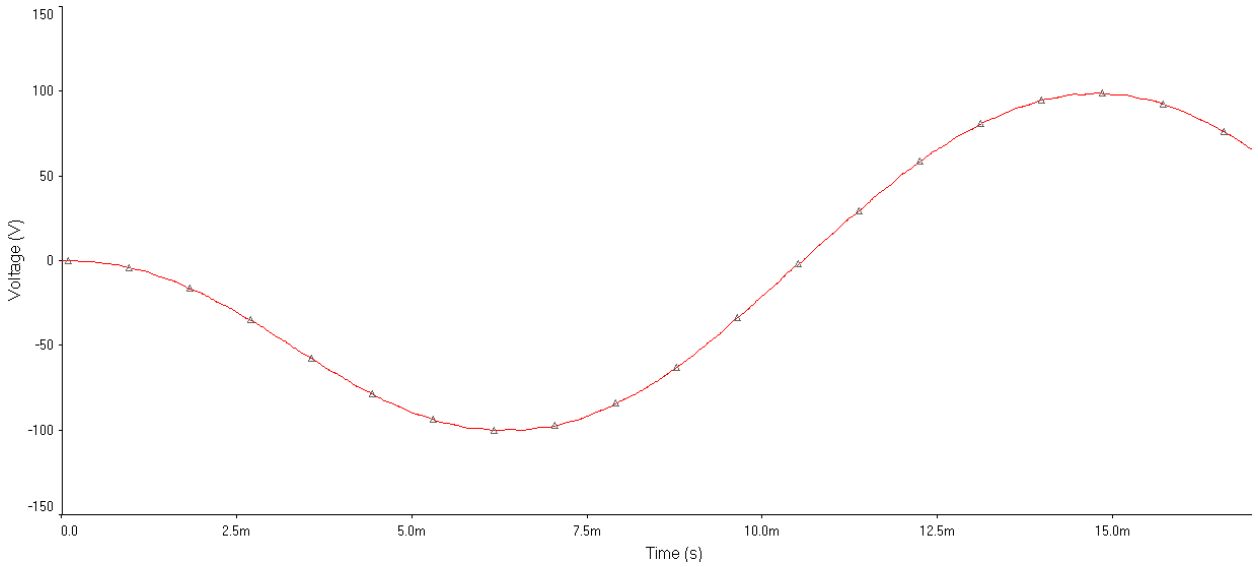

Figure 14: Simulated 3-Level PWM Output (Filtered)

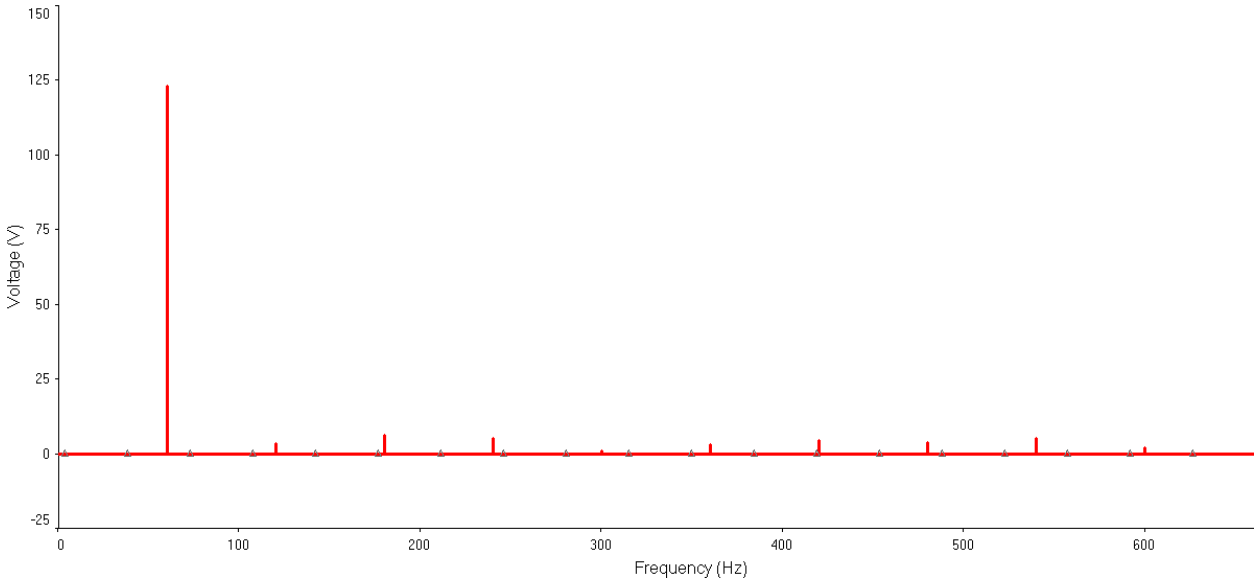

Figure 15: 3-Level PWM Harmonics Analysis of Unfiltered Output

The 3-Level PWM frequency plot shown in figure 15 markedly improved over those of the square and modified sine techniques. The primary frequency of 60Hz is the dominant in all three, but the magnitude of the harmonic frequencies is much reduced in 3-Level PWM, and the primary is of larger magnitude. When compared to the 2-level PWM, however, a couple things are noticed. First, the harmonics plot shows no higher level harmonics of significant magnitude. This represents the 3-Level signal following much more closely the desired sine wave. However, the primary frequency has a much lower voltage magnitude than that of the 2-Level design. The reason for this is the presence of other frequencies which are not harmonics of the 60Hz signal, which are caused by the switching of the signal from one polarity to the other, and back.

Examining 3-Level PWM in Practice

A 2006 – 2007 Worcester Polytechnic Institute (WPI) Major Qualifying Project (MQP) titled "DC/AC Pure Sine Wave Inverter" can be considered as companion to the analysis of the various PWM options. Some design considerations can be gleaned from it about inverter topology. The design documented in the report was a pure sine wave inverter using 3-level pulse width modulation using an analog logic control circuit. The control circuit, with its function generators, summer, and comparators, controlled MOSFET drivers which actuated the MOSFET's (with snubbers) connected to the high-side voltage and load with a 4-pole LC filter. Basically, a 60 Hz sine wave was generated with a "bubba oscillator" and compared with a high-frequency triangle wave that had a 60 Hz square wave summing component for separate levels of control during the two-half cycles of the sine wave. The logic that

resulted from the function generators controlled the two half-bridge MOSFET drivers that had independent high and low side output.

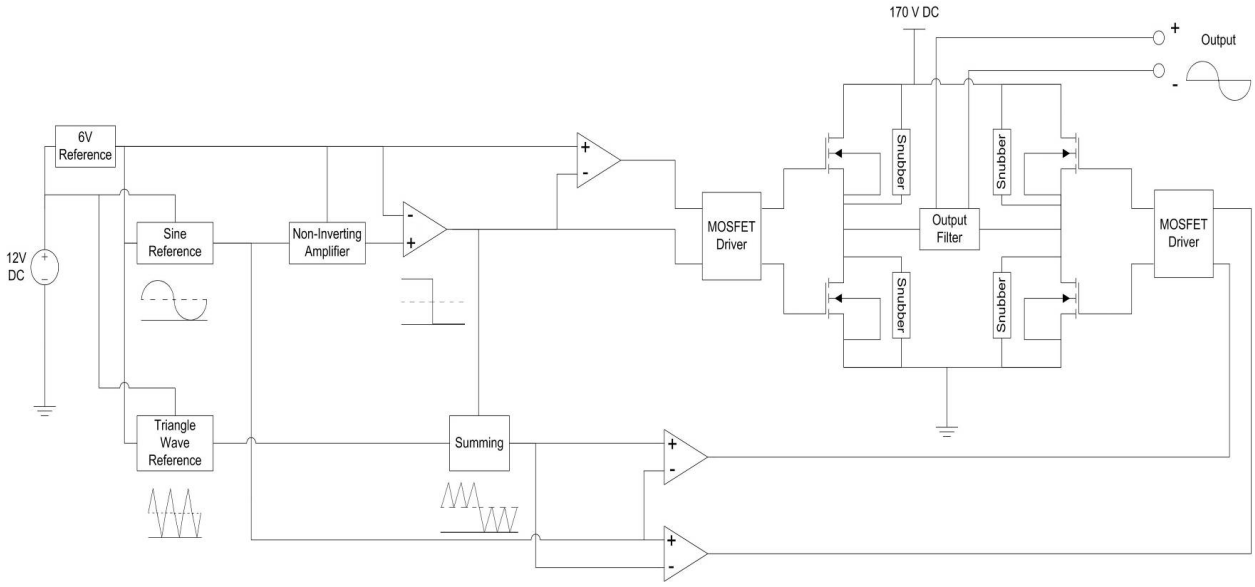

Figure 16: Block Diagram from "DC/AC Pure Sine Wave Inverter" MQP

The report provided a summative perspective of PWM sine wave inverters, but shortcomings of the project can be noted. While the final product produced a sine wave, the project team only tested with a 12 Volt high-side voltage. Thus, this project was more concerned with the generation of a sine wave from a DC source than producing a device that electronic devices can run from. The inverter design relied on a stiff high-side voltage to supply the load without any feedback to control their DC rail. In the "Results" section of the report, the team remarked:

> "While the operation of the inverter works under light or medium loads (above 50 [Ohms?] with 12V input), its output was affected by high frequency oscillations when heavier loads were connected."[5]

Such is the effect of lacking a feedback system. One of the goals of this project will be to build upon this MQP and implement a feedback system to provide stable operation up to the output goal. It is also noted that the cost of parts in the MQP was $65, which parallels the tentative budget for the parts in this project.

[5] (Doucet, 2007)

5-Level PWM

In order to create a PWM signal which more closely follows the desired sine wave output, the design described for the 3-level PWM technique can be expanded to 5-, 7- and 9+ level PWM. Each additional 2 levels added on top of the 3-level design adds an H-bridge (added in series), a comparator, and a summer. The added accuracy of the signal due to increasing the level therefore brings with it the addition of components, and the space, cooling, and power they require. Control signals must be created separately for each H-bridge (figure 18), each of which correspond to one layer of the sine voltage (figure 19). Higher level PWM also requires multiple isolated voltage buses. For example, the 5-level PWM circuit in figure 17 requires two isolated buses at 1/2 the voltage of the corresponding 3-level circuit. The buses must be isolated, as they need to be connected in series. In the 5-level PWM circuit, one half of each H-bridge is controlled by the square wave from the 3-level circuit, and simply controls polarity across the bridge. The other half of each bridge is controlled by the PWM output of each respective comparator. The resulting PWM signal is shown in figure 20, and the filtered sine wave output is shown in figure 21. One of the advantages of higher level PWM generation is that there is less of a voltage swing from the minimum and maximum of each step, which results in less power loss due to the slope up and down for each step (known as dV/dt losses). This reduced power loss results in higher efficiency for the inverter. This increased efficiency must be considered in balance with the addition of components and frequency effects which must be filtered out.

The frequency plot of the 5-level PWM technique can be seen to be improved over that of the 3-level scheme (figure 22). The harmonic frequencies are reduced, as in the 3-level technique, but the magnitude of the primary is significantly larger. Note that these plots show only harmonics of the 60Hz primary, and thus do not show the effects of the switching frequencies. The improvement of the 5-level PWM can, however, still be seen in the difference of the primary frequency's magnitude.

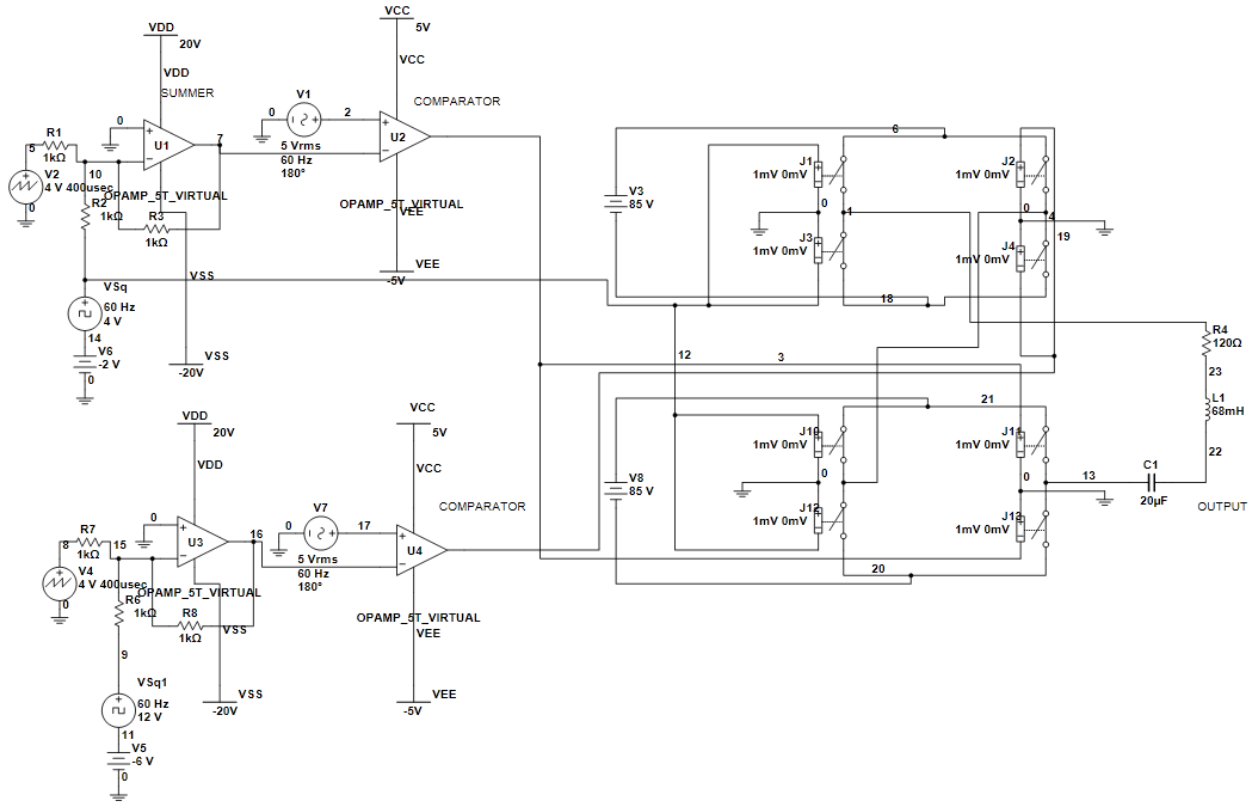

Figure 17:5-Level PWM Simulation Circuit

As can be seen in figure 15, the 5-level PWM circuit requires two isolated voltage sources, shown here as 85V DC sources, which can be added in series. A single 170V bus could not be used, as to connect it as we have here, the H-Bridges would be in parallel.

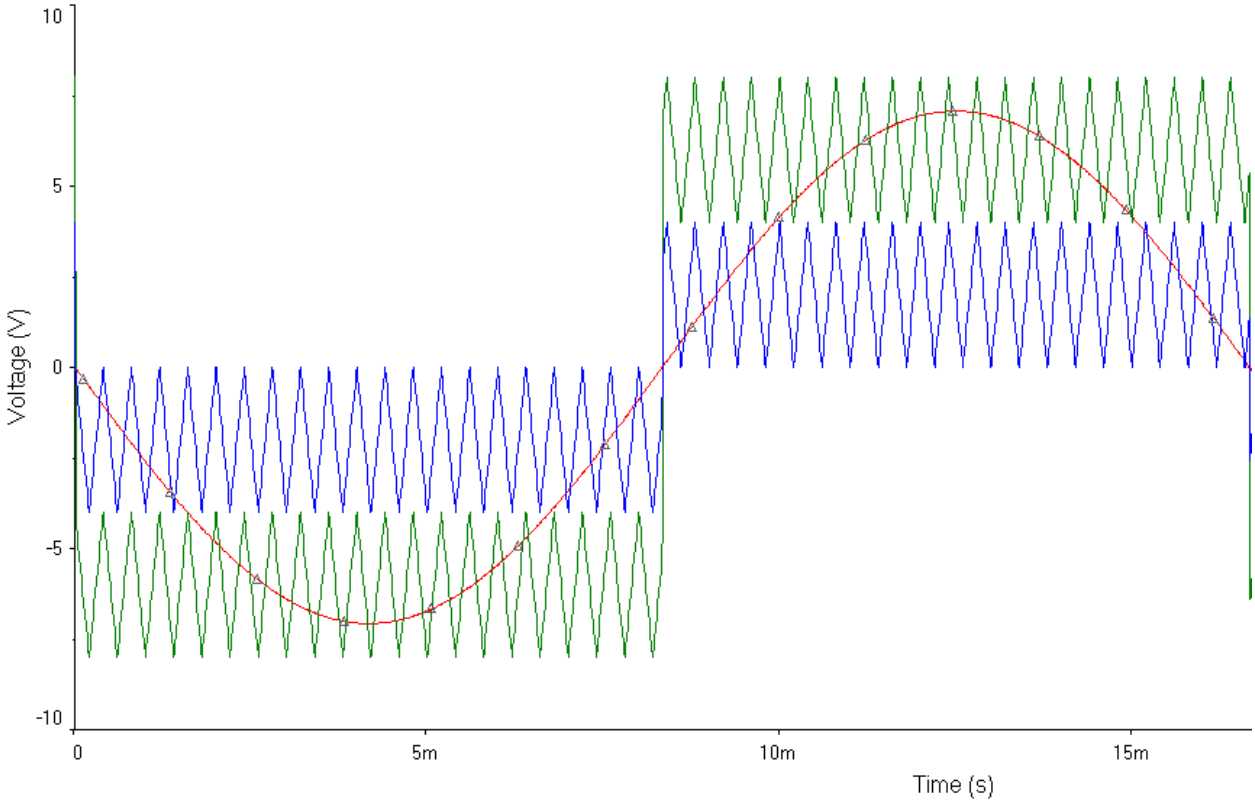

Figure 18: 5-Level PWM Comparison Signals

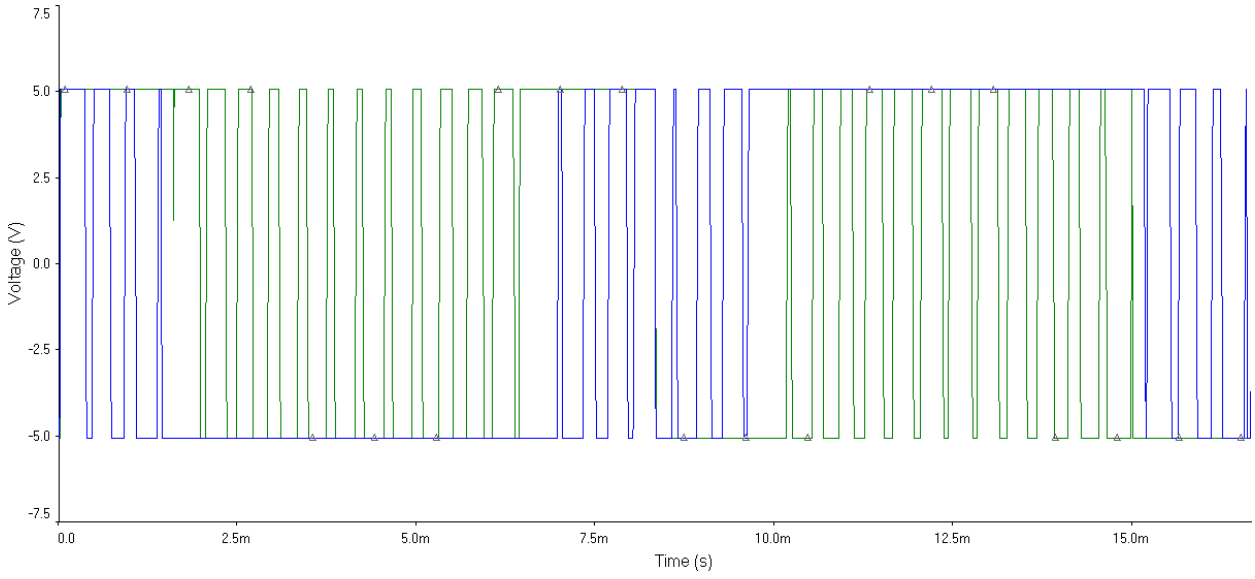

Figure 19: PWM Bridge Control Signals (superimposed)

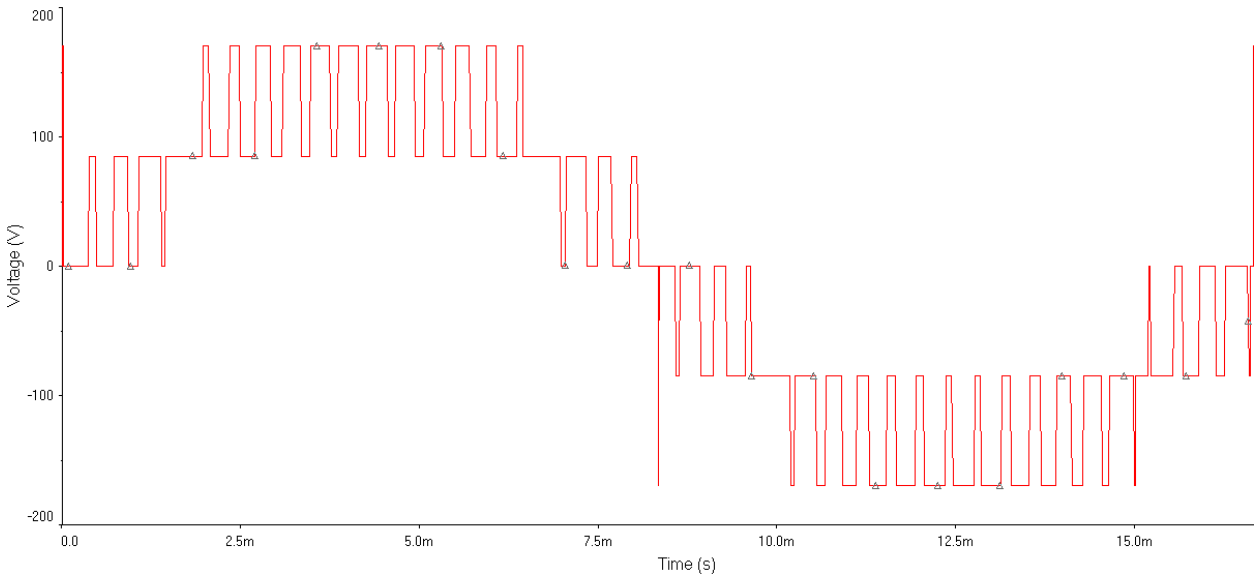

Figure 20: 5-Level PWM Output (unfiltered)

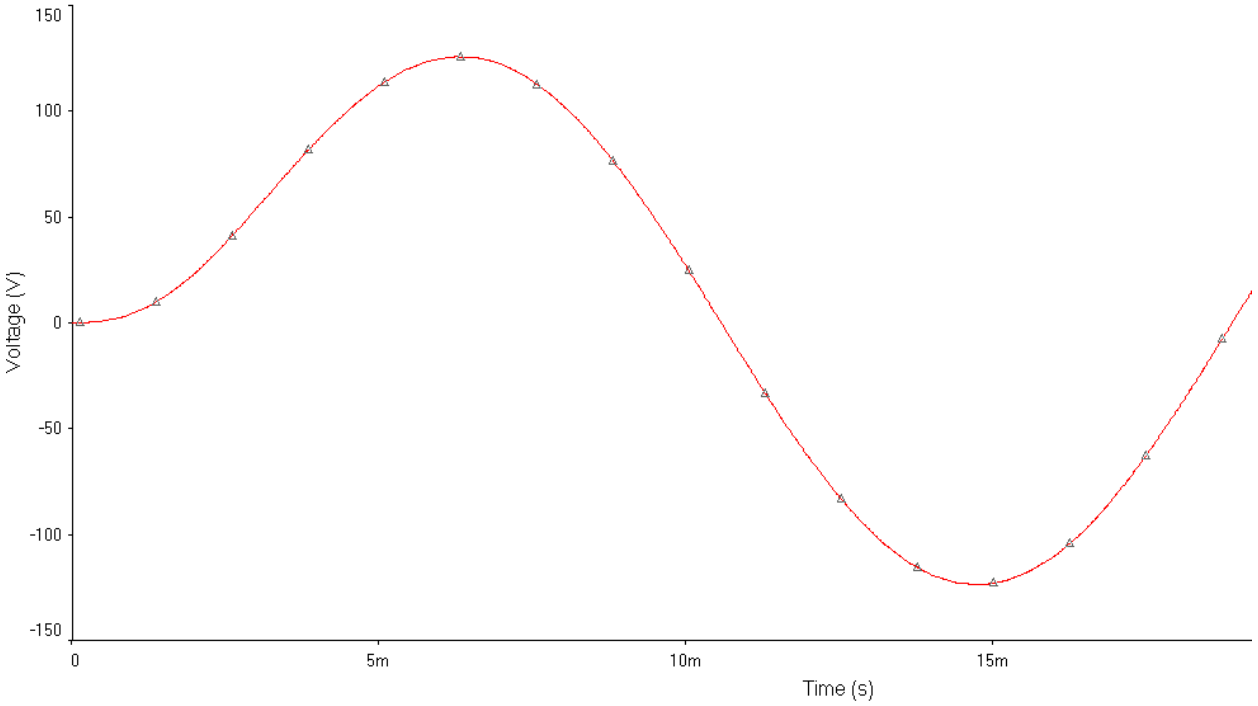

Figure 21: 5-Level PWM Output (filtered)

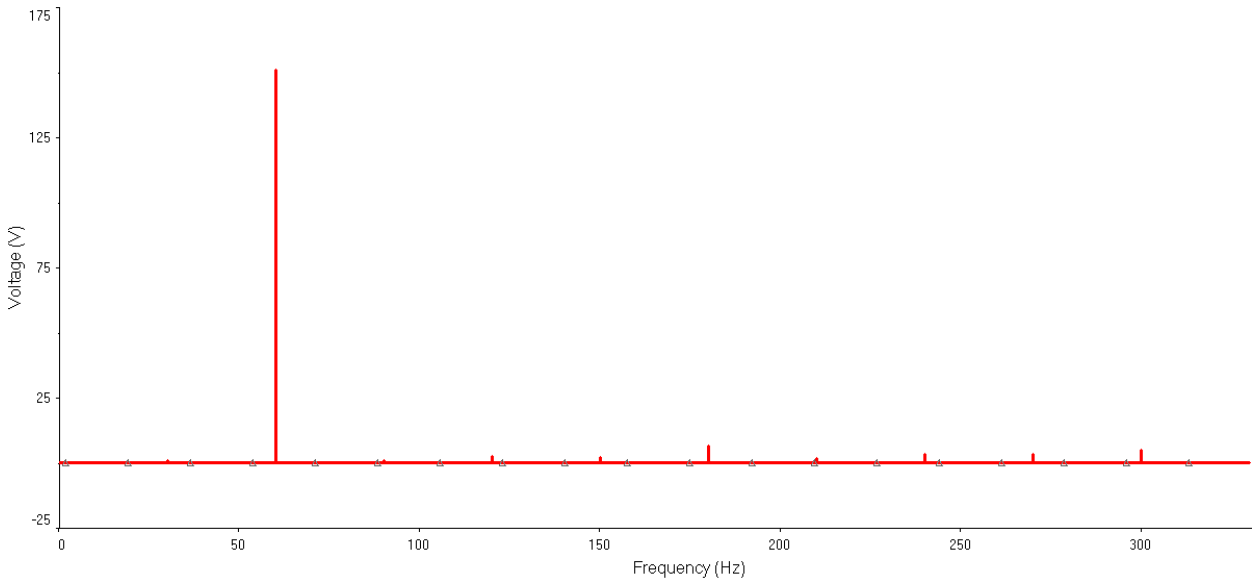

Figure 22: 5-Level PWM Harmonics Analysis of Unfiltered Output

The major downside of 5-plus level PWM designs is that it requires many more components to implement, with multiple DC voltage rails which must be placed in series. For our purposes, then, such a design is impractical and expensive. Though the potential advantages of these higher-level systems are certainly intriguing, this project focused on 3-level PWM as a balance between cost and efficiency.

IGBTs vs. Power MOSFETs

While designing this circuit, a choice had to be made between the two main types of switches used in power electronics. One is the power MOSFET, which is much like a standard MOSFET, but designed to handle relatively large voltages and currents. The other is the insulated gate bipolar transistor, or IGBT. Each has its advantages, and there is a high degree of overlap in the specifications of the two.

IGBTs tend to be used in very high voltage applications, nearly always above 200V, and generally above 600V. They do not have the high frequency switching capability of MOSFETs, and tend to be used at frequencies lower than 29kHz. They can handle high currents, are able to output greater than 5kW, and have very good thermal operating ability, being able to operate properly above 100 Celsius. One of

the major disadvantages of IGBTs is their unavoidable current tail when they turn off. Essentially, when the IGBT turns off, the current of the gate transistor cannot dissipate immediately, which causes a loss of power each time this occurs. This tail is due to the very design of the IGBT and cannot be remedied. IGBTs also have no body diode, which can be good or bad depending on the application. IGBTs tend to be used in high power applications, such as uninterruptible power supplies of power higher than 5kW, welding, or low power lighting.

Power MOSFETS have a much higher switching frequency capability than do IGBTs, and can be switched at frequencies higher than 200 kHz. They do not have as much capability for high voltage and high current applications, and tend to be used at voltages lower than 250V and less than 500W. MOSFETs do not have current tail power losses, which makes them more efficient than IGBTs. Both MOSFETs and IGBTs have power losses due to the ramp up and ramp down of the voltage when turning on and off (dV/dt losses). Unlike IGBTs, MOSFETs have body diode.

Generally, IGBTs are the sure bet for high voltage, low frequency (>1000V, <20kHz) uses and MOSFETs are ideal for low voltage, high frequency applications (<250V, >200kHz). In between these two extremes is a large grey area. In this area, other considerations such as power, percent duty cycle, availability and cost tend to be the deciding factors.

Our application in this project is 250W, with a 170VDC bus (ideally), and a switching frequency around 20kHz. These specifications make power MOSFETs the ideal choice for us. If our system was a larger, commercial application with a high power output, IGBTs would be the choice.

Amplitude Modulation

In PWM generation, two very important characteristics are m_a and m_f, where m_f is the ratio between the frequency of the triangle wave to the sine wave signal, and is generally an odd integer. This number is significant in that it determines the frequency of the harmonics in the PWM output signal. The significant components of this output are the primary, the harmonic at frequency m_f*f_c where f_c is the frequency of the sine wave control (as well as the primary output), and the harmonics at $m_{f+2}*f_c$ and $m_{f-2}*f_c$. M_f, therefore, determines the frequency of the harmonics of the output, which of course affects how easily they can be filtered out.

M_a is the ratio of the amplitudes of the sine wave and the triangle wave, and is always kept between 0 and 1, as a value above 1 will result in clipping and non-linear amplitude relationships. Between 0 and 1, though, the amplitude of the primary is linearly related to m_a. As the m_a ratio decreases, the amplitude of the primary also decreases. At the same time, though, the amplitude of the harmonics increase, and the m_f harmonic actually becomes larger than the primary just above 0.8 m_a.

Table 4: Normalized Fourier Coefficients[6]

M_a	1	0.9	0.8	0.7	0.6	0.5	0.4	0.3	0.2	0.1
N=1	1	0.9	0.8	0.7	0.6	0.5	0.4	0.3	0.2	0.1
$N=m_f$	0.6	0.71	0.82	0.92	1.01	1.08	1.15	1.20	1.24	1.27
$N=m_{f\pm2}$	0.32	0.27	0.22	0.17	0.13	0.09	0.06	0.03	0.02	0.00

In an unfiltered output, this can be very bad, especially if the load is not inductive. If there is a large inductive component, though, this will act as a low-pass filter, as the impedance will be very large as long as your triangle wave's frequency is also very high, since $Z_L=\omega L$. This can be further resolved by filtering your output with an added low-pass filter.

In order to test the bipolar PWM, we created two test circuits. The first is a virtual bipolar PWM circuit with an H-Bridge, which was operated with a bus voltage of 100V (the figure shows the configuration for the fourier comparison, i.e. 2V bus). The triangle wave signal was 2V in amplitude with a frequency of 20kHz. The sine wave signal was held at a constant 60Hz, but the amplitude was varied from 0.1414 to 1.3435 Vrms to vary the m_a of the system from 0.1 to 0.95. The filtered waveform at each value was then displayed. The individual waveforms were then combined into one graph for easy comparison. It should be noted that the magnitude of the waves decreased as m_a was decreased, but the wave-forms on the graph are normalized to magnitude, to show only the distortion present in the filtered output.

[6] (Hart, 2010)

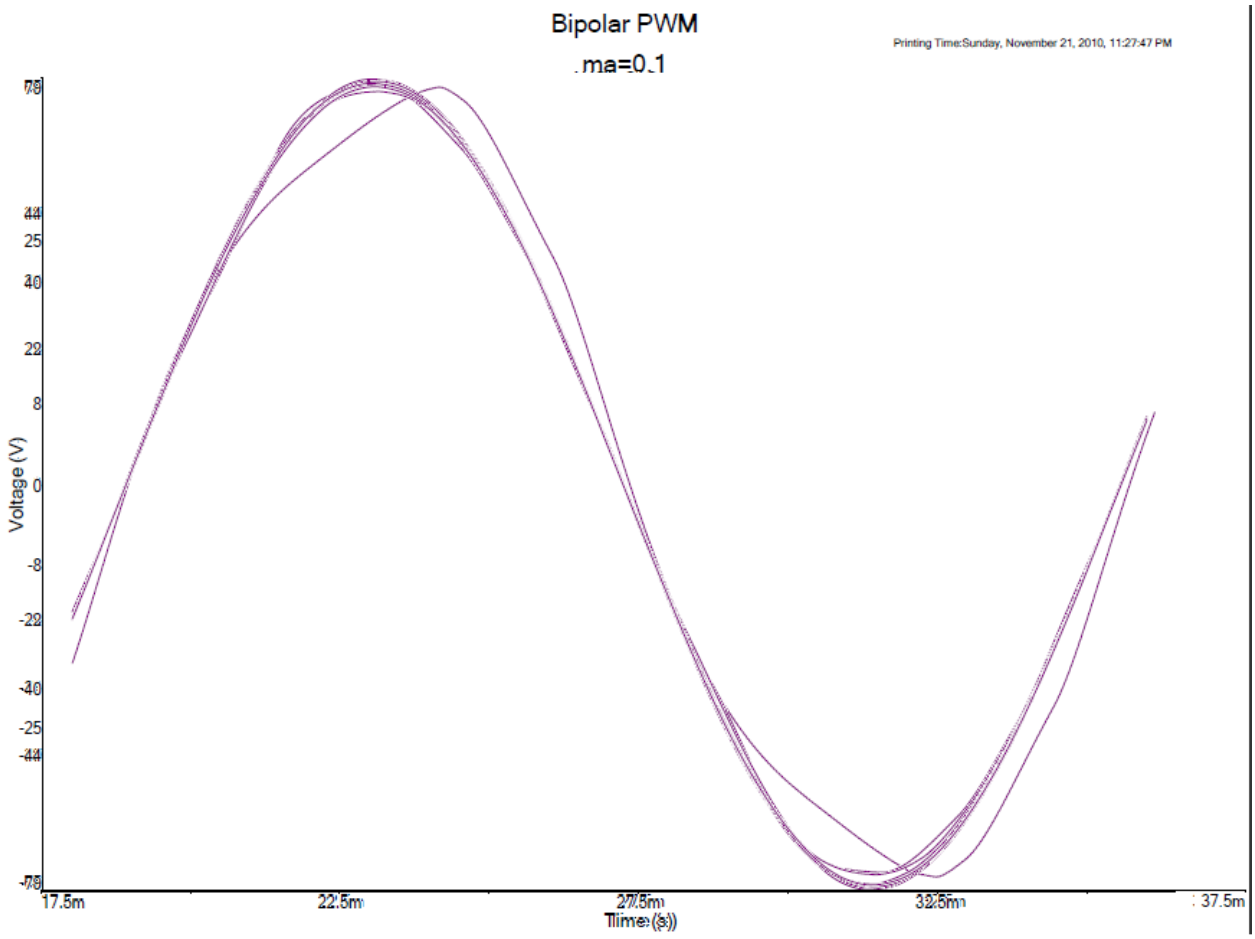

Figure 23: Filtered Outputs ma 0.1 to 0.95

There is no significant distortion of the filtered output even at very low values of m_a. There is some distortion at 0.3, 0.2, and 0.1, but it is not overwhelmingly large. The main downside of a low m_a, then, is the additional power loss of the harmonics in the filter. Because the impedance of the inductor in the filter becomes much higher at the harmonic frequencies, though, the currents involved in these losses are small.

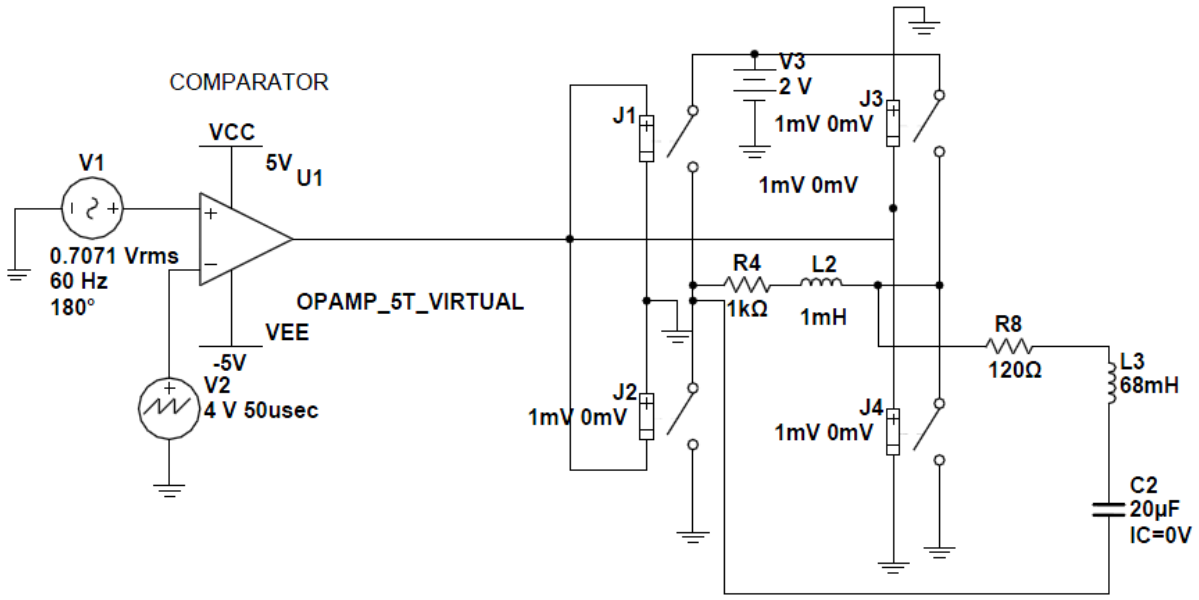

Figure 24: Bipolar PWM Test Circuit

If we implement a 3-level PWM circuit in our final design, the effect on the output of having a low m_a would be much reduced. In 3-level PWM, the present non-primary harmonics are much higher frequency, and are, in fact, higher than the switching frequency at $2m_{f\pm1}$, $2m_{f\pm3}$ and so on. This drastically reduces the total harmonic distortion of the output sine wave, and if the output is filtered, reduces the size of the filter components drastically as well. In addition, because the impedance of the inductor will be higher for the harmonics, the power losses will be even smaller.

H-Bridge Components and Power Losses

IRFP460A MOSFET

In order to move from theory to implementation, we needed to identify specific components for our design. First, we needed to determine what MOSFETs we wanted to use. We know that in an H-bridge, the highest voltage a single MOSFET that is off will experience is double the voltage of the DC power rail, which in our case is 2*170=340V. We want to have a healthy safety margin above this voltage as well, with doubling the value being a good idea. A rated voltage of 500-600V is therefore a good target for our MOSFETs. In addition, we are going to be providing approximately 250W for our output, which will be a 120Vrms sine wave. This means that the max rated current we should have coming out of our inverter will be 2.083A. We should certainly overshoot this value by some healthy margin, and in some ways our eventual choice was a little more than we need but if availability, cost, and other considerations allow this, it's not necessarily a bad thing. Our PWM output signal will switch at a frequency of 40kHz, which means our MOSFETs need to be relatively fast-switching as well. Eventually, we determined that the IRFP460A n-MOSFET will be sufficient for our design. The IRFP460A is rated at 500V, 20A, and is fast switching, with a t_{on} time of 55ns and a t_{off} time of 39ns.

IR2304 MOSFET Driver IC

In order to drive our MOSFETs in our H-Bridge, we used a MOSFET driver IC, specifically designed for driving a half-bridge. After considering various IC options, our choice was the IR2304, which is rated at 600V, with a gate driving current of 60-130mA and a gate driving voltage of 10-20V. The turn on and turn off times are equal, at 220ns, and the chip has a 100ns built-in dead time to prevent having both switches on one side of the H-bridge conducting at once, which is a good backup to prevent short circuit. The input and output diagram of our driver is shown below in figure 25.

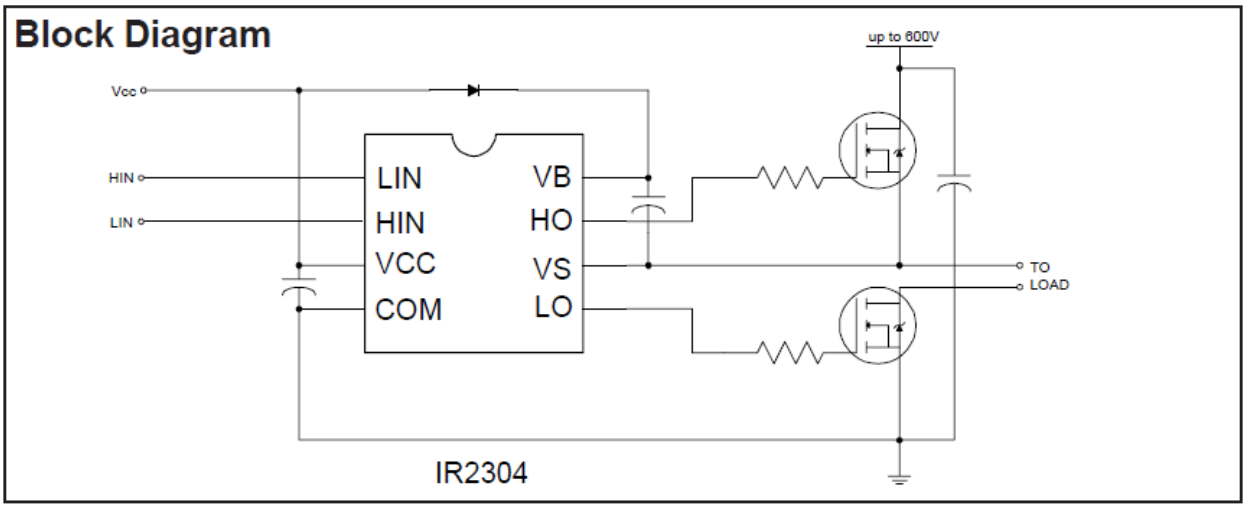

Figure 25: IR2304[7]

The capacitor shown between V_B and V_S is the bootstrap capacitor. This cap is required to keep the top n-MOS switch gate voltage higher than the source rail of 170V. The value for this cap can be found using the equation shown below, taken from IR document AN-978[8], and values from the MOSFET data sheet.

$$C \geq \frac{2\left[2Q_g + \frac{I_{qbs(max)}}{f} + Q_{Is} + \frac{I_{Cbs(leak)}}{f}\right]}{V_{cc} - V_f - V_{LS} - V_{Min}}$$

The values substituted into this equation were found either in our driver datasheet, our MOSFET datasheet, or in our circuit specifications. Q_g is the MOSFET gate charge, which is 105nC[9]. I_{qBS} is the driver quiescent current, which is 150uA. I_{LS} is the capacitor leakage current, approximately 250uA here, and Q_{IS} is 5nC. The frequency is 40kHz, and our V_{cc} supply voltage will be 10V. V_f will be zero, because we don't have an external diode in this configuration, and V_{LS} is the forward voltage of the MOSFETs,

[7] (International Rectifier, 2004)
[8] (International Rectifier, 2007)
[9] (International Rectifier)

which is 1.8V. Finally, V_{min} is the minimum difference between V_b and V_s, given as 0.3V in the datasheet. Using these numbers, we can calculate the minimum bootstrap capacitance value.

$$C \geq \frac{2[2 * 105nC + \frac{150\mu A}{40kHz} + 5nC + \frac{250\mu A}{40kHz}]}{10V - 0V - 1.8V - 0.3V} = 55.69nF$$

Power Loss and Heat

In order to determine the efficiency of our H-Bridge, and especially to determine the proper heat sink requirement for our design, we must first calculate of the power lost through each MOSFET while conducting, and due to switching. We will also compare the power loss of our final switching design to the more standard switching technique described in the background section, in order to identify the advantages and disadvantages of each design. First, we will calculate the power loss in the typical design, which has a fast switching PWM driven half-bridge, and a 60Hz square-wave driven half-bridge.

Typical PWM

In this typical design, the power losses through one half-bridge will be very different than that of the other half. Both MOSFETs in each half-bridge are switched constantly, but at very different rates. In the PWM-driven half-bridge, the switching can be approximated to be 50%, as the PWM wave will range from very high duty cycle to very low duty cycle, but it will do so symmetrically around the 50% rate, and therefore the average duty cycle will be 50%. The energy loss due to a single switching is found using the equation:

$$W_{on} = 0.5VIt_{on}$$

The voltage in this relationship is the maximum voltage a given MOSFET will experience, which will be when it is off, and sees the 170V rail on one side, and -170V on the other, meaning the value for the equation will be 340V. The current we expect to see through the MOSFETs while on can simply be found with our power rating of 250W. With a voltage of 120Vrms, we would expect to see a current of 250/120=2.083A. The time it takes for the switch to go from off to on, t_{on}, can be found in the data sheet, and for our IRFP460A, the value is t_{on}=55ns. These values together give a W_{on} of 19.47µJ. The calculation of the off switching losses are identical, simply replacing t_{on} with t_{off}=39ns, which gives W_{off}=13.81µJ. Because these two values are the switching losses for each single switch from one state to the other, the total loss per cycle can be found by simply multiplying these values by the number of

switches in a period. Assuming, as previously discussed, that the PWM has an average duty cycle of 50%, there will be one switch off and one switch on per switching period. The switching frequency of the PWM half-bridge is 40kHz, which means that the MOSFETs will switch, on average, 40,000 times a second each high and low. The energy lost per second of operation, then, is 40,000*(W_{on}+W_{off}), which is 1.331J/s=1.331W per MOSFET from switching. The other half-bridge switches at a rate of 60Hz, but otherwise has the same loss per switching, which means it's losses are 60*(W_{on}+W_{off})=1.997mW per MOSFET, which is drastically lower. This scheme has the obvious disadvantage, then, of splitting its switching losses between the two bridges, with most of the heat generation being on two MOSFETs, with the other two barely taxed at all.

The power loss from conduction will be the same for the two half-bridges, as the square wave has a duty cycle of 50%, and the PWM has an average duty cycle of 50%. The loss due to conduction per cycle is given by the relationship:

$$W_{Con} = V_{CE} I(DT)$$

where V_{CE} is given by the IRFP460A data sheet as 1.8V, the current is the previously calculated 2.083A, the duty cycle is 50% and the period is 1/Fs. Because we're interested in losses per second, we can simply drop the T from the equation (since we would be multiplying it by the switching frequency). This gives W_{cond}=1.87J per second, which means it has a power loss of 1.87W per MOSFET. In this scheme, then, each MOSFET on the PWM half-bridge will have a power loss of 1.87+1.331=3.21W, and each MOSFET on the slow side will have a power loss of 1.87+0.0019=1.88W, slightly more than half that of the fast-switching MOSFETs. The PWM half-bridge as a whole has a power loss of 6.42W, and 3.76W on the low-speed side. The entire H-bridge, therefore has a power loss of 10.18W.

Our Design

In our signal design, the load is spread more equally upon each of the MOSFETs in the two bridges. As previously described, each gate in our design switches is driven by PWM for half of each 60Hz period, and is held high for the other half, in the case of the low gates, and held low for the other half, in the case of the high gates. The switching losses will therefore be the same for each gate, and will be the same as the losses of the PWM-driven gates in the previous description, but will be only for a half-cycle. The losses from switching for each gate, therefore, will be 0.5*(40,000*(W_{on}+W_{off}))=1.331/2=0.665W per Mosfet. The losses due to conduction will be different for each half-cycle for each MOSFET. During the PWM-driven stages, the conduction losses will be the

same as those of the PWM-gates in the traditional implementation. For the other half-cycle, the high gates will be off, and the low gates will be on. The average duty cycles will therefore be 25% for the high gates, and 75% for the low gates. Using the same relationship given above, the power loss will be 1.8*2.083*0.25=0.937W for the high gates and 1.8*2.083*0.75=2.812W for each low gate.

The overall losses for each gate will be $W_{switch}+W_{cond}$, which will be 0.665+0.937=1.602W for each high gate, and 0.665+2.812=3.477W for each low gate. The losses for each half-bridge will be 1.602+3.477=5.079W, and 10.158W overall for the H-Bridge. Compared to the original scheme, the overall power losses are nearly identical. The difference is simply how this power is spread. In the original design, the switching losses were concentrated entirely in the two PWM-driven MOSFETs, whereas in our design the switching is spread equally across the entire bridge. To some degree, this is counteracted by the concentration of more conduction losses in the two low MOSFETs, so there are some disadvantages to both schemes. In an eventual PCB implementation, the two MOSFETs of each half-bridge would be adjacent to each other, so spreading the power losses across the two half-bridges will aid in dissipating the heat generated.

To determine the correct heat sinks to use in any final implementation of our design, we must complete a thermal analysis of our H-bridge, using the power losses we calculated above. The relationship we will use to do this is ΔT=P(Rθ)

$$\Delta T = PR_\theta$$

where ΔT is the allowable range of temperatures, P is the power lost through the MOSFET, and R_θ is the thermal characteristic of the MOSFET/heat sink system. First, we will assume that the ambient temperature will be 27°C, which is the high range of room temperature. The maximum operating temperature given in the MOSFET data sheet is 150°C, meaning ΔT=150-27=123°C. For our power value, we will err on the side of caution and use the higher of the two values, which is that of the low gates, for which P=3.477W. Rθ can be broken down into $R\theta_{JC}$, $R\theta_{CS}$, and $R\theta_{SA}$. The first two values are inherent to the MOSFET and are given by the data sheet as 0.45 and 0.24°C/W, respectively. The third value will be a property of the heat sink, and is the value for which we must solve. Using the relationship given,

$$123°C = 3.477W(0.45 + 0.24 + R_{\theta SA})$$

Solving this equation gives a maximum value of $R\theta_{SA}$ =34.68°C/W for our heat sink.

Filter Components

Our output of our H-bridge is ideally a 60Hz sine wave with a V_{rms} of 120V. Because it is encoded using a 40 kHz PWM signal it must be filtered. Due to the high voltage of our output, the only option is a passive filter, which is an inductor and capacitor in series, with the load connected across the capacitor. In our implementation, we desired a cut-off frequency comfortably below our switching frequency and above our ideal 60Hz output. In an LC filter, the cutoff frequency is given by the relationship

$$f_c = \frac{1}{\sqrt{LC} * 2\pi}$$

Using a capacitor of 15µF and an inductor of 33µH, we obtain a cutoff frequency of 7.153 kHz. We also needed components which are capable of handling the rated voltage and current output of our system, so we needed an inductor which could handle at least 2A, and a capacitor which could handle at least 170VAC. To this end, we chose the 1140-150K-RC inductor, which is rated for 27A and the 495-2965-ND Capacitor, which is rated for 275VAC, well above our requirements.

Control Signal Generation for 2-Level PWM

The theory of encoding a sine wave with a PWM signal is relatively simple. A sine wave is needed for the reference that will dictate the output, and a triangle wave of higher frequency is needed to sample the reference and actuate the switches. Generally, op-amps are used in generating sine waves, as they are in this project, but the process can also be done with a microcontroller with crystal oscillators. Within the vast library of op-amp circuits, more than one can serve as a sine-wave oscillator.

A Stable Operation Voltage

Signal generation begins with the power supply for the op-amps and IC's. As a battery's stored energy depletes, its voltage is reduced. Several of the amplifiers in the control signal generation circuits rely on the rail voltages to charge and discharge capacitors which cause a controlled oscillation. If V_{CC} and V_{EE} on the op amps vary during operation, so will the amplitude and frequency of the reference sine wave and sampling triangle wave.

The solution comes in the form of a linear voltage regulator. There are other types of voltage regulation, mainly switching regulators, but their benefits are of little use in powering op-amps and driver chips. Switching regulators are more efficient than linear regulators and they have the ability to boost voltages, but the supply voltage is well-defined and the op-amps require very little power relative to what a sealed lead acid (SLA) car battery can provide. Thus, the low ripple and simple connection scheme of a linear regulator is favored in this design.

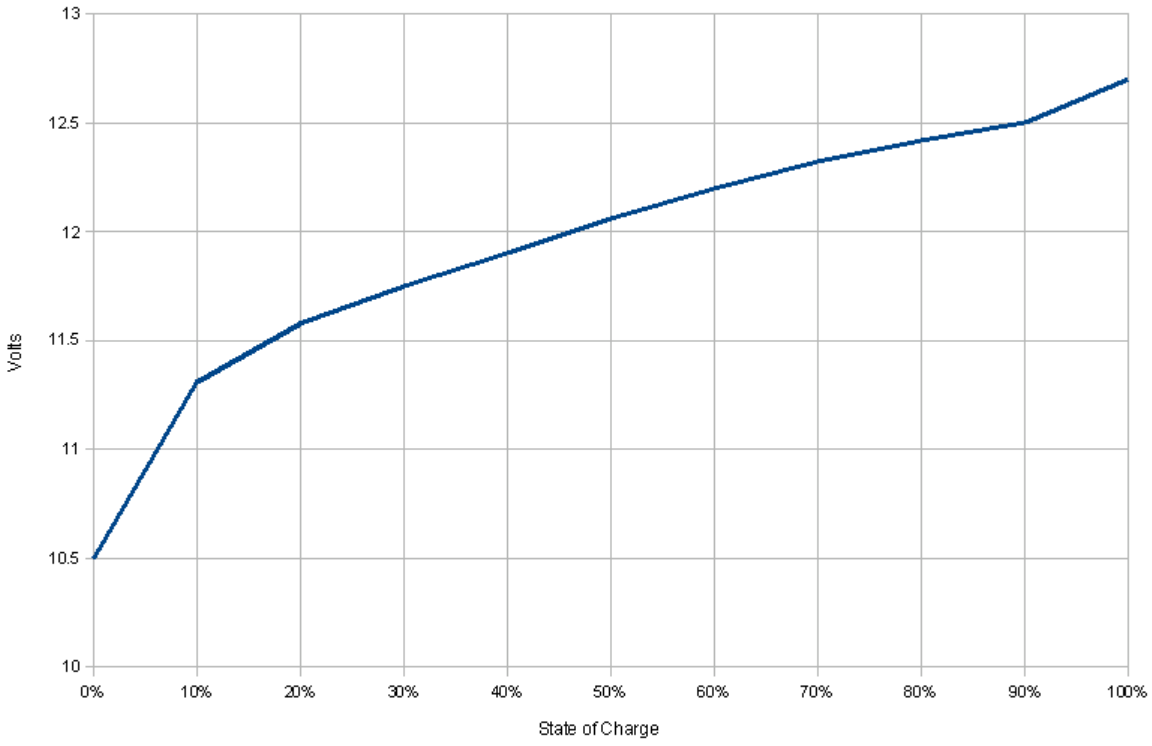

Figure 26: Voltage vs. State of Charge of a Sealed Lead Acid Battery[10]

The lowest assumed supply voltage for our design is 10.5 Volts. With a targeted nominal voltage of 10 Volts to operate the op-amps and MOSFET's, we plan to use a low-dropout (LDO) linear regulator such as the ROHM Semiconductor BAJ0BC0T 10V LDO that will ensure regulation down to V_{out} + .5V. Currently an LM317 adjustable regulator is used for prototyping purposes, as they are readily available. The LM317 works by maintaining a band gap voltage reference (about 1.25V) between its adjustment and output terminals. While this IC is working to maintain stable signal generation under a changing supply voltage, it can only do so with an adequate supply voltage. The dropout voltage of the LM317 depends on load current, and it ranges between 1 to 2.5 volts. On the test bench the LM317 was sourcing about 50 milliamps for all the op-amps and comparators, so the regulator failed to provide 10V when the bench supply was turned down to about 11.8V.

[10] (Deep Cycle Battery FAQ, 2009)

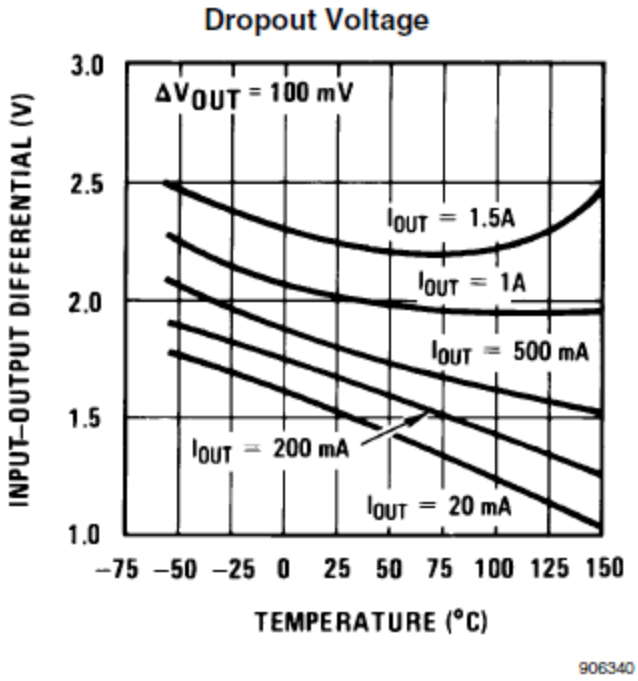

Figure 27: Dropout Voltage of the LM317 [11]

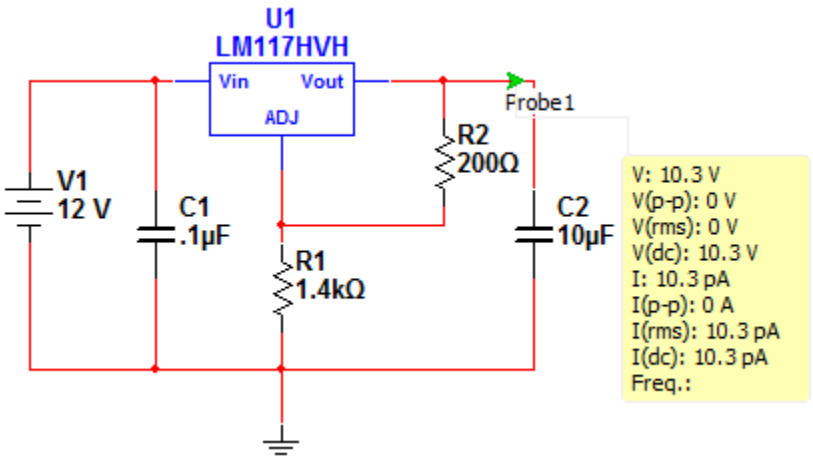

Figure 28: Voltage Regulation Circuit

[11] (National Semiconductor Corporation, 2011)

Triangle Wave Generator

The triangle wave generator is a Schmitt-trigger oscillator composed of a Schmitt trigger and an integrator, though it has a semi-regulated input voltage to the integrator with the addition of the 1N4154 fast-recovery clamping diodes. The equation for the frequency of oscillation is:

$$f = \frac{V_{diode}}{V_{sat+}} * \frac{R_3}{R_2} * \frac{1}{4R_{12}C_1}$$

It should be noted that a major source of error is the diode forward voltage which dictates the charge rate of C_1. It depends on the current-limiting resistor R_1 and, to some extent, temperature. The best option for determining this was to simulate or measure directly.

It also follows that the peak output voltage of the triangle wave should be:

$$V_{peak} = V_{sat+} * \frac{R_2}{R_3}$$

A high-pass filter is added to the circuit to eliminate the DC offset so that the triangle wave will be offset to the same voltage as the sine wave it is compared to.

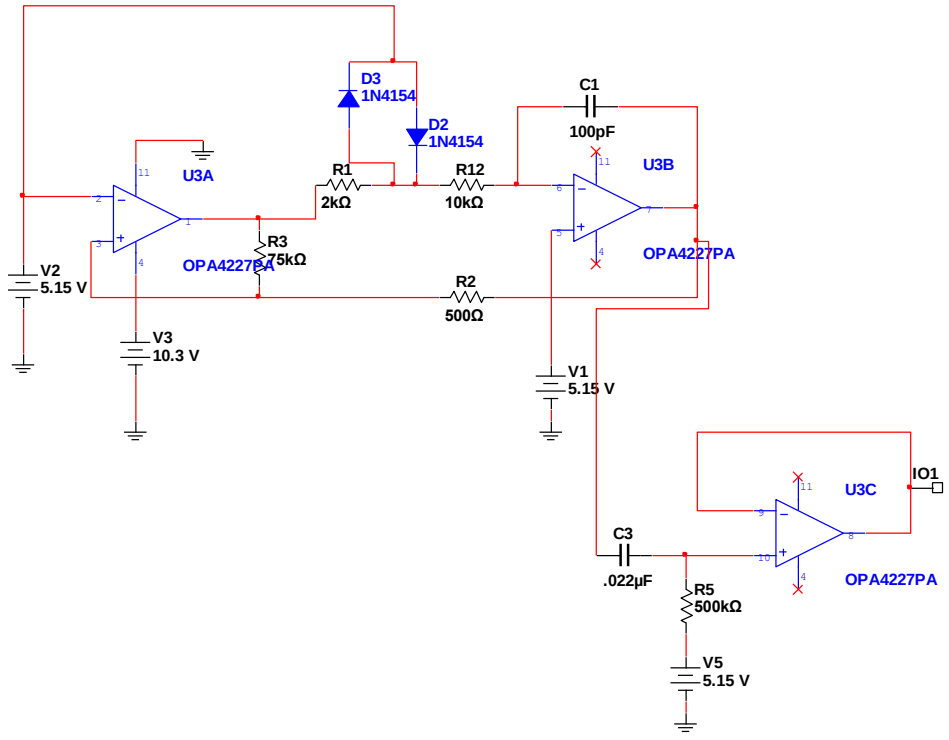

Figure 29: Triangle Wave Generator Circuit

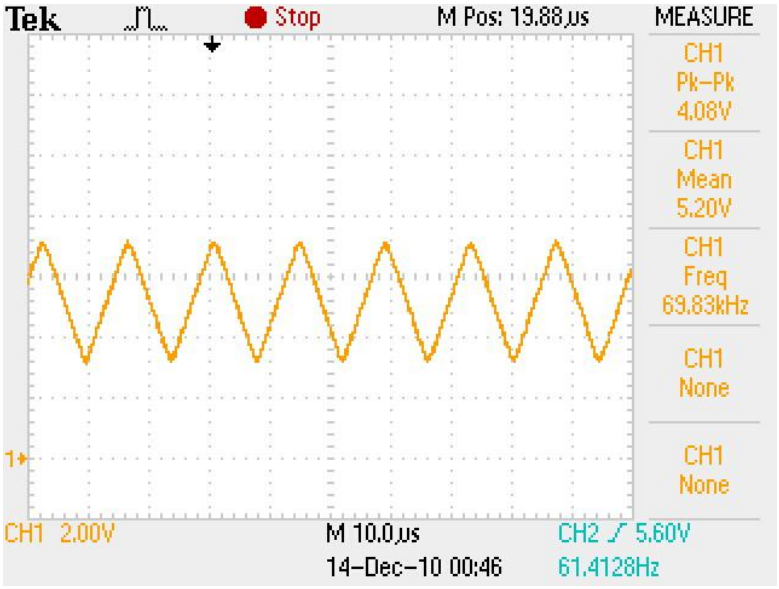

Figure 30: Output of the Triangle Wave Generator

Sine Wave Generator

Two different techniques for generating a 60 Hz reference sine wave were attempted, though both efforts were based on filtering a Schmitt-trigger oscillator (a square -wave generator). Since a Schmitt-trigger oscillator can produce a square wave by having a symmetric stimulus (such as a sine wave), a low-pass filter can produce a sine wave by filtering the harmonics and leaving the fundamental frequency alone. The spectral components of a square wave consist of a fundamental frequency that is the same as the square wave frequency, and all the odd-numbered harmonics multiplied by 1/k where k is the number of the harmonic. A low-pass filter with poles placed at the fundamental frequency can mitigate much of the harmonics, leaving a sine wave with about 2% THD, a figure deduced from simulation.

The circuit that generates the sine wave is composed of a Schmitt trigger oscillator and a fourth-order Butterworth Low-Pass active filter with a Sallen and Key topology. The whole circuit is made with a single LM348 (a quad 741 chip) and some passive components. The Schmitt trigger is basically a comparator with hysteresis. The non-inverting input voltage is a superposition of the input signal through the resistive divider (R4+R6) and the output of the amplifier through the resistive divider on the

non-inverting terminal. As the open loop gain of the LM348 is very high (104 dB) it will try to amplify the difference between the terminals to very high voltages, but the reality is that it will be limited to within the rails (V+ and V-). So, without negative feedback the op-amp will have two possible output states: V_- and V_+. The oscillation between output states is controlled by the resistor and capacitor on the inverting terminal. When the output is in its high state, the capacitor (C2) will charge through R7 until the voltage at the inverting terminal is higher than the non-inverting terminal. When it reaches that point, the Schmitt Trigger will change to its low state to allow the capacitor to discharge through R7. The cycle continues and the result is a square wave.

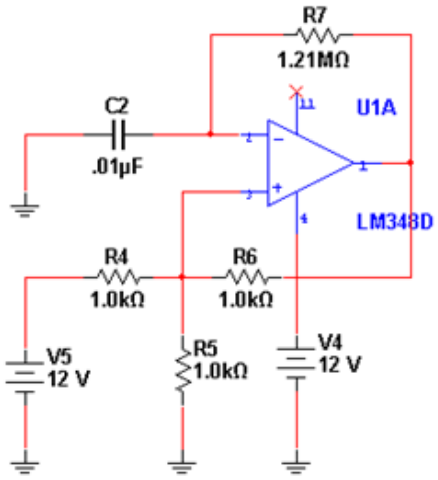

$V_+ = 6V * 1k/1.5k + V_o * 600/1.5k$

The possible non-inverting input voltages are 4V (from the input signal) + 4V (during the high state) or 4V + 0V during the low state. R and C are calculated from the half-period that it takes for the capacitor to go from the High to Low state, but the charge rate is the same.

$$4V = 8V\, e^{(-t/RC)}$$

$$.5 = e^{(-t/RC)}$$

$$.693 = t/RC$$

$$t = 1/60\ Hz / 2 = .0083\ s$$

Figure 31: Schmitt Trigger Oscillator

The low-pass filter is made using a Sallen and Key topology. Since the square wave is composed of a fundamental frequency sine wave (the same frequency as the square wave) and the odd numbered harmonics, a low pass filter can be designed to output just the fundamental sine wave by filtering out the harmonics. The current filter design provides a -40dB/decade drop off beyond 60 Hz and a -80dB/decade drop off beyond 100 Hz.

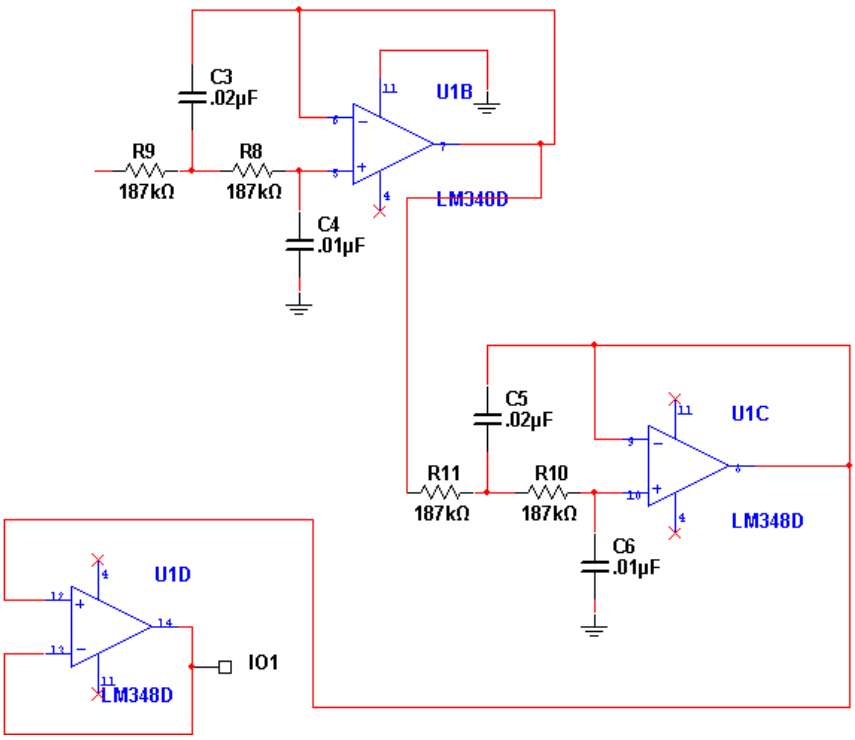

Figure 32: Butterworth Low-Pass Filter

$$\tan(45°) = \sqrt{\frac{C_3}{C_4} - 1} = 1$$

$$\frac{C_3}{C_4} = 2, C_3 = .02\ \mu F, C_4 = .01\mu F$$

$$2\pi(60Hz) = \frac{1}{R * \sqrt{.02\mu F * .01\mu F}}$$

$$R \approx 187k\Omega$$

$$\tan(45°) = \sqrt{\frac{C_5}{C_6} - 1} = 1$$

$$\frac{C_5}{C_6} = 2, C_5 = .02\ \mu F, C_6 = .01\mu F$$

$$2\pi(100Hz) = \frac{1}{R * \sqrt{.02\mu F * .01\mu F}}$$

$$R \approx 112k\Omega$$

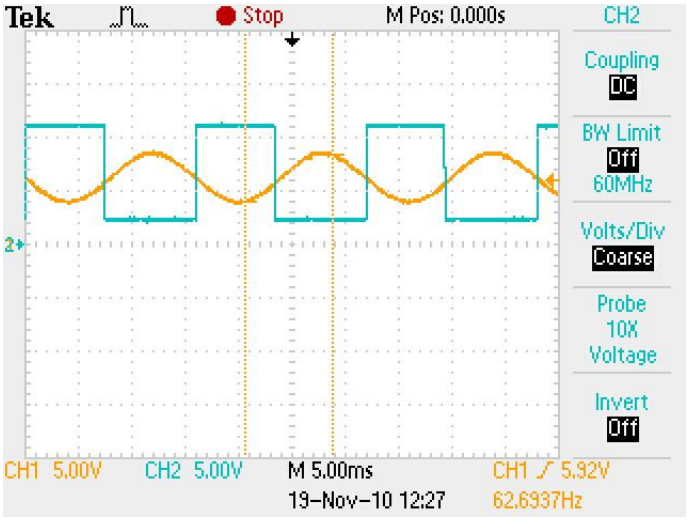

Figure 33: Square and Sine Waves from the Above Circuits

The output was as expected, an approximately 60 Hz sine wave. The 180 degree phase shift between the square and sine waves is from the filters, but that should not be a problem when controlling the switches. It appears as though the negative half-cycle on the square wave is longer than the positive half-cycle.

The shortcomings of the 741 amplifier are exposed. Firstly, it's slow. The slew rate affects the charge and discharge since the transition between charging and discharging is not instantaneous. Secondly, there is some input bias current that is causing some significant DC offset compared to our triangle wave. The worst offense to our attempt at a clean sine wave, though, is the asymmetric saturation voltages of the 741; the lowest its output can go with respect to the supply is not the same as the highest it can go with respect to signal ground. This is the reason for the longer negative swing on the output sine, compared to its positive swing. The revised sine wave generator replaces the LM348 with a TL084. It is faster in terms of slew, has less input offset current and is specified to have an output voltage that is 1.5V from either rail.

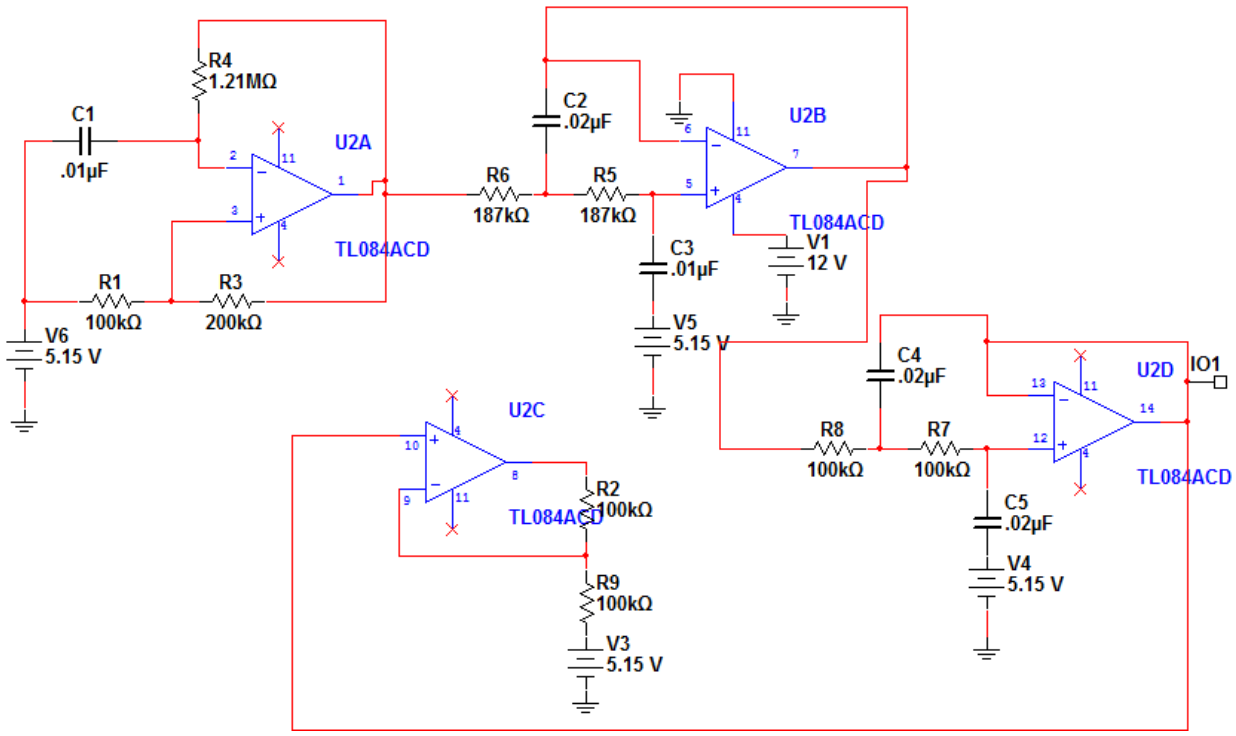

Figure 34: Revised Sine Wave Generator

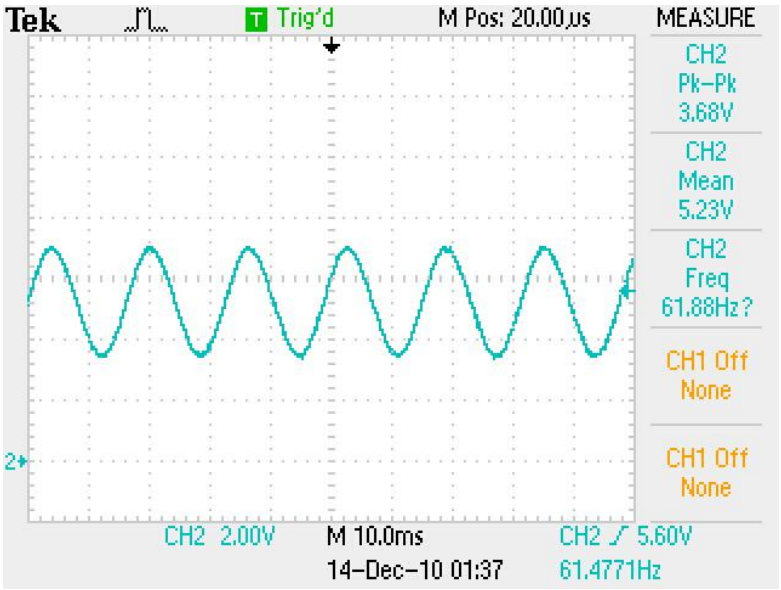

Figure 35: Sine Wave from the Revised Circuit

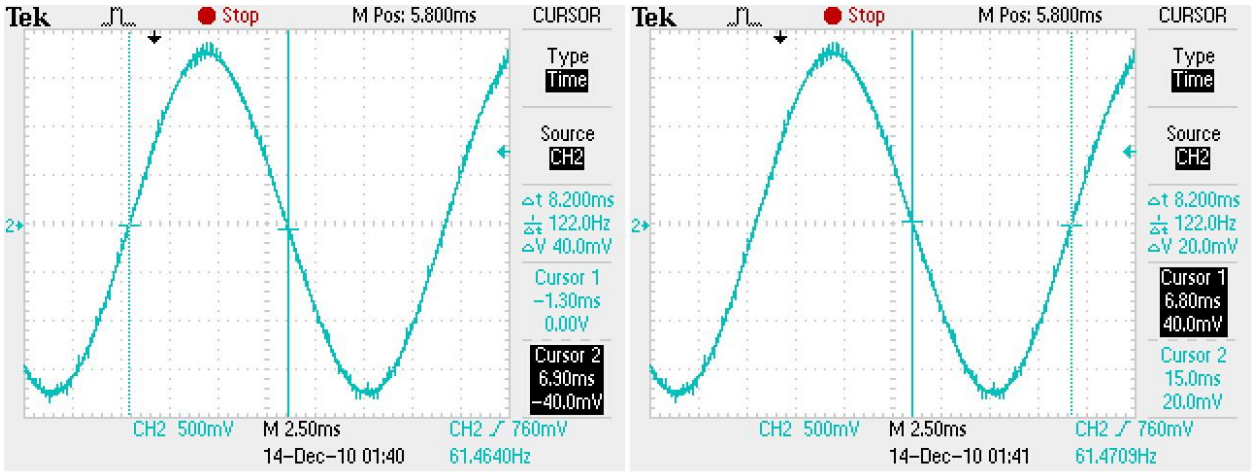

Figure 36: Comparison of Positive and Negative Swings of the 60 Hz Sine Wave

PWM Signal from Comparators

Sine wave inverters that utilize PWM for waveshaping have a comparator stage to generate the PWM signal. The high-frequency triangle wave is compared to the sine wave many times per sine wave cycle. The comparator output is a PWM signal whose duty cycle is related to how long the sine-wave amplitude is greater than the triangle wave. In other words, as the sine wave reaches its crest, the switching transistors are held closed longer to develop a greater voltage across the load.

The comparator used is a Motorola MC3302 that has four comparators per chip. The schematic for the MC3302 shows a differential pair driving a pull-down transistor. The differential pair amplifies the difference between its inverting and non-inverting inputs. The pull-down transistor is driven by the differential pair output. As soon as the transistor emitter becomes forward biased, it conducts current so that the entire source voltage (V_{CC}) drops across an external resistor. Since the load is connected in a common emitter configuration, the voltage to the load is approximately 0 volts when the inverting terminal is greater than the non-inverting terminal. Otherwise, the output is the full V_{CC}.

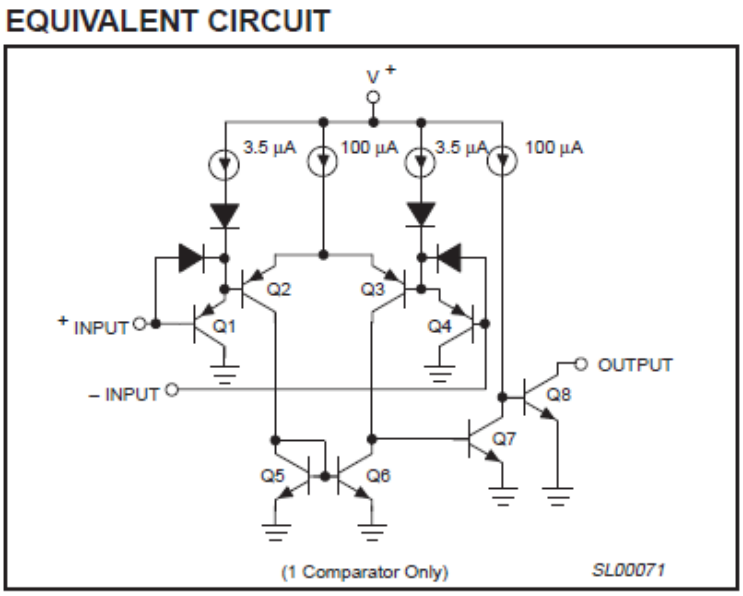

Figure 2. Equivalent Circuit

Figure 37: MC3302 Equivalent Circuit[12]

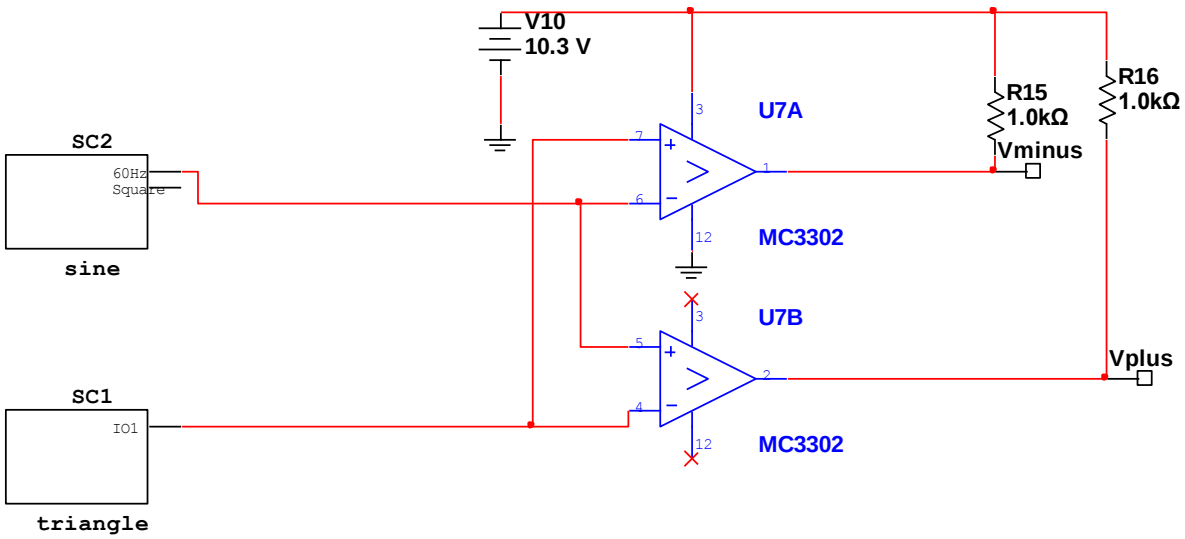

Figure 38: Comparator Circuit

In a two-level PWM system, one pair of switches is turned on to make current flow in one direction. For reference, this can be called the positive voltage direction. Alternately, another pair of switches allows current to flow in a direction opposite to the positive voltage direction. The four

[12] (Phillips Semiconductors, 1995)

switches form an H-bridge and it is in this manner that the two swings of the sine wave is generated across a load. As the reference sine wave approaches its crest, the PWM signal is dominated by the effect of the sine wave being greater than the triangle wave. Thus, the positive voltage direction switches stay on longer to develop the peak voltage of the sine wave. When the reference sine is at its minimum value (the valley) the PWM signal is dominated by the comparison of the triangle wave being greater than the sine wave most of the time. The result is a PWM signal that is the inverse of the positive voltage direction PWM signal. In application, we connected the signals to complementary inputs on two different comparators so that both waveforms are generated simultaneously to drive the N-channel MOSFET's of the H-bridge.

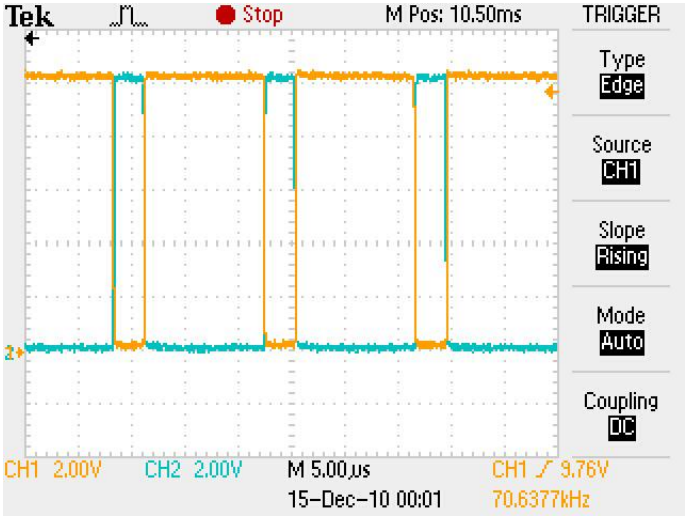

Figure 39 PWM Signals for Both Halves of the H-Bridge

One effect of having the reference sine wave amplitude less than the triangle wave amplitude is that the output will not reach the source voltage. This is called amplitude modulation, defined as the ratio of the amplitude of the reference wave to the sampling wave. In our circuit, we achieved an amplitude modulation of about 90%, meaning that the minimum time that the triangle wave will sample beyond the sine wave is 10% of the duty cycle. Since the switch duty cycle never reaches 100%, the peak voltage across the load will be a fraction of the source voltage. The consequence is that we need to have a source voltage greater than our desired peak voltage across the load.

At this point, we abandoned the 2-level PWM system in hopes of being able to implement a feedback system with a 3-Level PWM system while gaining switching efficiency.

Signal Generation for 3-Level PWM

The signal generation circuit for our 3-Level PWM centers around the use of the Texas Instruments TL494, a common PWM controller chip. The TL494 generates a PWM signal by comparing an internally generated saw-tooth wave with an error signal. Common applications for this chip are DC/DC converters, where an output voltage is programmed by resistors in the error feedback path that is referenced to some DC voltage signal. In make out DC/AC converter, we used the error amplifiers with no feedback from the output so that the error signal is the signal we want encoded in the PWM output.

Features of the TL494

Programmable Switching Frequency

The internal saw-tooth wave which samples the error input can be adjusted by connecting a resistor and capacitor to ground on the R_T and C_T pins (pins 4 and 5). In our application we, used single-ended output by connected the output transistors in parallel. For single-ended output (as opposed to a push-pull output transistor configuration), the switching frequency is determined by the equation $f = 1/R_T C_T$.

Two Error Amplifiers

Depending on design needs, up to two error signals can be used. As an example, one error signal can control the PWM to maintain the desired output while another can be used to limit current. A current sensing resistor would be used to convert current in to a voltage signal which could be compared to some reference threshold.

Minimum Dead Time (Maximum Duty Cycle)

By default, the maximum duty cycle of the PWM signal coming from the TL494 is 97%. This can be decreased by applying a voltage to the DTC pin (pin 4) under the following guidelines:

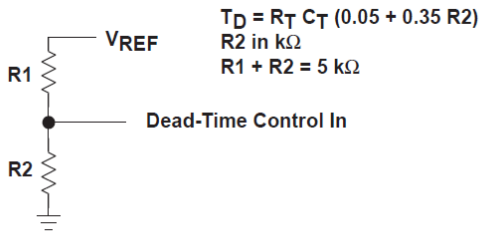

Figure 29. Tailored Dead Time

Figure 40: TL494 Dead Time Control[13]

Using the TL494

Our use of the TL494 concerns mainly the manipulation of the input to the error amps on the chip. The TL494 works in the same fashion as the PWM generation of the 2-Level PWM circuit above. An input signal is connected to an error amp input, and it is compared to a saw-tooth wave. Since this IC is catered to DC/DC converters, we had to make accommodations in our reference signals.

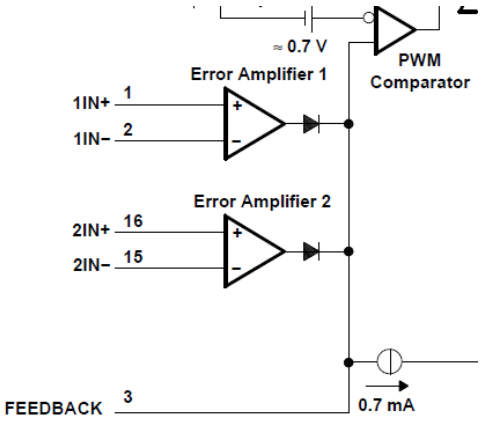

Figure 41: TL494 Inputs

A single TL494 can only produce a 2-Level PWM signal. There is no level shifting of the internal saw-tooth wave, nor are there multiple PWM outputs that are needed for a 3-Level PWM system. For a DC/DC converter, this is no need for anything more than a single feedback signal and a single carrier wave to sample it. The chip's bias towards DC/DC converters is also apparent in the PWM behavior. As

[13] (Griffith, 2005)

the error signal goes down (the DC level is falling), the chip compensates by increasing duty cycle to bring it back up.

The solution to the problems associated with using the TL494 for our inverter application comes in three parts: externally level shifting the sine wave reference by creating reference half-waves to eliminate the need to level-shift the carrier wave, inverting them to produce the maximum PWM duty cycle as the sine wave reaches its peaks, and using two TL494's to produce each half of the sine wave output.

Emulating the level shifting carrier wave typical in 3-level PWM systems required using op-amp rectifiers on the reference sine wave. The op-amp precision rectifier works by turning on diode D2 (Figure 42: Precision Rectifiers for Half-Wave Generation) whenever the input is greater than signal ground. This has the effect of bypassing any current that would go through R3, preventing it from developing a voltage. Since the output is connected to the virtual ground, it is equal to it. When the input is less than signal ground, the circuit behaves like a regular inverting amplifier with the gain equal to –R3/R2. Since this circuit rectifies only the half of the sine wave that is less than signal ground, an inverted sine wave is used with another precision rectifier to create the second half-wave for PWM signal comparison.

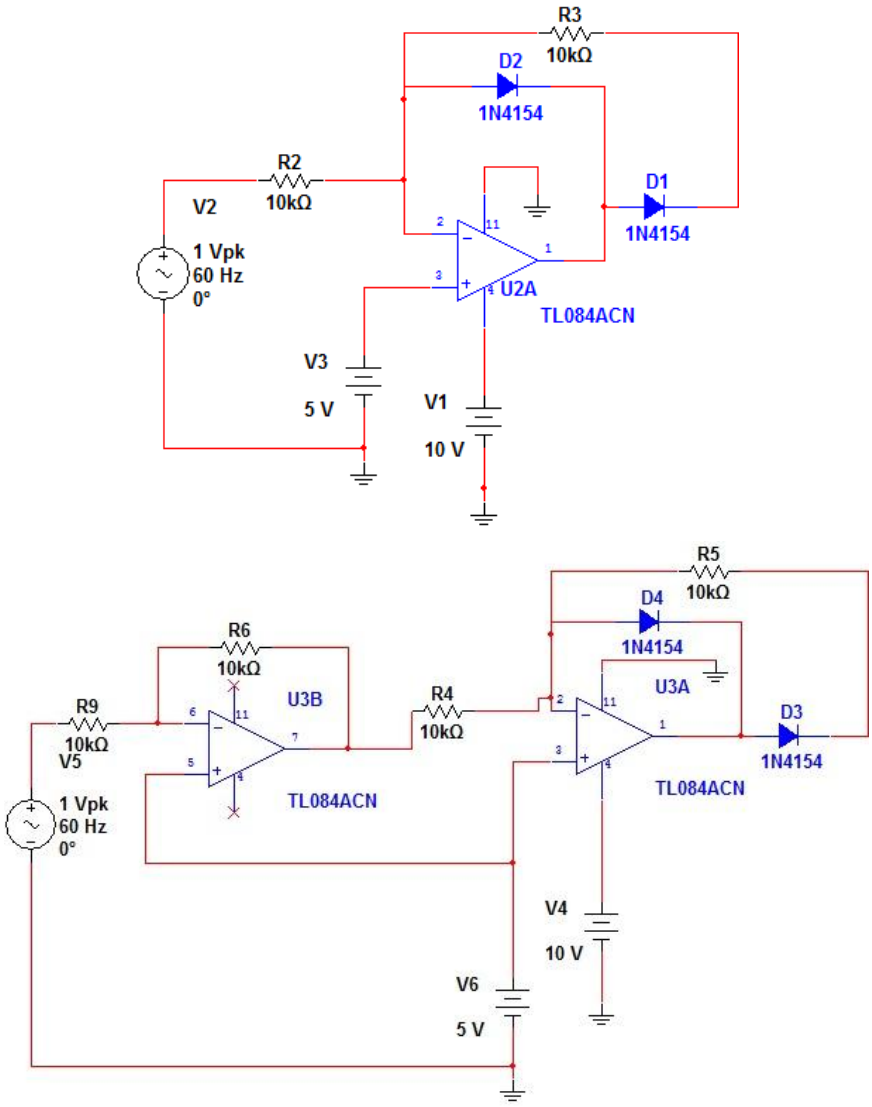

Figure 42: Precision Rectifiers for Half-Wave Generation

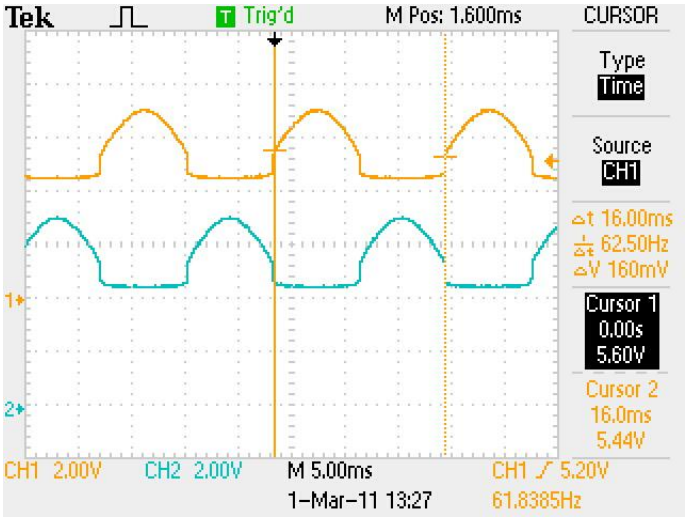

Figure 43: Half-Wave Rectifier Outputs

The results of using the precision rectifiers are two half-rectified sine waves that are equal in amplitude and 180° out of phase compared to each other. There is a slight distortion created by the negative feedback compensating for the forward drop across the output diode, but the signals are still usable. These signals should produce the produce the necessary PWM signals when sampled with a carrier wave, but the TL494 produces a smaller duty cycle as the error signal gets larger. This can be thought of as an increasing DC level at the output, and the TL494 compensates by delivering shorter pulses. So, as each of the half-waves reaches its peak, minimum duty cycle occurs. This is the opposite of the desired effect. The solution is simply to invert the half waves.

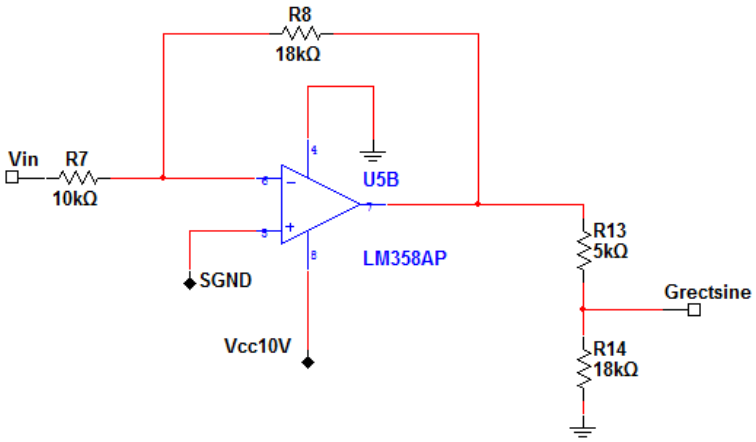

Figure 44: Inverting Gain Stage for the Half Waves

The LM358 is chosen for the inverting gain stage of the half waves due to its ability to output a voltage very close to its minus rail. This translates to more headroom for adjusting maximum duty cycle, as the TL494 reaches maximum PWM duty cycle as the input reaches 0 Volts (while minimum duty cycle occurs when the input is at about 3 volts). It should be noted that R13 and R14 adjust the DC Level of the half-wave and R8 and R7 adjust the amplitude of the half wave. The values above were experimentally determined to produce the least crossover distortion of the output sine wave while maintaining a reasonable amplitude.

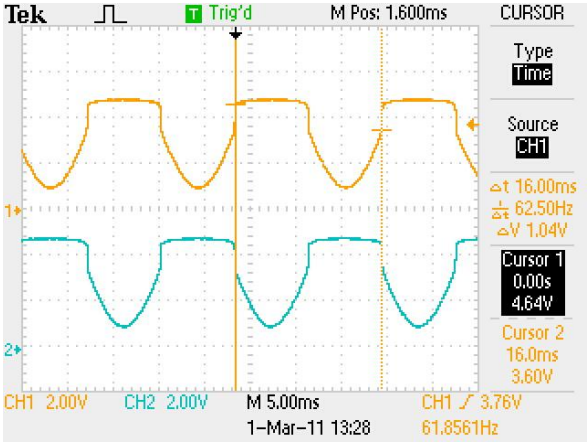

Figure 45: Outputs of the Inverting Amplfiers

At this point, the signals are ready to use in the TL494's. We programmed a switching frequency of 40 kHz with R9 = 25k Ω and C2 = 1000 pF. We tied the output transistors together for single-ended output (OTC pin tied to ground). The error amp is connected for unity gain at the FB pin.

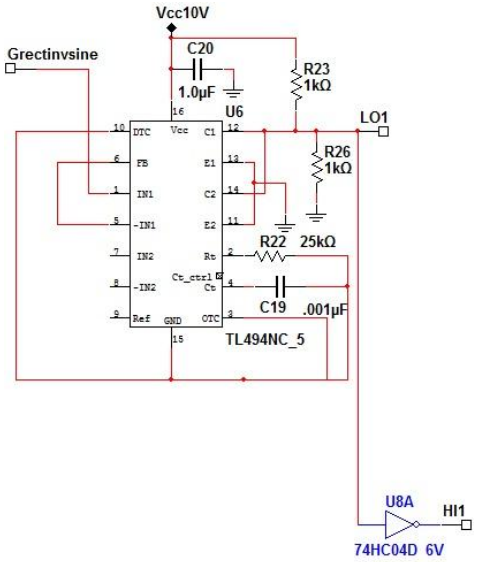

Figure 46: TL494 Configuration

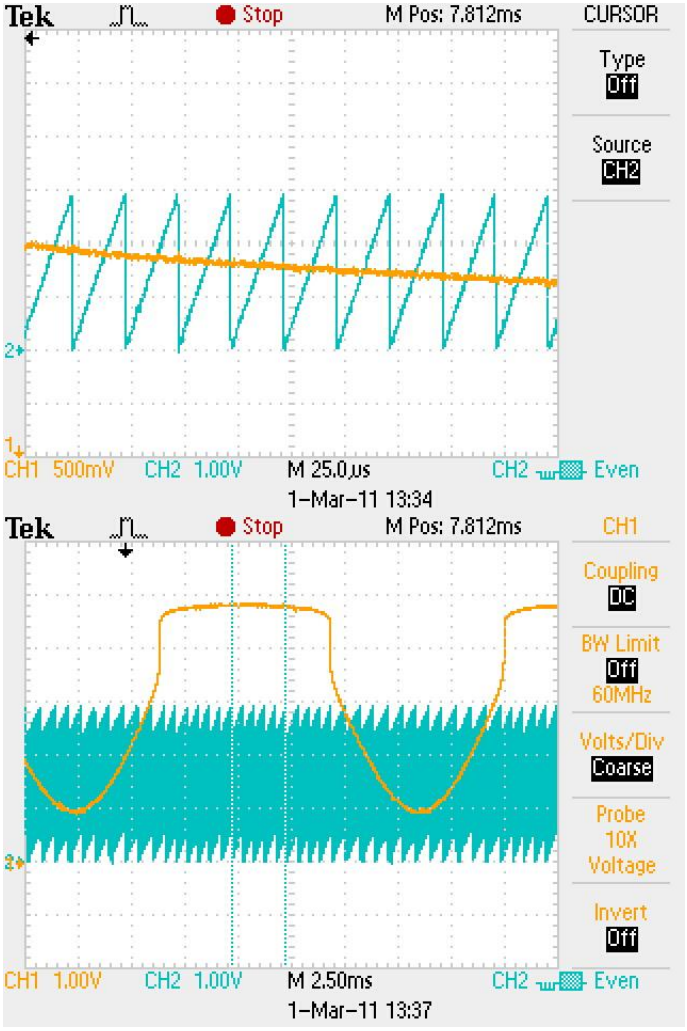

Figure 47: Sampling the Input with a Saw-Tooth Wave

Upon examination of the output at the pull-down transistor, we realized that the outputs were the inverse of what we need. The duty cycles were correct, but where we expected a logic 1, there was a logic 0. We solved this by dividing the voltage in half at the TL494 collectors to make the output compatible with 74-series logic inverters. Serendipitously, we already had a 5 Volt source needed for 5-Volt logic chips by way of the TLE2426 we were using for our signal ground. Since V_{CC} for all the chips was 10 Volts, the TLE2426 divides that in half to produce a signal ground while being able to sink or source 20 mA.

Later on, we would realize that the signal at the TL494 collector would be useful to drive the low-side gates on our MOSFET H-bridge, with the inverted signal driving the high-side gates. This

discovery came about after having charging issues with the bootstrap capacitors. We had been ignorant of the fact that the bootstrap capacitor needs to be grounded in between cycles so that V_{cc} can replenish the charge on it. We had left the bottom gates off when we weren't pulsing current from its corresponding high gate. Since the bootstrap capacitor is connected to the load filter, bottom plate of the capacitor always stayed at its boosted voltage from being connected to the load. Since V_{cc} is only 10 Volts and the high-side voltage is much greater than that, the bootstrap diode cannot become forward biased. The solution was to use the inversion of the signal driving the high-hate on the same side, the signal coming directly from the TL494.

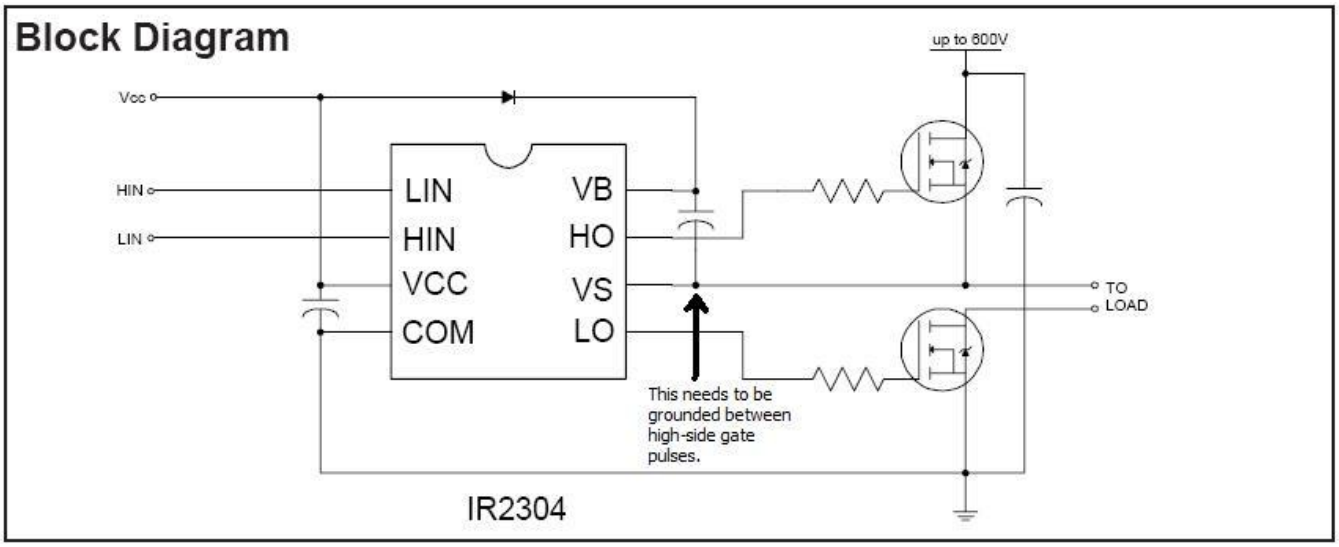

Figure 48: Grounding the Bootstrap Capacitor[14]

[14] (International Rectifier, 2004)

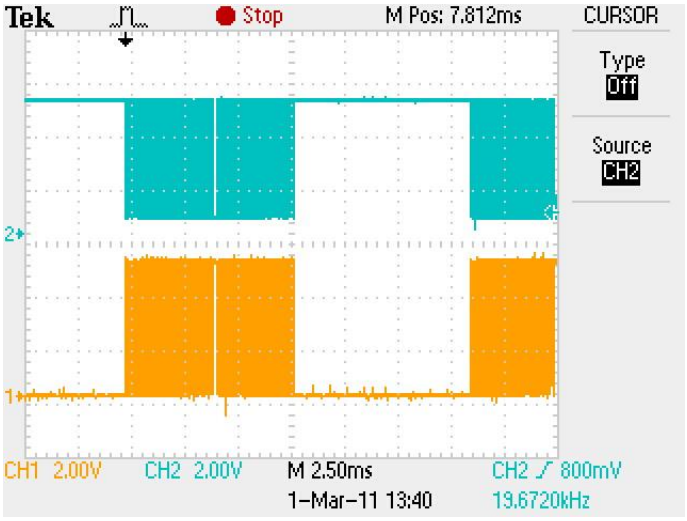

Figure 49: PWM Signal from the TL494 (Top) and its Inversion (Bottom)

Figure 50: Alternating PWM Signals for Both High Side Gate Half-Cycles

Using these signals, we were able to drive the H-bridge using the TL494 chip to spread PWM switching across the four MOSFETs equally, while still ensuring that the Vs node is pulled to ground every cycle, ensuring the proper operation of the bridge.

Results

Once we had determined the specifications of our overall design, we built a prototype of the final circuit shown below, in figure 51. The signals going into each IR2304 driver IC were detailed previously, with LIN1 and HIN2 in phase, and vice versa.

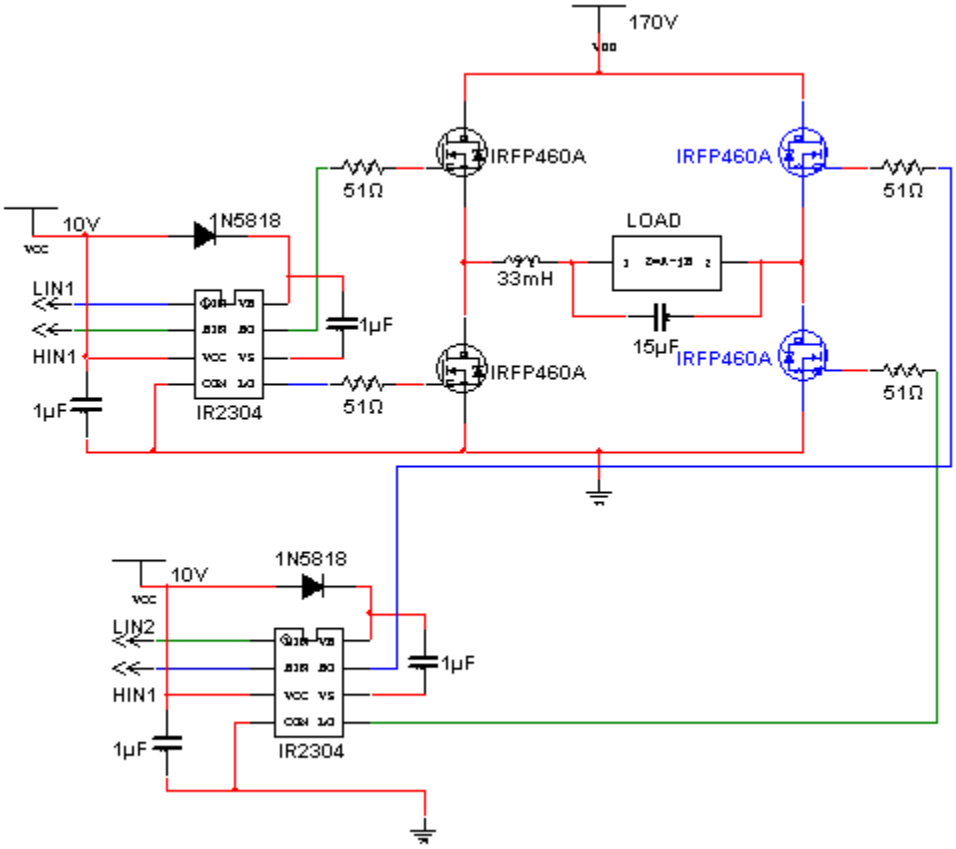

Figure 51: Final Inverter Design

The preliminary prototype consisted of the low-voltage signal generation circuits on breadboard, with the MOSFET driver circuit soldered on a protoboard, due to the high voltage rail. The H-bridge itself was constructed on a wooden board, with the MOSFETs attached to heat-sinks obtained from a 400W power supply, with an off-the-shelf square-wave inverter used for the high voltage rail. Due to the fact that this supply only contained a high voltage rail of approximately 145VDC, our testing was done at this level instead of 170VDC. The off-the-shelf supply and the signal-generation circuitry were powered by a single 12VDC car battery, which was regulated to 10V for the signal generation circuit.

Once the prototype was constructed, it was tested both at low-voltage and high-voltage. The low-voltage testing was conducted using the 12VDC car battery both as the VCC regulator source and as the H-bridge DC rail. As such, the output was a 12V PWM signal, which was filtered and used to power a 12V halogen car headlight. Testing at low-voltage allowed us to safely test our setup and perform basic troubleshooting before moving on to high voltage.

Low-Voltage Test

The prototype was tested first at low voltage, with a 12VDC battery supplying both the H-Bridge, and the VCC regulator. Using this source, the inverter was connected to a 12VDC halogen car headlight as a load, with a low-voltage filter of the same value as that described in the previous section. The MOSFET gate voltage wave-forms under this load are shown in figure 53. Some distortion can be seen, but the Waveforms otherwise look as they should. Channel 1 shows V_{gs} for the high gate of the half-bridge, showing that it must be boosted above that of the DC rail.

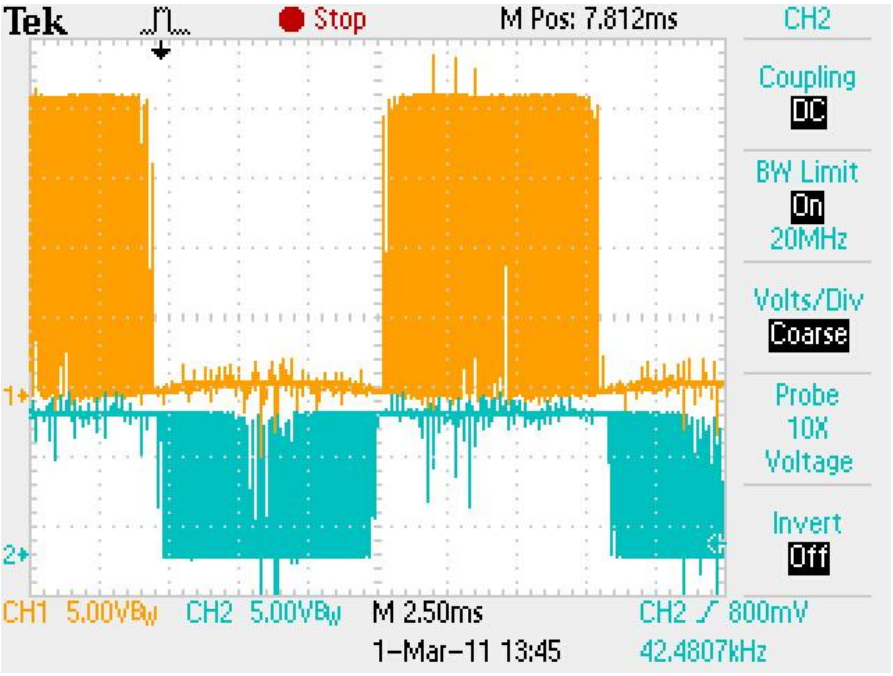

Figure 52: Low-Voltage Test Half-Bridge Vgs Waveforms

The filtered waveform across the 12VC headlight load is shown below in figure 53. The output of our low-voltage test was nearly ideal, with very little distortion. This verifies that our generated PWM signal did indeed encode a sine wave which is sufficiently free of distortion.

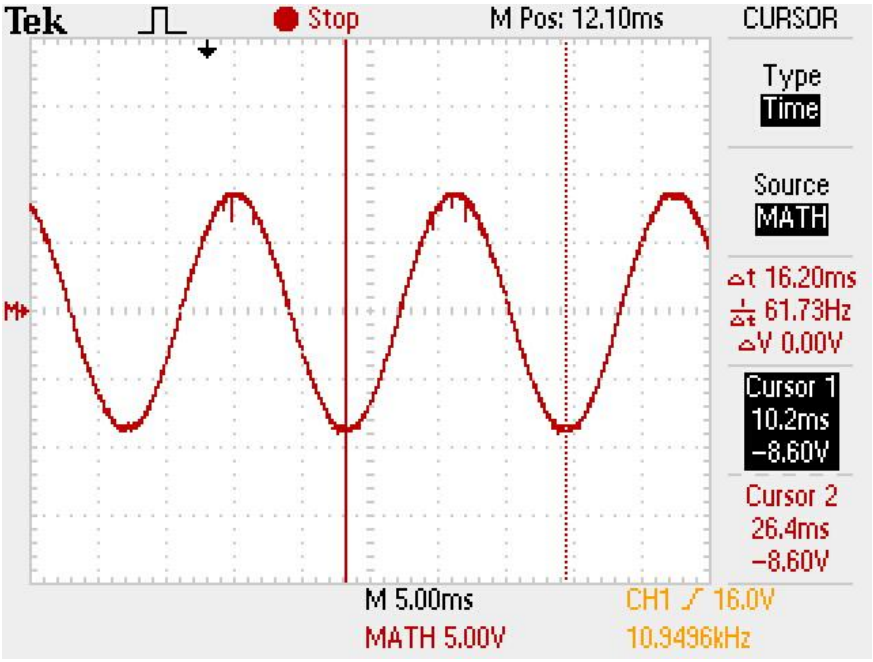

Figure 53:Filtered Low-Voltage Output across 12VDC Headlight

Figure 54 below shows the sine wave output, zoomed in on the cross-over point. This distortion is due to the adjustment of the offset values in our signal generation circuit, and should, in theory, be optimized further. In this case, the dead-time is smaller than 250µs, which is less than 1.5% of the sine wave's period. Though it is not perfect, this degree of distortion should be acceptable for our purposes. It is certainly far better than the "distortion" inherent to a square wave or modified sine wave inverter.

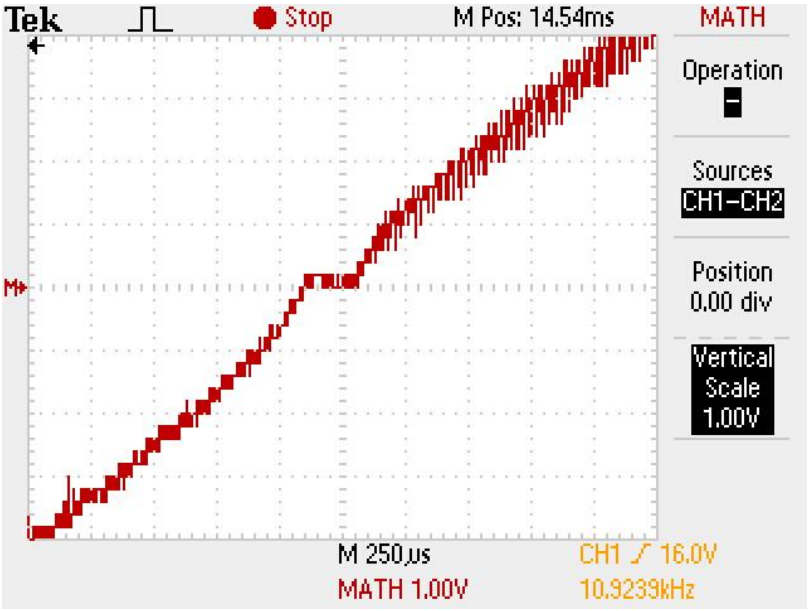

Figure 54: Low-Voltage Output Cross-Over Distortion

High Voltage Testing

200W Resistive Load

Once we had confirmed that our prototype operated correctly at low voltage, we tested it at high-voltage, by using the DC-DC boost stage of an off-the-shelf modified sine wave inverter, specifically its 145VDC rail. We still powered the VCC regulator off of the 12VDC car battery, as well as the DC boost. We also ran into some trouble with our filter, which will be detailed as well. For our test, we first connected two 100W incandescent light bulbs in parallel for our load. This load would be close enough to our rated power to let us know if we had any major problems with our design.

Figure 55, below, shows the gate voltages of one half-bridge while operating under these load conditions. There is some degree of feedback distortion that can be seen in the high gate waveform, but it remains high enough to operate the MOSFET properly. The distortion present in the low gate voltage is also troublesome, and can be seen as well in figure.

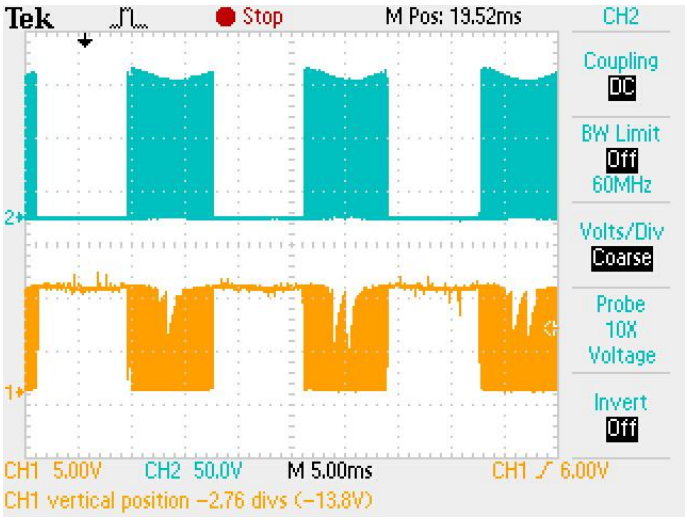

Figure 55: High Voltage Half-Bridge Vgs Waveforms

Figure 56 shows the filtered output across our resistive load, and illustrates the same distortion we could see on the low gate voltage above. This distortion was accompanied by severe overheating of our MOSFETs, and caused us quite a bit of trouble until it was figured out. Eventually, through much troubleshooting involving replacement of components, and operating under various conditions, we were able to determine that the problem lay in our filter capacitor. Our original selection was a ceramic 15µF capacitor rated for 250VDC. It was chosen due to the fact that our capacitor will see a maximum of 170V (145 in our test setup), but we didn't realize that there are other considerations which come in to play when operating with AC. Our filter capacitor was getting overloaded and breaking down. Once the prototype was operated without the capacitor, it operated correctly (albeit without a filter), and the overheating issue was completely resolved. The capacitor specified in the H-Bridge design section takes this lesson into account, and therefore is rated for an AC voltage of 250V. We have not yet replaced the capacitor for further testing, and the remaining tests were therefore performed with the capacitor removed.

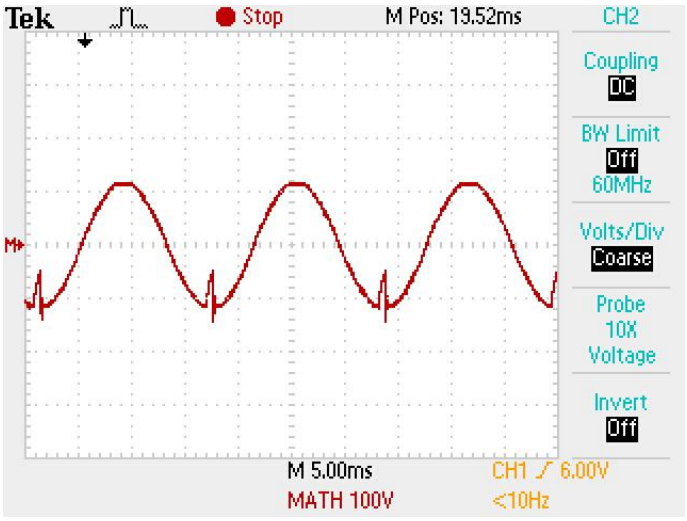

Figure 56: High-Voltage Filtered Output Waveform (showing Breakdown Distortion)

Figure 57, below, shows the output waveform across the 200W light bulb load, with the capacitor removed, the worst distortion of previous test is now gone, though the voltage still dips to some degree at both extremes. The fact that the sine output was sufficient with the filter, apart from the break-down distortion, and that the output without the filter was essentially the same as before, but with the distortion gone, can be taken to mean that our output would be ideal if we had the filter.

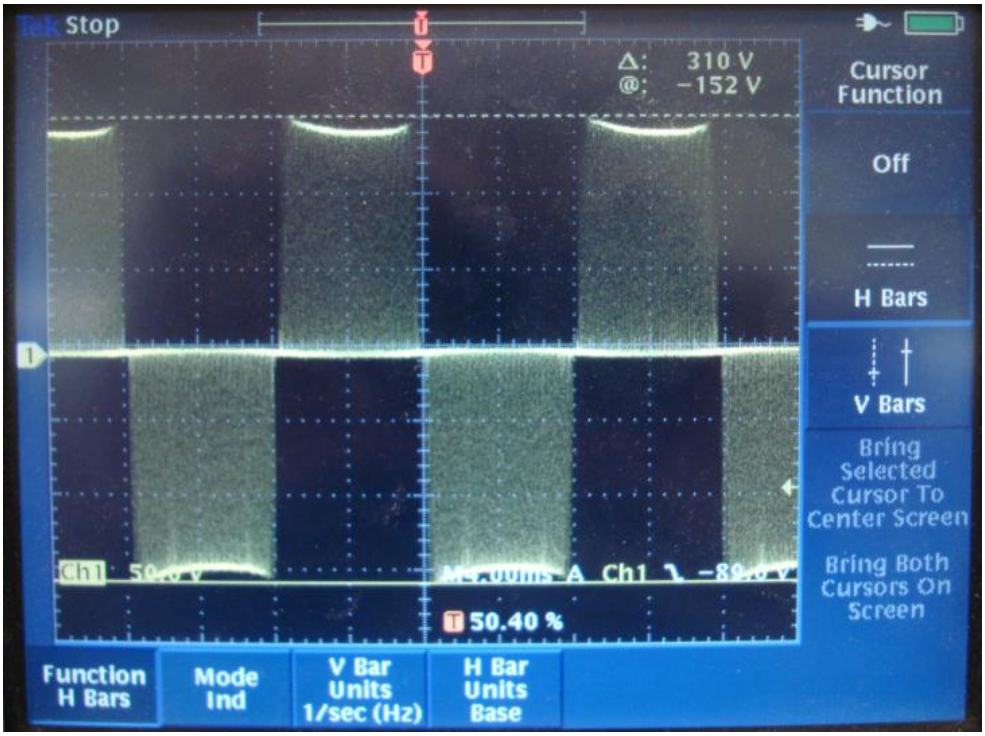

Figure 57: Unfiltered High-Voltage Output with a 200W Load

The dipping of the waveform in the middle of each section of PWM is due to the voltage drop of our DC bus we used for testing our circuit. The edges are sustained without difficulty, as the duty cycle is low, but as the duty cycle increases to nearly 100% in the middle of the PWM block, the supply has trouble maintaining the voltage. This issue would have been addressed by our initially proposed DC boost stage feedback scheme, where the output voltage drop would have been compensated for by raising and lowering the bus voltage.

Figure 58: Unfiltered Output FFT w/200W Resistive Load

Figure 58 shows the FFT of the output waveform in this test, performed actively by the oscilloscope. In this scope image, we can see the two areas of most importance to us. First, the large peak, which is all the way to the left in this image, is the 60Hz sine wave fundamental frequency, shown zoomed in, in figure 59. This is the primary frequency which will be retained by our filter, and go through to the load. The two larger peaks to the left are interesting to note. They both represent the PWM switching frequency, which is 40kHz. The presence of two distinct peaks, one at 38.9kHz, the other at 40.9kHz, is an artifact of our signal creation circuit. Ideally, there should be one peak centered on 40kHz, but our design generates the PWM for the top half of the sine wave completely isolated from the PWM for the bottom half of the sine wave. Each component in the generation circuit has a

tolerance level, and variations from component to component will result in a frequency which is not exactly 40kHz. In our circuit, though, the two PWM signals are isolated, never interacting with each other until they meet at the load. The result is that the two tolerance effects are separate, and will result in two different frequencies, near the ideal 40kHz, but due to two isolated tolerance cascades.

Figure 59: Output FFT showing 60Hz peak

Inductive Load Test

Next, we used our inverter to power a 120VAC plug-in power rotary tool, which is rated for 96W, as an inductive load. The output while powering the rotary tool at full speed (but with low torque- we weren't grinding anything) is shown below in figure 60.

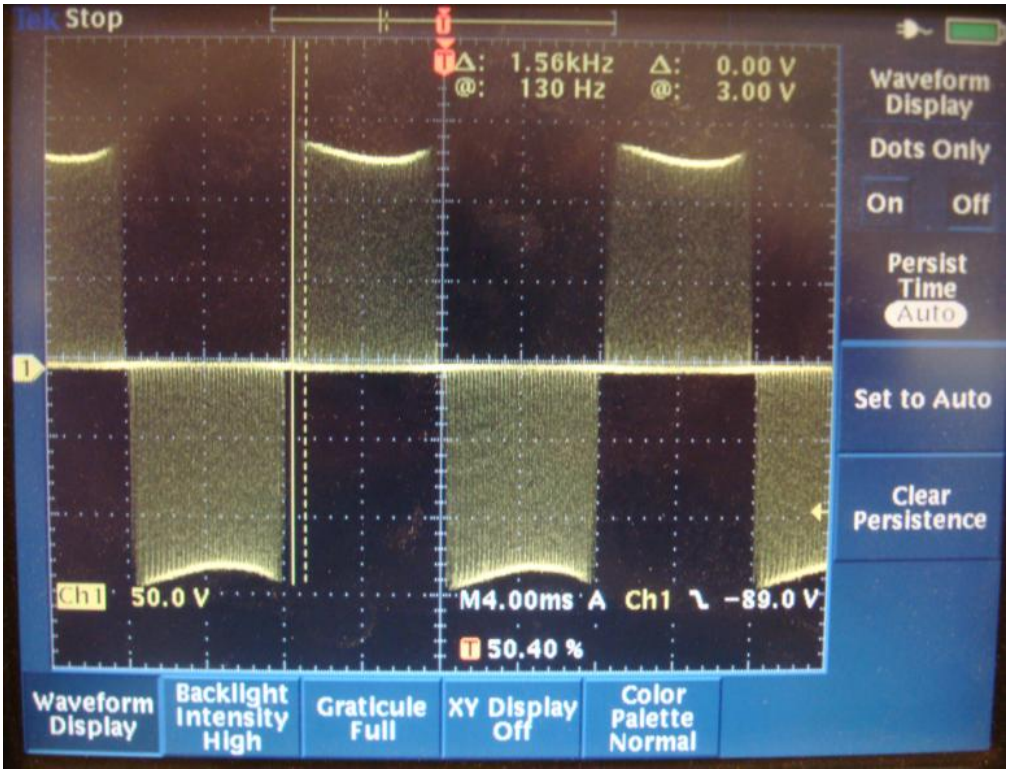

Figure 60: Unfiltered Output with Inductive Load

The unfiltered PWM output while running the rotary tool is nearly identical to that of the resistive load. There is no additional noise, and merely a slightly increased dip in the voltage, representing a different current load from the DC bus. It should be noted that this waveform is after the rotary tool has spun up to speed, with no load apart from spinning the chuck. Torque requires an increase in current, which means that the initial turning on of the motor requires an inrush current. When the rotary tool was initially turned on, the waveform dipped considerably, coming to rest at this steady state after a second or two.

Printed Circuit Board

One of the goals for this project was to produce a working PCB. The final product took on a two-tier design to keep the footprint within a 3" by 5" design constraint. A logical choice was made to separate the low-voltage control components and the high-voltage power h-bridge, and to connect them together with an inter-board connector. Along with reducing noise through capacitive and inductive coupling, such a design allows for modularity. Different control circuits can be plugged into the

h-bridge while the h-bridge itself can be used in a standalone fashion for other purposes. To reduce prototyping cost, the boards were fabricated in a one piece design that would be separated at the time of assembly.

Translating the design to a PCB brought with it various improvements. The PCB has a large copper ground plane which reduces signal noise by coupling capacitance between traces to ground instead of to other traces. Secondly, all the IC's have bypass capacitors placed close to their physical location to decouple them from the power supply in order to decrease input ripple. The virtual ground IC (TLE2426) now has the noise reduction pin connected to ground for better noise performance, as well as a capacitive divider at its output for voltage stability and accuracy under load.

In order to allow for use in other potential applications and with other control circuits, the H-bridge PCB has some generic features which are unused in our application. The four MOSFET positions have through holes for either TO-247 or TO-220 package MOSFETs. They are meant to be attached to Ohmite F-series heat sinks which have a range of thermal resistance ratings and height. The inductor footprint is meant for Bourns 1140-series ferrite chokes with 1.15 inch lead spacing which gives the user the ability to use inductors ranging from 6.8 to 1000 µH. Capacitors from the Nichicon EC range can be used, up to 16 µF.

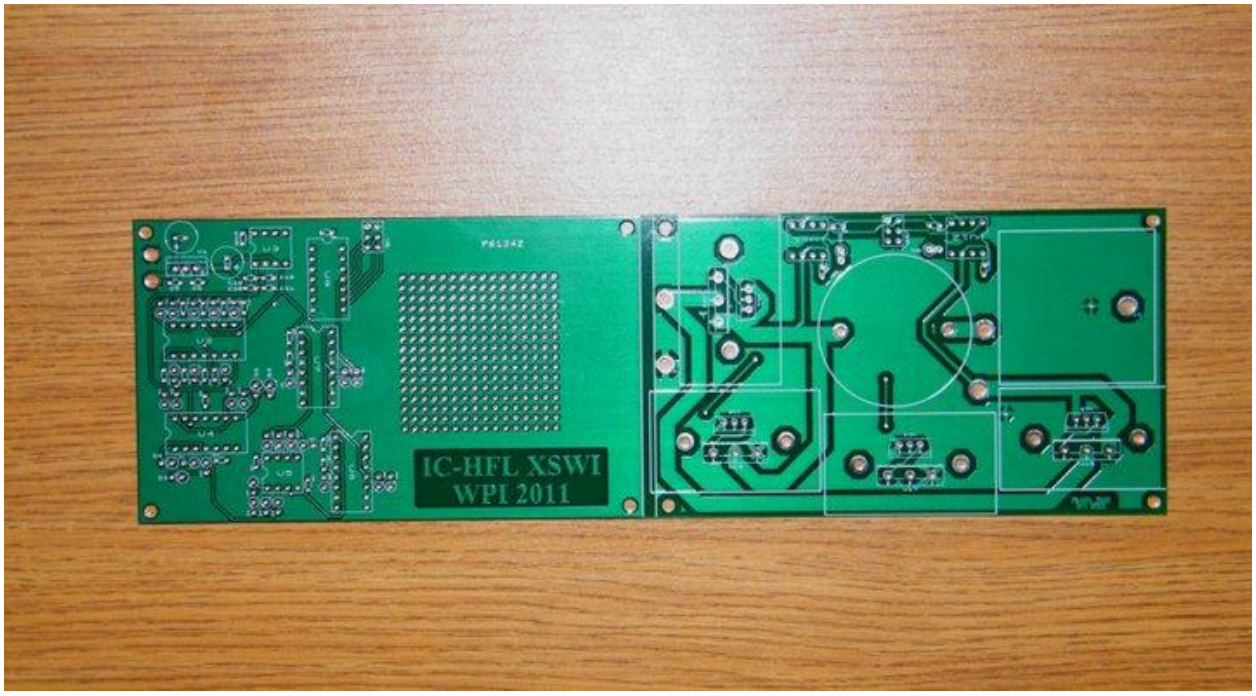

Figure 61: Sine Wave Inverter PCB

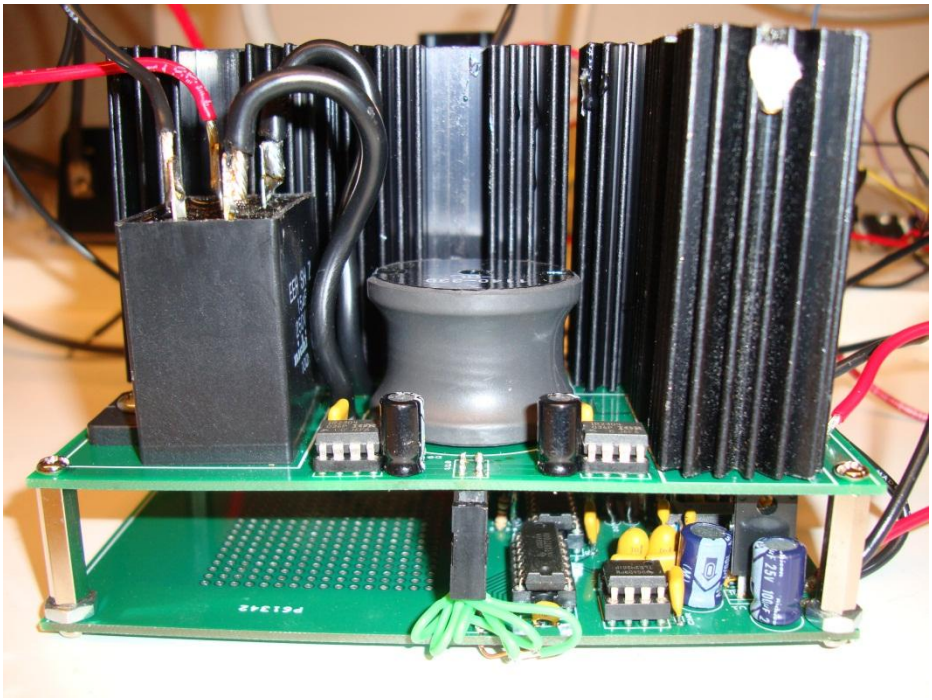

Figure 62: Populated PCB

The boards performed as expected once assembled (figs. 63, 64), but there are several improvements to be made due to oversights. On the control board, for example, the input power wire holes are too big. Also, the output PWM signals have been re-routed after noticing that the output at the PWM controller only gets to about 1V from ground for a logic"0" signal. The solution was to use the other inverters on the 74HC44 chip to invert the once-inverted signals from the PWM controller again to obtain the original waveform, except that the logic "0" value would be closer to ground. This was done to prevent any conflict with the MOSFET driver maximum low-input threshold. The most important change to the control board would be to reverse the silkscreen for the TL084's, as the chips were laid out backwards. The only problem this presents is that the V+ and V- terminals are switched. Apart from this this inconsistency, the quad op-amps are symmetric.

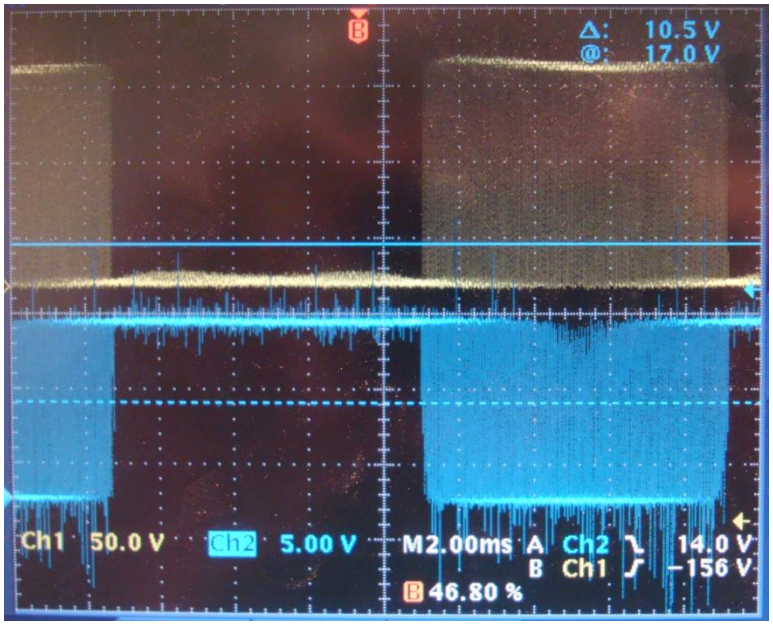

Figure 63: PCB gate voltage waveforms (one half-bridge)

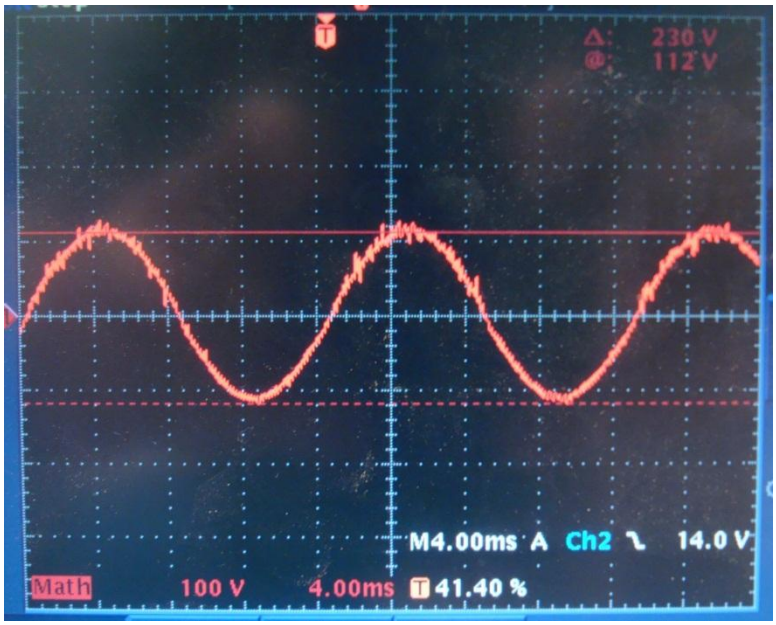

Figure 64: PCB filtered output waveform

On the H-bridge board, the biggest improvement that can be made is to change the heat sinks so that the MOSFETS can be placed close to the driver IC's, in order to minimize the length of the gate traces. Also, gate resistors need to be included in the board, as in our final PCB prototype, they had to be soldered in manually, bypassing the trace.

Power Efficiency

In order to determine the power losses, and therefore the efficiency of our PCB design, the power into and out of the inverter were experimentally determined. In order to determine the powers, we needed to determine first the voltage and current at the two points. Voltage was a simple matter of using a digital multimeter to measure the voltage of the H-bridge, and again to measure the RMS voltage of the output voltage waveform. In order to determine the currents, though, we needed to use an indirect measurement, using a known resistance in-line with the circuit, and measuring the voltage drop across this resistance. This allowed us to calculate the current going into and out of our inverter. The results of these measurements are shown below.

	Vin/out (Measured)	Resistance (Measured)	Vdrop (Measured)	Current (Calculated)	Power (Calculated)
Input	130VDC	0.05	0.11VDC	2.2ADC	286W
Output	91.55Vrms	0.017	0.046Vrms	2.76Arms	252W

Using these values, we calculate a power efficiency of 88% for our inverter, which is well within design specifications of Efficiency ≥ 75%. It should be noted that this power efficiency is for the unfiltered output. Using the LC filter we discussed earlier reduces the power output considerably, burning far too much energy as heat in the MOSFETs of the H-bridge. At this point, the exact cause of this is unknown, and is still being investigated.

Conclusion and Recommendations

Ongoing blackouts exacerbate the problem of inaccessible healthcare in developing countries. While it is commonplace in the United States to have hospitals equipped with uninterruptible power systems, such a practice only serves to bolster a grid developed with ample funding and technology. While Americans give nary a thought to the possibility, power outages are an everyday expectation for sub-Saharan African villagers.

Affordable pure-sine wave inverters are necessary to provide an expedient, if not total, solution to underdeveloped grids. This logic can be taken further with the concept of microgrids. By lacking centralized power generation, developing countries have an opportunity to use solar panels to create localized grids. This is a driving force behind low-cost inverter technology.

This WPI MQP consisted of the design of an affordable pure-sine wave inverter using 3-level PWM and MOSFET switches in an H-bridge configuration, in which an op-amp based logic control circuit was used to control MOSFET drivers to actuate H-bridge MOSFET's. Due to complications mid-way through the project, the DC-DC boost stage is assumed, and not created. Feedback was included in our DC-DC design, and was removed with the removal of its system. A major focus for potential future improvement is therefore to implement a feedback system, which our design lacks. This can be done in two ways: to alter the DC rail voltage in the DC-DC boost phase, as was the case in our initial design, or to alter the duty cycle of the PWM signal in the DC-AC inverter phase.

If cost and simplicity had not been design constraints, it also would have been interesting to pursue a 5-level PWM implementation of the same inverter. It would have brought with it higher efficiency, less noise, and easier filtering, and, despite the additional complexity, it would be an exciting area of potential future work.

Perhaps the biggest area of potential improvement of our project is the design and implementation of a DC-DC boost phase which would convert the 12VDC car battery source to a 170VDC rail for use with the H-bridge. Our workaround using an off-the-shelf inverter's DC boost rail allowed us to sufficiently prototype and test our inverter, but it was certainly not the same as a DC-DC phase specifically designed and optimized for our implementation.

Ultimately, we ended this MQP project with a working DC-AC inverter prototype, which operated efficiently within our rated power range of up to 250W. With the assistance of the DC boost

phase of the off-the-shelf inverter, we showed that our inverter design was able to take a 140VDC source, and convert it to a pure-sine wave using 3-level PWM with minimal power loss. The major source of power loss in our system, the H-Bridge, burns only 10W, merely 4% of the rated power of our design. That means that any DC-DC boost phase designed in future implementations would be able to burn 16% of the power, and still be within the design specifications.

It should be noted that efficiency suffers while using our designed filter. The filter components are not rated for high frequency use, so the component values are severely derated from the manufacturers' specifications. Due to this, we feel that the inductor was not sufficiently choking the current into the capacitor. Since the PWM is acting like a series of turn-on transients, the peak current into the capacitor is very high, leading to the heating of the MOSFET's. The solution to this would be to increase filter component size or to increase switching frequency to a point where small components rated for high frequencies can be used. As a proof of this concept, we noted that MOSFET heating was decreased when we doubled our effective inductance in the filter by connecting another inductor of the same value in series.

In the end, we successfully tested the viability of our design, using a signal scheme which is, to our knowledge, unique, and results in the spreading out of power losses across the H-bridge. Testing showed that our design is able to output a sufficiently pure sine wave with minimal distortion, which can be used to power relatively intricate electronic devices, precisely as desired. Though the addition of a DC boost phase and feedback would be desirable for a complete design, our work in this MQP could be directly inserted into such a design unaltered with more than a reasonable expectation of success.

References

Deep Cycle Battery FAQ. (2009). Retrieved October 15, 2010, from Northern Arizona Wind and Sun: http://www.windsun.com/Batteries/Battery_FAQ.htm#Battery%20Voltages

Doucet, J. D. (2007). *DC/AC Pure Sine Wave Inverter.* Worcester, MA: Worcester Polytechnic Institute.

Griffith, P. (2005, February). Designing Switching Voltage Regulators With the TL494. Dallas, Texas, USA: Texas Instruments.

Hart, D. (2010). *Power Electronics.* McGraw-HIll.

International Rectifier. (2007, March 23). Application Note AN-978: HV Floating MOS-Gate Driver ICs. El Segundo, California, USA: International Rectifier.

International Rectifier. (2004, September 10). IR2304(S) & (PbF) Half-Bridge Driver. El Segundo, California: International Rectifier.

International Rectifier. (n.d.). IRFP460 Datasheet. datasheetcatalog.com.

Inverters R Us. (2010). *Inverters R Us*. Retrieved October 10, 2010, from Inverters R Us: invertersrus.com

National Semiconductor Corporation. (2011, February 25). LM117/LM317A/LM317 3-Terminal Adjustable Regulator. Santa Clara, California , USA: National Semiconductor Corporation.

Phillips Semiconductors. (1995, November 27). LM139/239/239A/339/339A Quad Voltage Comparator. Phillips Semiconductors.

Samlex Power. (2010). 300 Watt Pure Sine Wave Dc-AC Inverter PST-30S-12A/PST-30S-24A Owners Manual. Coquitlam, British Columbia, Canada: Samlex Power.

Waste to Watts. (2010). *Solution-Based Recycling*. Retrieved October 20, 2010, from Waste to Watts: waste2watts.org

Appendix A: Circuit Schematic

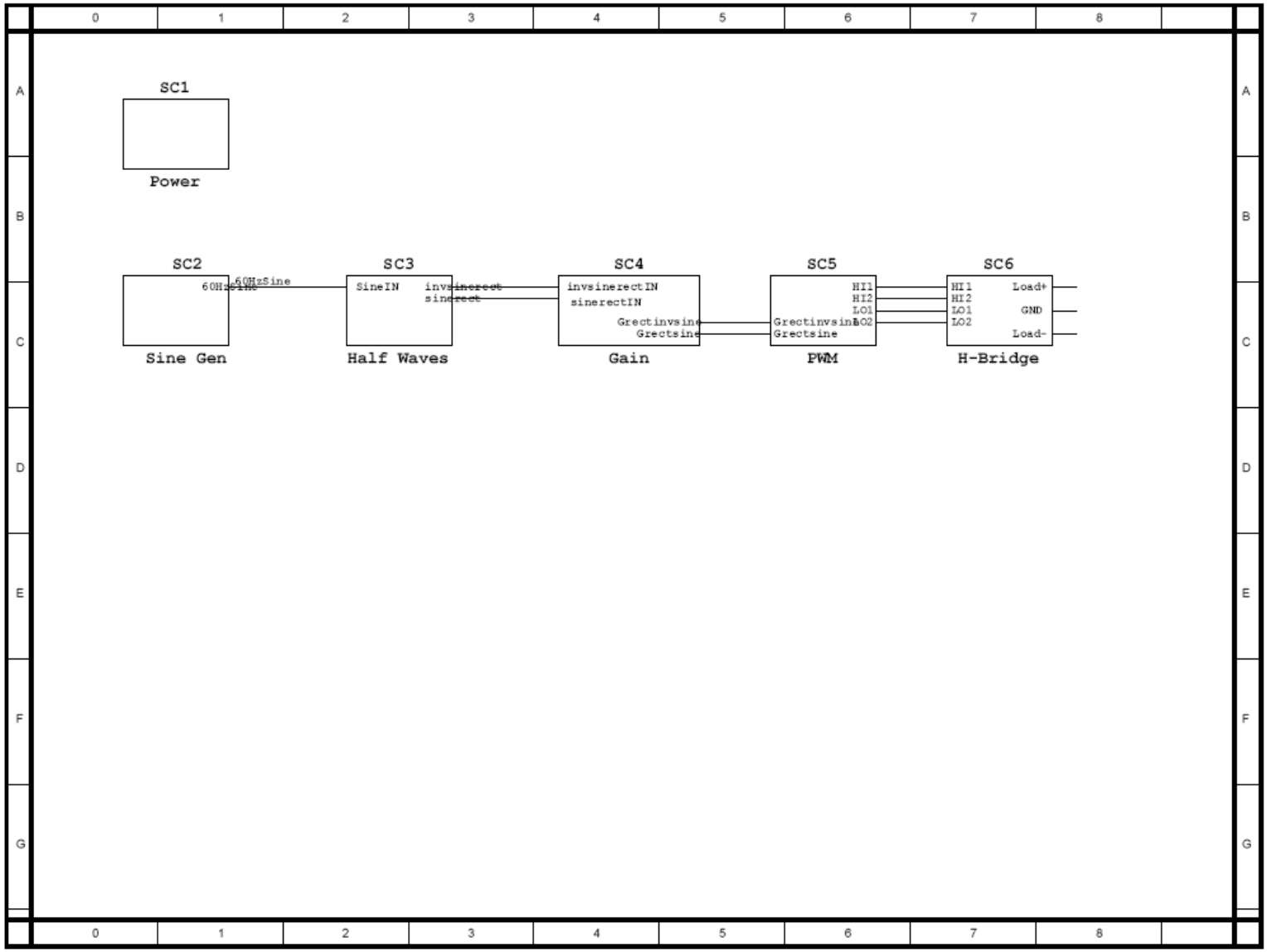
SC1
Power
SC2
60HzSine
Sine Gen
SC3
SineIN
invsinerect
sinerect
Half Waves
SC4
invsinerectIN
sinerectIN
Grectinvsine
Grectsine
Gain
SC5
HI1
HI2
LO1
LO2
Grectinvsine
Grectsine
PWM
SC6
HI1
HI2
LO1
LO2
Load+
GND
Load-
H-Bridge

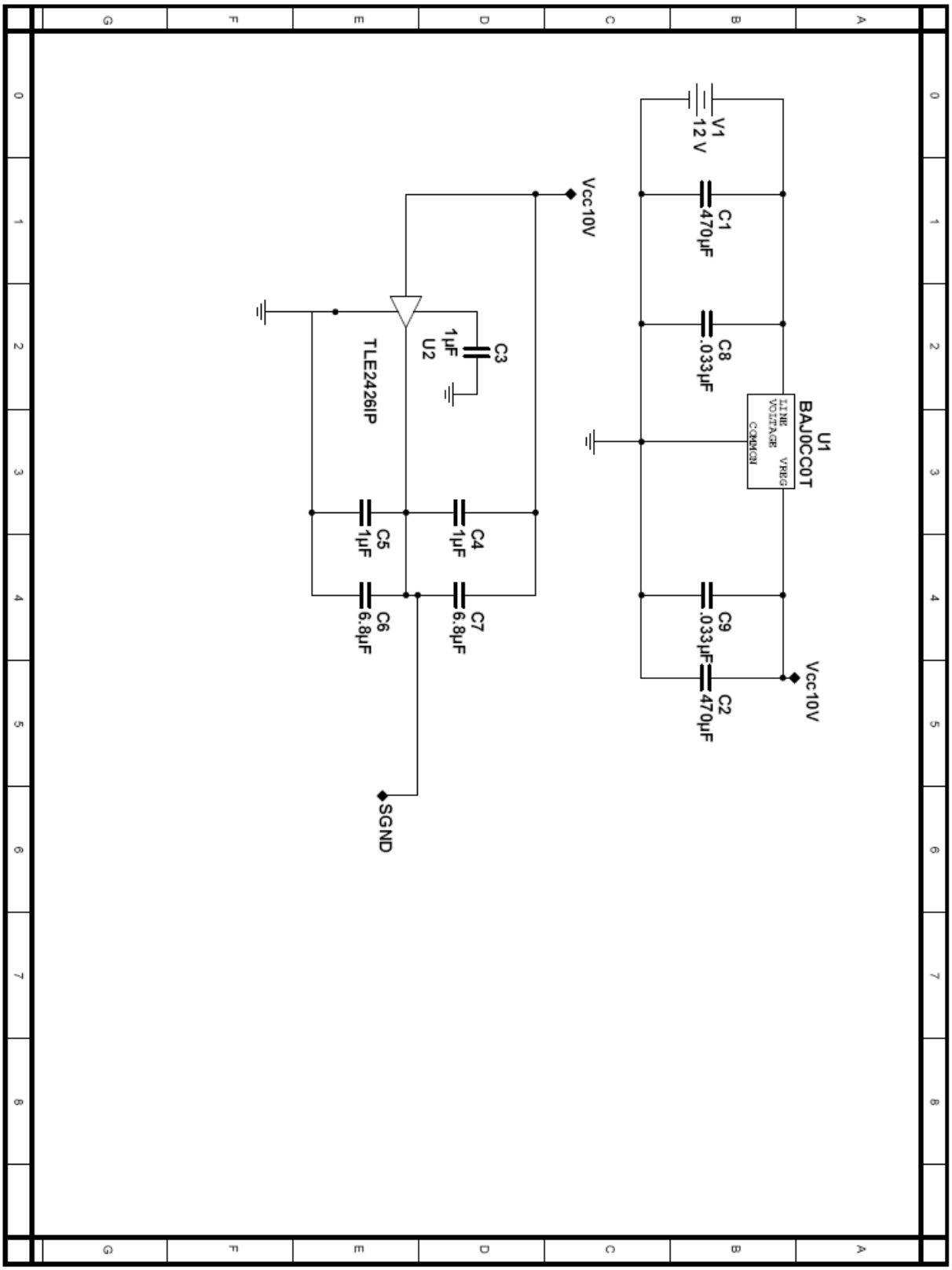
V1
12 V
C1
470µF
C8
.033µF
U1
BAJ0CC0T
LINE VOLTAGE
COMMON
VREG
C9
.033µF
C2
470µF
Vcc10V
Vcc10V
C3
1µF
U2
TLE4266IP
C5
1µF
C4
1µF
C6
6.8µF
C7
6.8µF
SGND

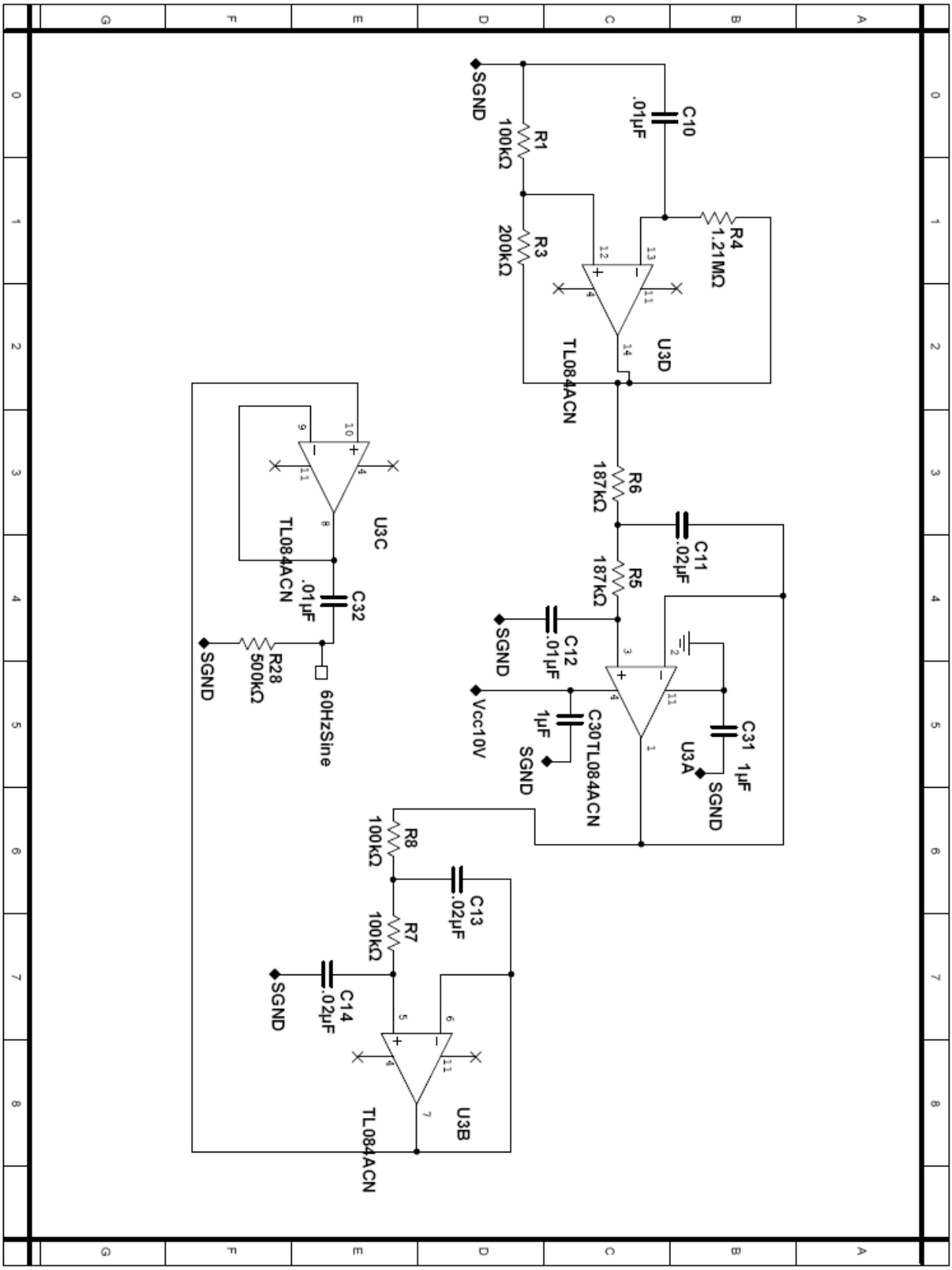
SGND
C10
.01µF
R1
100kΩ
R4
1.21MΩ
R3
200kΩ
U3D
TL084ACN
R6
187kΩ
C11
.02µF
R5
187kΩ
C12
.01µF
SGND
Vcc10V
C30
1µF
SGND
TL084ACN
C31 1µF
U3A
SGND
U3C
TL084ACN
C32
.01µF
R28
500kΩ
SGND
60HzSine
R8
100kΩ
C13
.02µF
R7
100kΩ
C14
.02µF
SGND
U3B
TL084ACN

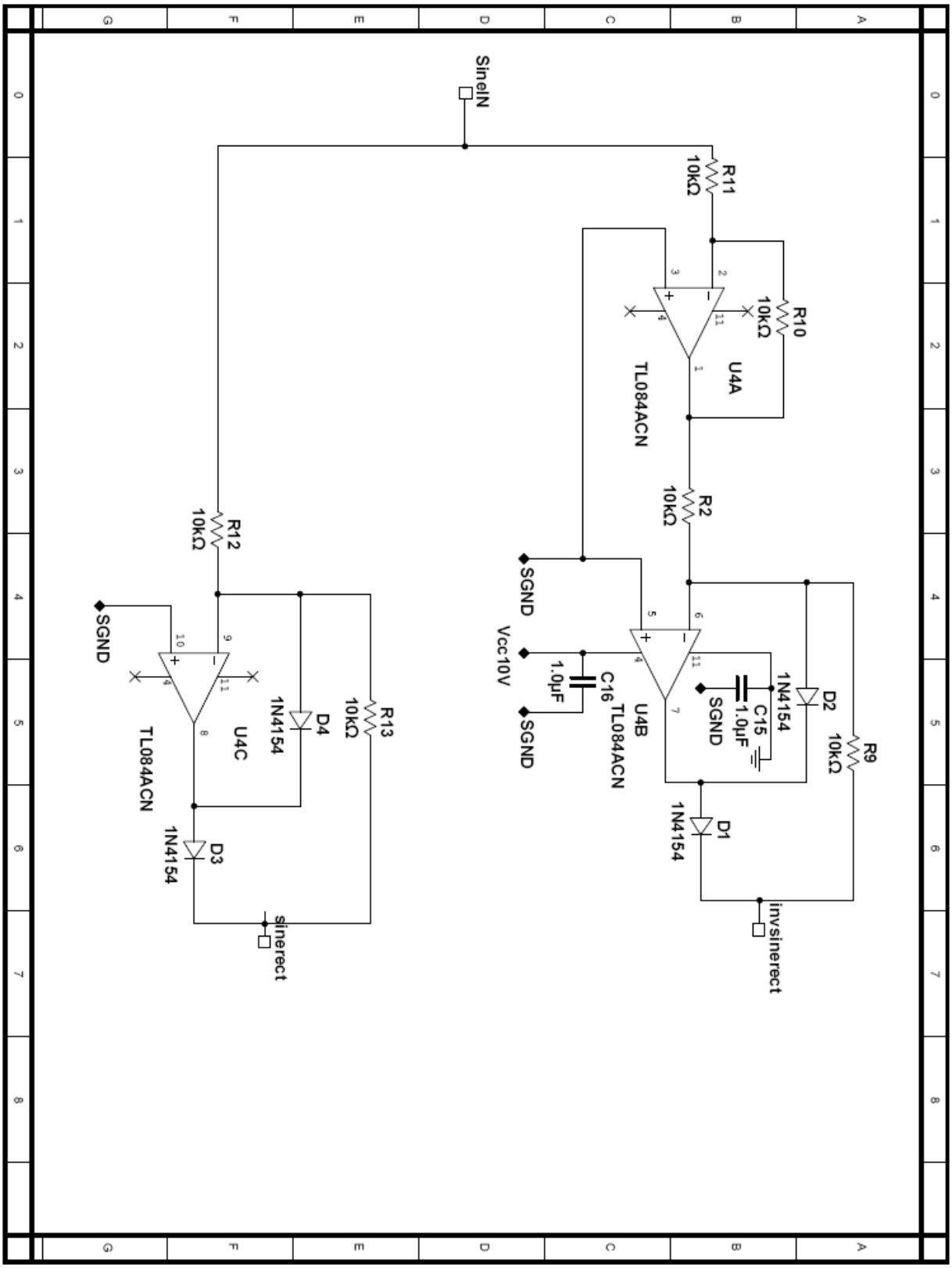
SineIN
R11
10kΩ
R10
10kΩ
U4A
TL084ACN
R2
10kΩ
R12
10kΩ
SGND
Vcc10V
1.0µF
C16
U4B
TL084ACN
C15
1.0µF
1N4154
D2
R9
10kΩ
D1
1N4154
invsinerect
SGND
SGND
R13
10kΩ
D4
1N4154
U4C
TL084ACN
D3
1N4154
sinerect

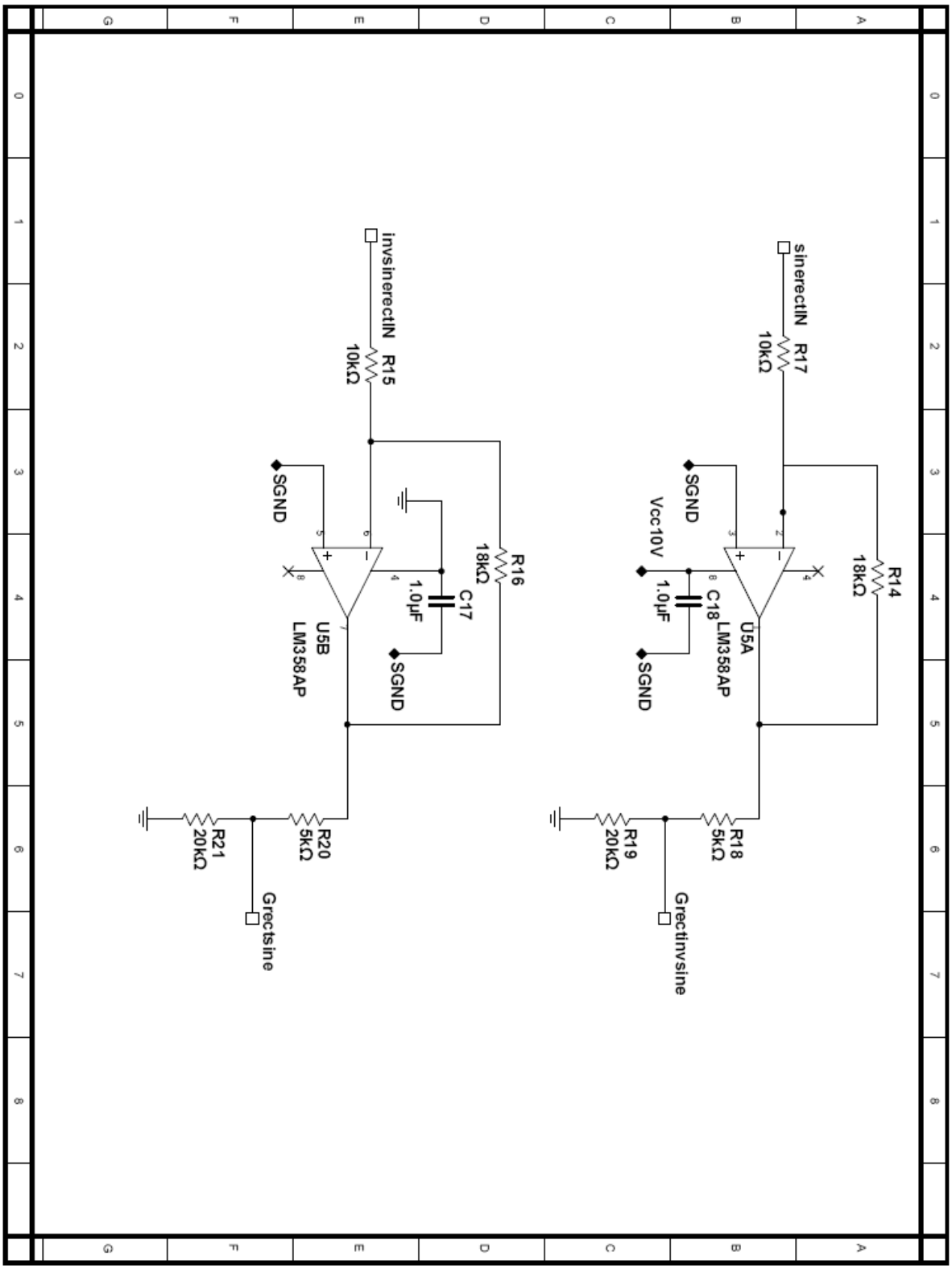
sinerectIN
R17
10kΩ
R14
18kΩ
SGND
Vcc10V
C18
1.0µF
SGND
U5A
LM358AP
R18
5kΩ
R19
20kΩ
Grectinvsine
invsinerectIN
R15
10kΩ
R16
18kΩ
SGND
C17
1.0µF
SGND
U5B
LM358AP
R20
5kΩ
R21
20kΩ
Grectsine

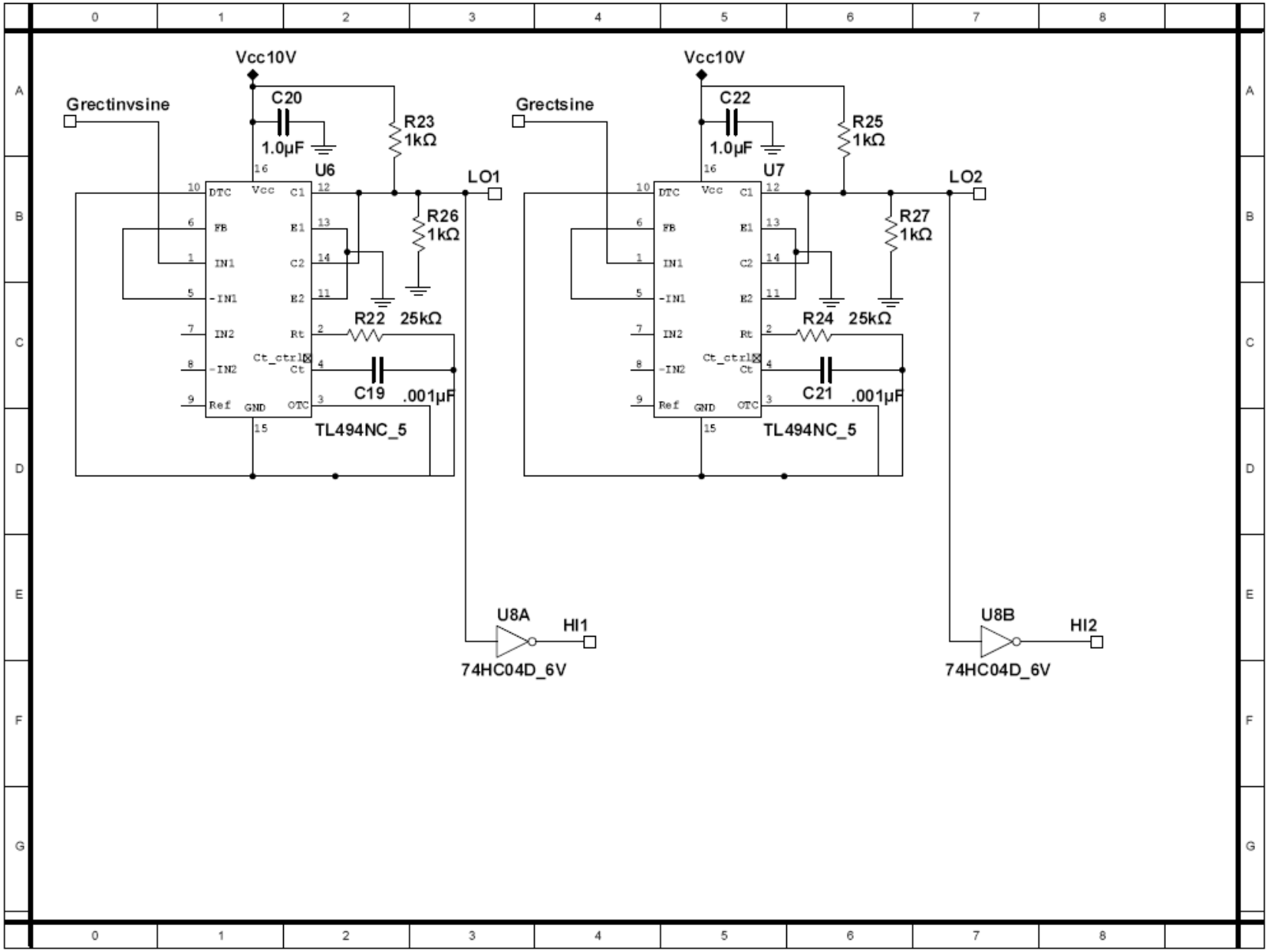
Vcc10V
Grectinvsine
C20
1.0µF
R23
1kΩ
U6
LO1
R26
1kΩ
R22
25kΩ
C19
.001µF
TL494NC_5
U8A
HI1
74HC04D_6V
Vcc10V
Grectsine
C22
1.0µF
R25
1kΩ
U7
LO2
R27
1kΩ
R24
25kΩ
C21
.001µF
TL494NC_5
U8B
HI2
74HC04D_6V

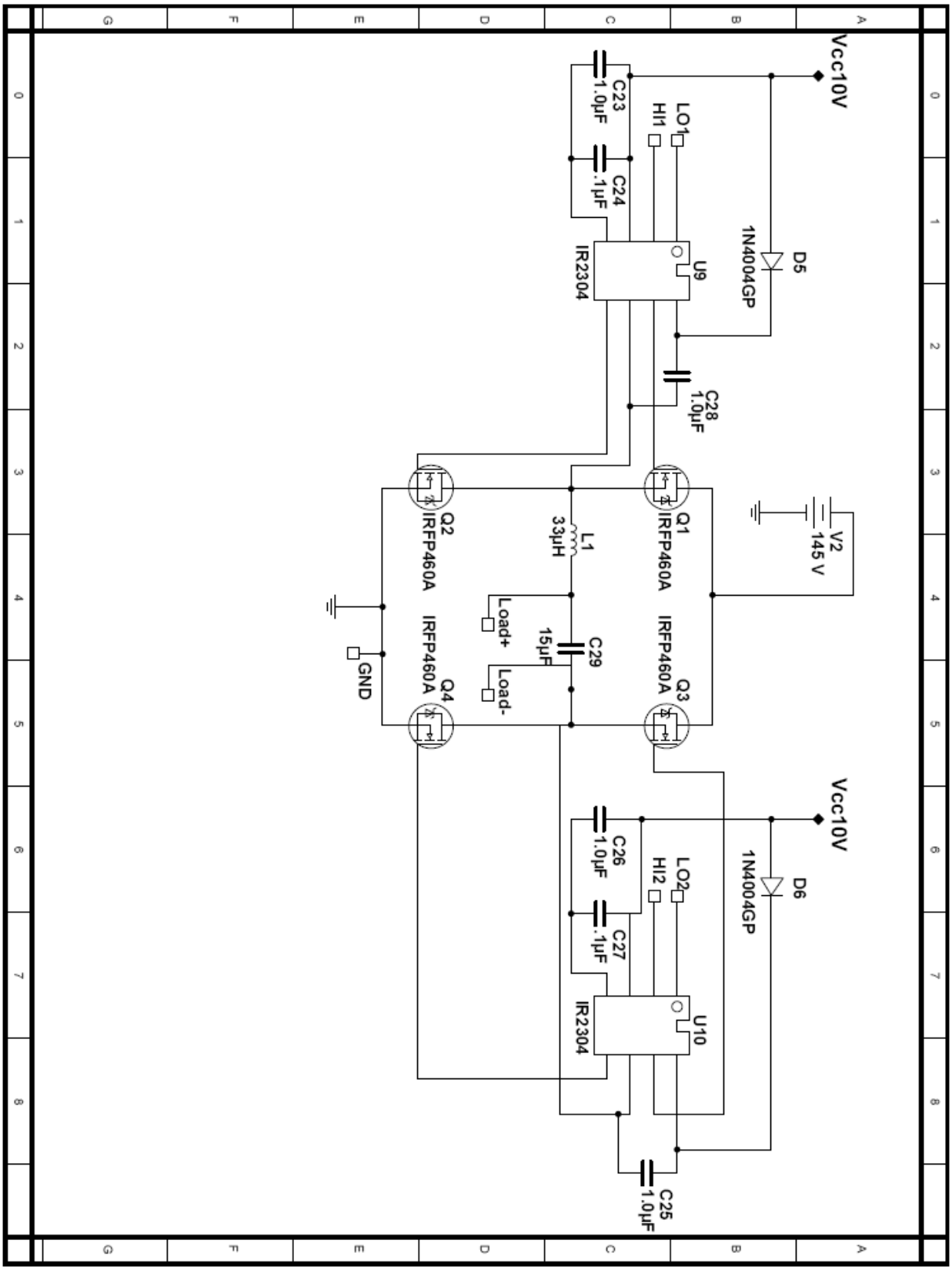
Vcc10V
C23
1.0µF
C24
.1µF
LO1
HI1
IR2304
U9
D5
1N4004GP
C28
1.0µF
Q1
IRFP460A
Q2
IRFP460A
L1
33µH
V2
145 V
Load+
C29
15µF
Load-
GND
Q3
IRFP460A
Q4
IRFP460A
Vcc10V
C26
1.0µF
C27
.1µF
LO2
HI2
IR2304
U10
D6
1N4004GP
C25
1.0µF

PCB Top Silkscreen

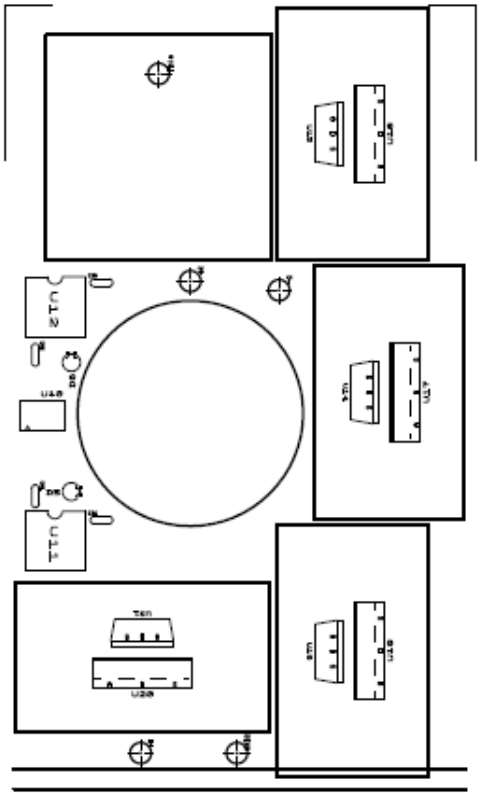

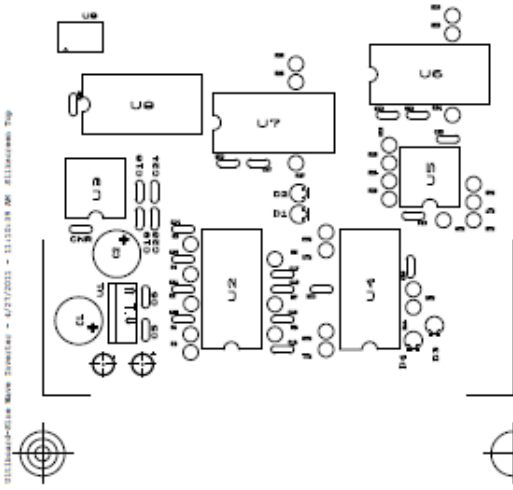

PCB Top Copper

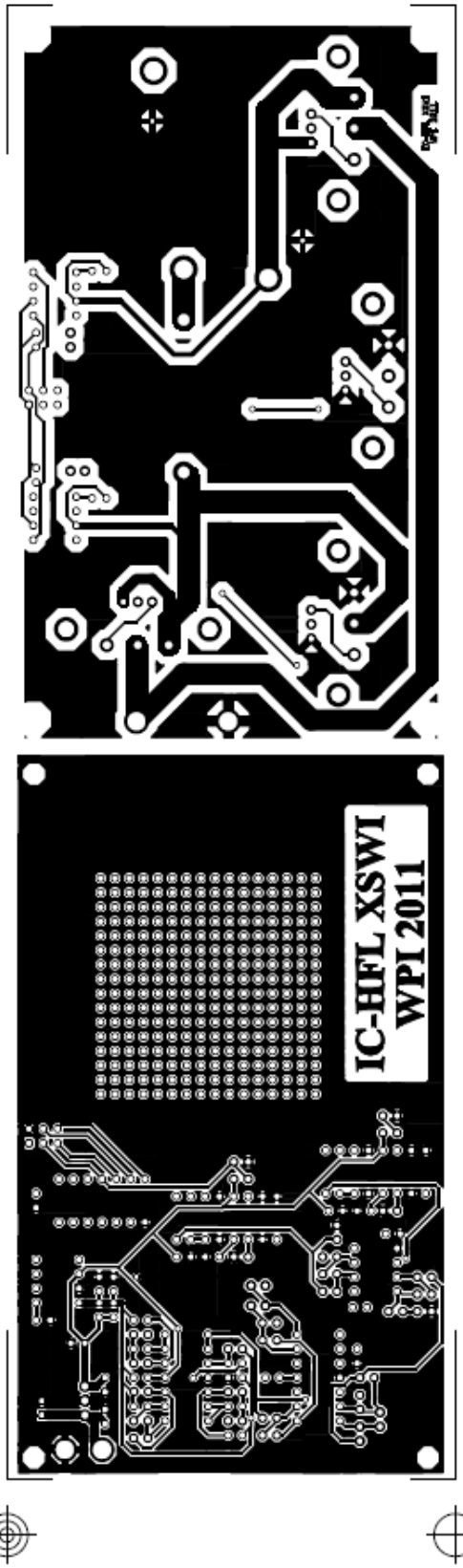

PCB Bottom Copper

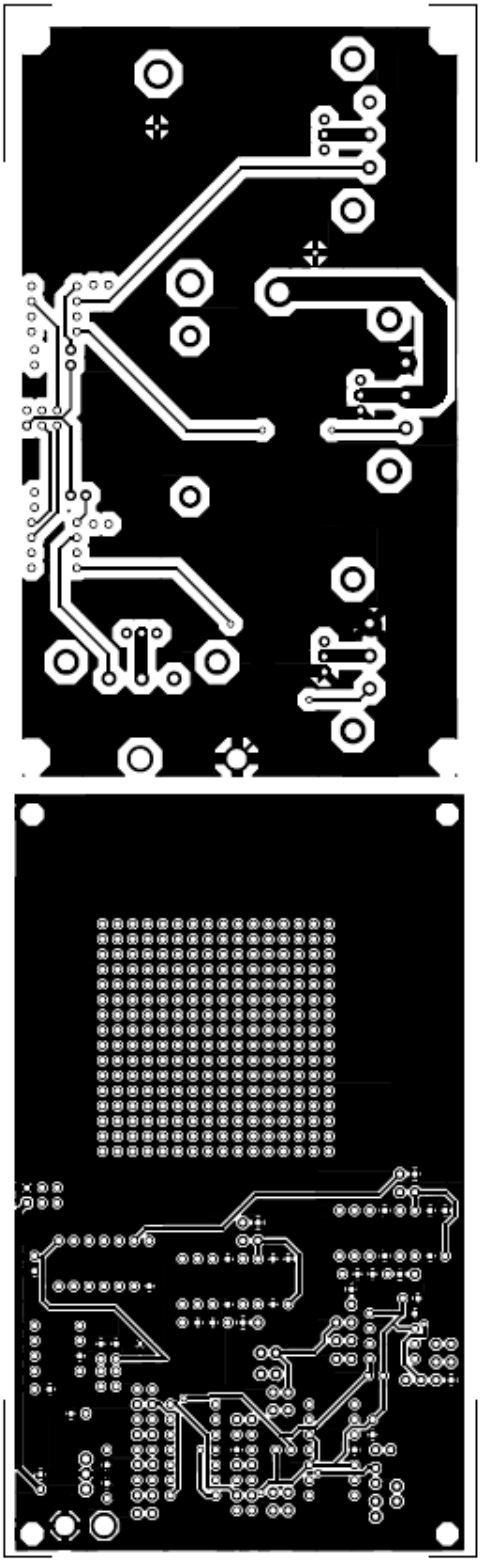

Appendix B: Parts List

Passive Components	Quantity	Price	Subtotal
33 uH Inductor	1	6.37	6.37
15 uF 250V AC Cap	1	10.47	10.47
470 uF Electrolytic Cap	2	0.39	0.78
.33 uF Cap	2	0.28	0.56
1 uF Cap	16	0.35	5.6
6.8 uF Cap	2	1.23	2.46
.01 uF Cap	6	0.24	1.44
.02 uF Cap	3	0.13	0.39
1000 pF Cap	2	0.27	0.54
100K Ohm Resistor 1/4W	3	0.10	0.3
200K Ohm Resistor 1/4W	1	0.10	0.1
187K Ohm Resistor 1/4W	2	0.10	0.2
10K Ohm Resistor 1/4W	8	0.10	0.8
18K Ohm Resistor 1/4W	2	0.10	0.2
5K Ohm Resistor 1/4W	2	0.10	0.2
20K Ohm Resistor 1/4W	4	0.10	0.4
1K Ohm Resistor 1/4W	4	0.10	0.4
500K Ohm Resistor 1/4W	1	0.10	0.1
			0
Integrated Circuits			0
BAJ0CC0T 10V LDO	1	1.82	1.82
TLE2426 Rail Splitter	1	1.61	1.61
TL084 Op-Amp	2	0.72	1.44
LM358 Op-Amp	1	0.46	0.46
TL494 PWM Controller	2	0.73	1.46
IR2304 MOSFET Driver	2	3.10	6.2
74HC04 Hex Inverter	1	0.47	0.47
			0
Semiconductors			0
1N4154 Diode	4	0.04	0.16
1N4004 Diode	2	0.09	0.18
IRFP460A 500V MOSFET	4	6.28	25.12
		Total	70.23